An integrated perspective into human relational memory

Shahin Tavakol
Integrated Program in Neuroscience
McGill University, Montreal, QC, Canada
Submission Date: December 2023

A thesis submitted to McGill University in partial fulfillment of the requirements of the degree of Doctor of Philosophy.

To Jowana & Waran

To understand something is conditional on the existence of its evidence in your mind.

~ Sûrewerdî ~

TABLE OF CONTENTS

ABSTRACT

Relational memory consists of multi-domain cognitive processes involved in information encoding and retrieval. These relational domains include episodic, semantic, and spatial memory, and they operate by binding discrete domain-specific elements of subjective experience into a coherent mental scheme. For example, in episodic memory, successive spatiotemporal events are combined into an autobiographical abstraction known as an episode. Similarly, in semantic memory, facts and notions are organized into a hierarchy of conceptual categories, and in spatial memory, the physical locations of surrounding objects are mapped out into a mental repository known as a cognitive map.

These distinct forms of relational memory have typically been studied separately, be it in animal models or humans. In the rodent literature, early studies were conducted using radial arm and water mazes, with experimental results supporting a role of the hippocampus in episodic and spatial cognition. At the same time, patients with brain lesions were being assessed in the context of various behavioral memory paradigms, further pointing to the involvement of the medial temporal lobes and underlying hippocampal and parahippocampal structures in information encoding and retrieval. With the advent of neuroimaging technologies, novel assessment protocols and tools, such as functional magnetic resonance imaging and virtual reality, enabled researchers to ascertain a wide range of cortical contributions to relational memory across all domains. Even so, the field still lacked an integrated evaluation paradigm for effectively addressing phenotypic variations in episodic, semantic, and spatial memory in the same individuals and across different populations.

Thus, the overarching objective of my PhD has been to develop a standardized relational memory platform for investigating differences in behavioral, structural, and functional phenotypes across healthy and clinical populations. In this thesis, I present, first, the *integrated relational evaluation paradigm* (iREP), which is the framework we have designed and used to investigate relational memory in humans, and then, the results of three complementary studies pertaining to (*i*) the overlapping structural and functional correlates of relational memory in healthy controls, (*ii*) the behavioral phenotyping of healthy and clinical populations, and (*iii*) the variations in task-based functional connectivity patterns in both populations.

In the first study, we applied the iREP to a group of healthy individuals, and discovered an integrated structure-function substrate of spatial memory in medial and lateral temporal cortices. In the second study, we compared behavioral responses across all iREP measurements between healthy individuals and patients with temporal lobe epilepsy, and observed a graded pattern of cognitive deficits in the clinical cohort, with episodic being most affected, followed by spatial, and semantic showing mixed results. In the final study, we examined patterns of functional connectivity across relational domains in the same groups, and found strong correspondence between multi-domain cross-cohort behavioral and functional variations. Together, our studies establish a novel framework for examining relational memory in different populations, with results pointing to an integrated behavioral, structural, and functional pattern across domains.

RÉSUMÉ

La mémoire relationnelle se compose de processus cognitifs multi-domaines impliqués dans l'encodage et la récupération de l'information. Ces domaines relationnels incluent la mémoire épisodique, sémantique et spatiale. Chacun de ces domaines cognitifs fonctionne en liant les éléments discrets de l'expérience subjective, générant ainsi une représentation mentale cohérente. Par exemple, dans la mémoire épisodique, les événements spatio-temporels successifs sont combinés pour créer une abstraction autobiographique connue sous le nom d'épisode. De même, dans la mémoire sémantique, les faits et notions sont organisés en une hiérarchie de catégories conceptuelles, et dans la mémoire spatiale, les emplacements physiques des objets environnants sont cartographiés dans un référentiel mental connu sous le nom de carte cognitive.

Ces formes distinctes de mémoire relationnelle ont généralement été étudiées séparément, que ce soit chez les modèles animaux ou chez l'homme. Dans la littérature sur les rongeurs, les premières études furent menées à l'aide de labyrinthes d'eau et de bras radiaux, avec des résultats expérimentaux soutenant un rôle de l'hippocampe dans la cognition épisodique ainsi que spatiale. En même temps, des patients présentant des lésions cérébrales furent évalués dans le cadre de divers paradigmes comportementaux de mémoire, indiquant, en outre, la participation des lobes temporaux médians et des structures sous-jacentes, tels que l'hippocampe et le parahippocampe, dans l'encodage et la récupération d'information. Avec l'avènement des technologies de neuroimagerie, de nouveaux protocoles et outils d'évaluation, telles que l'imagerie par résonance magnétique fonctionnelle et la réalité virtuelle, ont permis aux chercheurs de déterminer un large éventail de contributions corticales à la mémoire relationnelle dans tous les domaines. Néanmoins,

le domaine manquait d'un protocole intégré pour étudier les variations phénotypiques de la mémoire épisodique, sémantique et spatiale chez les mêmes individus et dans différentes cohortes.

Or, l'objectif principal de mon doctorat a été de développer un cadre d'évaluation mnésique pour examiner les différences comportementales, structurelles et fonctionnelles chez les populations saines et cliniques. Dans cette thèse, je présente, d'abord, le paradigme d'évaluation relationnelle intégrée (PÉRi), qui est l'outil que nous avons développé et utilisé pour étudier la mémoire relationnelle chez l'homme, puis, les résultats de trois études complémentaires relatives à (i) les corrélats structurels et fonctionnels de la mémoire relationnelle chez les individus sains, (ii) le phénotypage comportemental de populations saines et cliniques et (iii) les variations de connectivité fonctionnelle issues des tâches de mémoire dans les deux populations.

Dans la première étude, nous avons appliqué le PÉRi à un groupe d'individus sains et avons découvert un substrat intégré structurel-fonctionnel de mémoire spatiale dans les cortex temporaux médians et latéraux. Dans la deuxième étude, nous avons comparé les réponses comportementales du PÉRi entre participants sains et patients souffrant d'épilepsie du lobe temporal, et avons observé des déficits cognitifs gradués dans le groupe clinique. Dans l'étude finale, nous avons examiné les motifs de connectivité fonctionnelle entre les domaines relationnels dans les mêmes groupes, et avons trouvé une forte correspondance entre les variations comportementales et fonctionnelles à travers cohortes et domaines cognitifs. Ensemble, nos études établissent un nouveau cadre pour examiner la mémoire relationnelle dans différentes populations, avec des résultats qui démontrent une intégration des diverses formes de mémoire relationnelle sur le plan comportemental, structurel et fonctionnel.

ACKNOWLEDGMENTS

I would first like to thank my supervisor and mentor, Boris Bernhardt. When I started working with him, I was still a green graduate student with very little experience in—what a wise man once called—"serious science". Boris took me under his wing and taught me the ways of the brain, and I will forever be grateful to him.

Over the course of my PhD studies, my committee members, Nathan Spreng and Jorge Armony, provided me with great assistance. I would not have been able to accomplish all my objectives had it not been for their, at times, cut and dry, albeit always constructive and honest comments.

My deepest thanks also go to my fellow MICA lab mates: Reinder Vos de Wael, Sara Larivière, Jessica Royer, Qiongling Li, Alex Lowe, Donna Gift Cabalo, Hans Auer, Nicole Eichert, Linda Horwood, Casey Paquola, Oualid Benkarim, Bo-Yong Park, and Raul Rodriguez-Cruces. I would also like to thank our external collaborators Lorenzo Caciagli, Jonathan Smallwood, and Beth Jefferies for their indefatigable support. Further thanks go to our MRI personnel, David Costa, Ronaldo Lopez, the late Louise Marcotte, Soheil Quchani, Michael Ferreira, and Ilana Leppert.

Last, but certainly not least, I would like to thank my rock, Jowana Waissi. Her love and friendship have sustained me through thick and thin. Words cannot describe how much I love and appreciate her. She gifted me with the most precious thing in my life, our beautiful baby daughter, Waran, who is sitting in my lap as I am writing this sentence. ☺

I would like to end this acknowledgement section with some parting words about my sister, Shilan, who left us midway through my PhD. Losing her was the single most devastating experience of my life. How I wish she could have met Waran. I will cherish her memories forever.

CONTRIBUTIONS TO ORIGINAL KNOWLEDGE

In *Project I*, we introduced the *integrated Relational Evaluation Paradigm* (iREP), a novel cognitive task battery optimized for use in the MRI environment, which combines three difficulty-modulated probes that collectively tax the episodic, semantic, and spatial domains of relational memory. Administering this new assessment platform in a group of healthy individuals, we detected integrated structure-function markers confined to the medial and lateral temporal cortices that are associated with interindividual differences in spatial cognition.

In *Project II*, we leveraged the iREP to study relational memory in patients diagnosed with temporal lobe epilepsy (TLE) and age- and sex-matched healthy controls. We examined between-group behavioral disparities and their underlying socio-demographic and clinical presentations. For the first time, we have demonstrated within single subjects that TLE patients present with a graded pattern of mnemonic deficits wherein the episodic system is most affected by disease, followed by the spatial system, with the semantic system being relatively unaffected.

In *Project III*, we contextualized our behavioral findings from *Project II* within network-level functional topographies derived from task-based neural dynamics. We observed similar multivariate patterns across episodic, semantic, and spatial domains, where controls and patients differed in their whole-brain connectivity profiles and behavioral performances. We further established the presence of domain-specific functional motifs that converge within the limbic system.

Our work lays the analytical foundations of an integrated memory framework that, we hope, will significantly streamline the study of human relational cognition in different populations.

CONTRIBUTIONS OF AUTHORS

Project I

Shahin Tavakol: study and task design, data acquisition, image processing, statistical analysis, manuscript writing; Qiongling Li/Jessica Royer: data acquisition, manuscript editing; Alex Lowe: data acquisition; Reinder Vos de Wael/Sara Larivière/Casey Paquola: manuscript editing; Elizabeth Jefferies/Tom Hartley: task design, manuscript editing; Andrea Bernasconi/Neda Bernasconi: manuscript editing; Jonathan Smallwood: task and study design; Veronique Bohbot: discussion, manuscript editing; Lorenzo Caciagli: task and study design, analysis; Boris Bernhardt: study supervision, funding

Project II

Shahin Tavakol: study and task design, data acquisition, image processing, statistical analysis, manuscript writing; Valeria Kebets: analysis, editing of manuscript; Jessica Royer/Qiongling Li/Hans Auer: data acquisition, manuscript editing; Jordan DeKraker: image processing; Elizabeth Jefferies: task design, manuscript editing; Neda Bernasconi/Andrea Bernasconi: manuscript editing; Christoph Helmstaedter: task design, manuscript editing; Jorge Armony/R. Nathan Spreng: analysis, manuscript editing; Lorenzo Caciagli: study and design; Birgit Frauscher: patient identification, manuscript editing; Jonathan Smallwood: task and study design; Boris Bernhardt: study supervision, funding

Project III

Shahin Tavakol: study and task design, data acquisition, image processing, statistical analysis, manuscript writing; Valeria Kebets: analysis; Jessica Royer/Qiongling Li/Hans Auer: data acquisition; Elizabeth Jefferies: task design; Lorenzo Caciagli: study and design; Birgit Frauscher: patient identification; Jonathan Smallwood: task and study design; Boris Bernhardt: study supervision, funding

LIST OF FIGURES AND TABLES

Project I

Project II

Project III

LIST OF ABBREVIATIONS

ATL: anterior temporal lobe

DLPFC: dorsolateral prefrontal cortex

DMN: default mode network

fMRI: functional magnetic resonance imaging

IFC: inferior frontal gyrus

iREP: integrated Relational Evaluation Paradigm

LV: latent variable

lTLE: lateral temporal lobe epilepsy

MICA: multimodal imaging and connectome analysis

MRI: magnetic resonance imaging

MTL: medial temporal lobe

mTLE: medial/mesial temporal lobe epilepsy

PLS: partial least squares

rs-fMRI: resting-state functional magnetic resonance imaging

TLE: temporal lobe epilepsy

vmPFC: ventromedial prefrontal cortex

1 GENERAL INTRODUCTION

1.1 Relational memory

That human memory is a complex system composed of multiple cognitive domains is a foregone conclusion today, but it was not always the case. In fact, prior to landmark works on relational cognition pertaining to episodic memory (Penfield & Milner, 1958; Scoville & Milner, 1957; Tulving, 1972), semantic memory (Collins & Quillian, 1972; Quillian, 1966), and spatial memory (Milner, 1965; O'Keefe & Dostrovsky, 1971; Tolman, 1948), the field was dominated by behaviorism, itself, borne out of the necessity to bring empirical integrity to the study of the mind (Watson, 1924). Even so, in attempting to bring experimental rigor to psychology, behaviorism hamstrung itself by severely constraining its own practical scope as it endeavoured to describe all manner of behavior in terms of stimulus and response (Watson, 1924). Ironically, while its inception was iconoclastic in essence, behaviorism eventually collapsed under the weight of its own theoretical axioms. In hindsight, the imposition that all observations should admit of an explanation through the narrow lens of the stimulus-response paradigm was an oversight, one that would ultimately lead to the downfall of behaviorism as a systematic approach to understanding human nature.

The upshot of two simple rodent experiments conducted by Edward Tolman in 1948 would mark the beginning of a paradigm shift away from behaviorism. At the outset of *Cognitive maps in rats and men* where he related his findings, Tolman distinguished his own views from those of behaviorists, claiming that something akin to a field map of the surroundings gets established in the rat's brain when it navigates a new environment (Tolman, 1948). His first experiment involved an elevated maze consisting of a starting shaft that led into a circular compartment, which further

appended an exit shank with orthogonal bends, ultimately terminating in a food-containing goal-box. Rodents were trained on this contraption across twelve trials spread out over four nights (*i.e.*, three trials per night), where they learned to run directly and unhesitatingly from the starting path to the food-box. Following this conditioning phase, the exit shank was replaced by a series of radial arms, thus forming the so-called "sun-burst" maze, and the rodents were allowed to navigate the apparatus once more from the starting shaft to the goal-box. Remarkably, after realizing that the originally learned path was no longer available, 36% of rodents, which amounted to over four times the number expected under the null hypothesis, chose the same radial arm that led in the direction of where the food-goal would have been during the initial training phase. Tolman argued that his rats were exhibiting a kind of goal-oriented navigational phenotype that simply did not fit the stimulus-response model. In the ensuing experiment, Tolman wanted to know whether this behavior was indeed the result of a "broad comprehensive" cognitive map that integrated across a wide range of environmental cues or some other form of "strip-like and narrow" local encoding mechanism that was tuned to the specific goal destination. To this end, two groups of rodents were conditioned in a simple T-maze over the course of seven days across twenty trials. The first group, which counted twenty-five rats, was trained to reach the food-box on one side of the bifurcation (*i.e.*, left), while the second group, also twenty-five, learned to access the other one (*i.e.*, right). As in the previous experiment, the distal section of the maze was substituted for a series of radiating paths. In addition, the entire apparatus was flipped upside down such that *left* now corresponded to *right* and vice versa. During the testing phase, 84% of rodents selected a single arm to run on within seven minutes. In both groups, a significant portion of rats chose "not the paths which pointed directly to the spots where the food had been, but rather paths which ran perpendicularly to the corresponding sides of the room" (Tolman, 1948). Thus, most rodents in both cohorts had

settled on the same relative paths they had been conditioned to follow, even though the absolute paths had been reversed. In other words, those that were trained to go left continued to go left, even though left was now right, and vice versa. Overall, while the first spatial orientation experiment strongly pointed to the implication of a cognitive map, rather than a stimulus-response mechanism, in informing the navigation choices of rodents, the second one suggested that this map is, indeed, a comprehensive mental representation, which is to say one that does not depend exclusively on a given focal point. Speculating about how his findings may apply to the human condition, Tolman maintained that while cognitive maps may enable pathfinding behaviors in spatial spaces, they may additionally allow us to navigate social ones as well. In the closing statements of his manuscript, he wrote that major societal issues, such as the discrimination of minorities, arise from our failure to generate broad social cognitive maps in which the well-beings of different demographic groups are interlinked (Tolman, 1948).

In retrospect, Tolman's works marked a stark departure from behaviorism, breathing new life into a field that seemed to have crystalized because of a lack of explanatory power over complex behavioral phenomena. They additionally laid the theoretical groundwork for generalizable models of human cognition that bridge the gap between multiple mental domains. Soon after, arguably the earliest formulation of the relational memory framework was proposed in an obscure doctoral dissertation by M. Ross Quillian, where he advanced a model of semantic memory consisting of a constellation of interconnected concept nodes related to one another via "associative links" (Quillian, 1966). These nodes come in two flavors, "type" nodes, which sit atop an abstractive hierarchy within a "plane", and "token" nodes, which make up the bulk of the plane, with *intra*-plane token-to-token connections and *inter*-plane token-to-type associations (Quillian, 1966).

Thus, any given concept can be construed as a cluster of interlinked planes, each one composed of an apex type node related to downstream token nodes that are either connected to each other within the same plane or to other singular type nodes across different planes. Take for example the concept of *dog*. What is a dog? Is it an animal? Is it "man's best friend"? Is it a canine? Is it a thing that goes, "woof, woof"? According to this model of semantic memory, *dog* can be understood as an abstraction that integrates across a collection of intersecting conceptual planes, some that describe *animal*, some others that define *canine*, and yet others that illustrate concepts such as *man* and *friendship*, or even *woof* as an onomatopoeia. What is important to note is that there is no intrinsic hierarchy or configuration across planes, nor are the planes themselves rigid constructs; only when a specific node is indexed does a transient structural order emerge within the entire semantic constellation, a phenomenon akin to a memory engram. Accordingly, while the apex node *dog* may recruit other nodes such as *animal* or *canine*, at any other instant, it may become itself a secondary type node—if not a subordinate token node—in the semantic sequences running downstream from type nodes for *puppy* or *furry*. Hence, Quillian's model of semantic memory postulated a self-contained conceptual paradigm in which individual nodes take form through conformational permutations of the system. While novel in its detailed account of how concepts are formed via associative links, the core of Quillian's thesis, that semantic referents are built upon pre-existing ones, harkens back to much older schools of thought. One example comes from Sûrewerdî, the 12th century Kurdish mystic, who observed in his treatise *The Shape Of Light*: "As long as you cannot construct the form of something in your mind, you cannot possibly know it, because the realization of a thing [*i.e.*, dog] has to correspond to something [*i.e.*, animal, canine, etc.]" (Suhrawardī, 1998). While Quillian's thesis specifically delt with the semantic memory

system, he conjectured that its underlying principles of information storage could just as easily apply to other cognitive domains, such as visuo-spatial memory (Quillian, 1966).

On the heels of Quillian's thesis came Endel Tulving's seminal work on episodic memory. Interestingly, Tulving's conceptualization of episodic cognition was a direct offshoot of the semantic memory framework laid out by Quillian and others (Collins & Quillian, 1972; Quillian, 1966). In Tulving's own words, "A new kind of memory that has recently appeared on the psychological scene is 'semantic' memory. As far as I can tell, it was first used by Quillian (1966) in his doctoral dissertation […] A useful concept in science frequently is one whose definition not only makes very clear what it includes, but also what it excludes […] To facilitate subsequent discussion, I will refer to this other kind of memory, the one that semantic memory is not, as 'episodic' memory. I will refer to both kinds of memory as two stores, or as two systems, but I do this primarily for the convenience of communication, rather than as an expression of any profound belief about structural or functional separation of the two" (Tulving, 1972). In a later work, Tulving described episodic memory as having emerged as an "embellishment" of the more archaic semantic memory system by way of evolution (Tulving, 2002). In fact, he maintained that the major differences between these two mnemonic systems pertain to the nature of the information being stored (*i.e.*, spatiotemporal relations between events *vs* abstract relations between conceptual referents) and their inherent susceptibilities to information transformation or loss, with the episodic system being much more liable to alteration than the semantic (Tulving, 1972).

With the emergence of new models of relational memory, it became necessary to uncover its neural correlates. It 1957, the first definitive evidence of mnemonic substrates would be produced by

Brenda Milner, pointing to the importance of the hippocampus and surrounding structures of the medial temporal lobe (MTL) in sustaining episodic and spatial memory (Scoville & Milner, 1957). An immediate corollary of Milner's findings was the development of animal protocols designed to study the function of hippocampus. In one such experiment, John O'Keefe and Jonathan Dostrovsky recorded directly from the dorsal CA1 hippocampal subfield of rats while they were being passively manipulated across a rectangular platform and held down at specific locations while facing different directions (O'Keefe & Dostrovsky, 1971). They found that several electrode subunits responded to the location and heading direction of the rat. Based on their observations, the researchers concluded that the hippocampus must somehow be providing "the rest of the brain with a spatial reference map". Thus, the idea of the cognitive map, as initially conceived by Tolman, had been reawakened after laying somewhat dormant. Then, in 1978, O'Keefe and Lynn Nadel co-authored their influential book *The Hippocampus as a Cognitive Map*, in which they described the hippocampus as a "cognitive-mapping system", which is predicated on the actions of specialized CA1 cell populations that make up so-called "place units … whose firing pattern is dependent on the location of the animal in an environment" (O'Keefe & Nadel, 1978). Notably, they also introduced the dichotomous notion of *egocentric* (or relative) vs. *non-egocentric* (or absolute) spatial systems, maintaining the role of the hippocampus in the latter, where the first one is a body-centered cognitive map that changes as a function of the subject's position and heading direction, whereas the second is a stable representation of the surroundings predicated on the inter-relationships of items that populate it irrespective of the subject. This type of spatial mapping, that is, the hippocampal-dependent non-egocentric, is commonly referred to as "allocentric" in the literature (Chan et al., 2016; Guderian et al., 2015; Sierk et al., 2019). Moreover, the authors hypothesized that the neural mechanisms that instantiate the cognitive map need not exclusively

pertain to spatial relationships. In fact, they argued that semantic relationships between words, symbols, or concepts could also be represented in the brain in the form of "non-spatial maps" (O'Keefe & Nadel, 1978), harkening back to Quillian's semantic memory framework (Collins & Quillian, 1972; Quillian, 1966). While the discovery of place cells in the rat hippocampus was the first of its kind as far as cellular substrates of the cognitive map go, it would not be the last. Since then, several other specialized neurons have been discovered in both humans and animals, each one specially tuned to respond to a unique property of physical space. They include, among others, place cells in the human (Ekstrom et al., 2003), entorhinal grid cells (Hafting et al., 2005; Jacobs et al., 2013), border cells (Sargolini et al., 2006), and head direction cells (Savelli et al., 2008; Solstad et al., 2008).

Building on the works of O'Keefe, Dostrovsky, and Nadel, in 1993, Neal J. Cohen and Howard Eichenbaum wrote their highly touted *Memory, Amnesia, and the Hippocampal System*, where they drew upon converging evidence across human and animal models of memory dysfunction to synthesize the relational memory framework as we know it today. They described the functional role of the underlying structures of the MTL, which includes the hippocampus and parahippocampus, as a relational system that indexes highly processed neocortical patterns, effectively binding them to form multidomain representations that go beyond spatial relationships (Cohen & Eichenbaum, 1993). Indeed, they maintained that the characterization of hippocampal neurons as mere "place cells" does not do justice to the breadth of associative processes in which they are directly involved, instead opting for the more general "relational cells". In the years since, relational memory theory has been widely adopted and evaluated (Eichenbaum & Cohen, 2001; Hannula et al., 2006; Konkel et al., 2008; Ryan & Cohen, 2003; Tavakol et al., 2022; Tavakol et

al., 2021), with revised versions of the framework, such as the Tolman-Eichenbaum machine, which proposes a role for entorhinal grid cells in laying out an abstract scaffolding onto which hippocampal place cells bind multisensory representations (Whittington et al., 2020). Beyond hippocampal contributions, contemporary neuroimaging findings anchor relational memory domains to underlying neural architectures that span the entire neocortex. For example, the consolidation of episodic engrams is believed to be mediated by the concerted activity of the ventromedial prefrontal cortex (vmPFC) and anterior temporal lobe (ATL), which are actively associated with the anterior hippocampus (Eichenbaum, 2017; Moscovitch et al., 2016). The ATL appears to be specifically engaged in semantic memory in conjunction with the inferior frontal gyrus (IFG), where symbolic prompts are processed across hemispheres, with greater left-sided involvement for lexical stimuli (Hoffman & Morcom, 2018; Jackson, 2021; Rice et al., 2015). According to the hub-and-spoke model of semantic cognition, conceptual knowledge is formed when modality-specific sources of semantic information from primary and association cortices converge upon the ATL, which acts as a transmodal hub that integrates them into a coherent and generalizable mental construct (*i.e.*, a concept) (Patterson & Lambon Ralph, 2016; Rogers et al., 2004; Schapiro et al., 2013). With respect to spatial memory, findings point to the retrosplenial, parahippocampal, and posterior parietal cortices as important areas (Baumann & Mattingley, 2021; Qiu et al., 2019), with one framework positing the integration of hippocampal-dependent allocentric representations with extra-hippocampal egocentric schemes via the retrosplenial cortex (Bicanski & Burgess, 2018; Byrne et al., 2007; Dhindsa et al., 2014). These modern network-level models of relational memory exemplify the latest paradigm shift in contemporary neuroscience, wherein function and disease are increasingly described in terms of whole-brain network dynamics, a change in how we conceptualize the brain that has been primarily driven by

advancements in neuroimaging in tandem with novel analytical tools, such as connectomics (Tavakol et al., 2019).

1.2 Neuroimaging and experimental platforms

Today, magnetic resonance imaging (MRI) can be used to derive high-resolution structural and functional properties of the brain, enabling direct assessments of relational memory behavioral phenotypes and their underlying neural properties. These analyses are further streamlined for group-level comparisons thanks to well-established volumetric (Collins et al., 2003; Dadar et al., 2018) and surface-wide brain templates (Fischl, 2012; Glasser et al., 2013; Kim et al., 2005), which are commonly used to register subject-specific biomarkers to a shared brain space. For example, native T1-weighted (T1-w) anatomical images can be leveraged by modern automated segmentation tools to produce surficial representations of the neocortex and hippocampus upon which various metrics can be expressed along surface vertices (Bernhardt et al., 2016; Caldairou et al., 2016; Fischl, 2012; Goubran et al., 2020; Kim et al., 2014; Kim et al., 2005; Romero et al., 2017; Wang et al., 2012). In many studies of relational memory that use structural MRI (sMRI), the main objective has been to identify variations in specific morphological properties (*i.e.*, neocortical thickness, gray matter volume, hippocampal dentation, etc.) that are associated with behavioral outcome measures of episodic (Aslaksen et al., 2018; Beattie et al., 2017; Travis et al., 2014; Zammit et al., 2017), semantic (Chen et al., 2019; Paulin et al., 2020; Snowden et al., 2019; Snowden et al., 2018), and spatial cognition (Abrahams et al., 1999; Hartley & Harlow, 2012; Maguire et al., 2000; Tavakol et al., 2021). Modern computational toolboxes offer the option of generating models of neocortical surface and approximating thickness. For example, FreeSurfer, which is cross-validated with histological and manual data (Cardinale et al., 2014; Kuperberg et

al., 2003; Rosas et al., 2002), incorporates a pipeline that consists of brain extraction from a T1-w image, segmentation of the brain by tissue type (*i.e.*, white matter, grey matter, blood vessels, etc.), generation of pial and white matter meshes, and alignment of subject-specific surfaces to fsaverage template while minimizing geometric distortions (Dale et al., 1999; Fischl et al., 1999). For the segmentation of hippocampal subfields, one powerful method capitalizes on a multi-template surface-patch algorithm that produces unfolded surfaces that run through the core of each subfield (Bernhardt et al., 2016; Caldairou et al., 2016; Vos de Wael et al., 2018). Once the native T1-w image undergoes correction for intensity non-uniformity, it is then standardized for intensity and linearly registered to MNI152 volumetric template. The image is subsequently partitioned into left and right subiculum, CA1-3, CA4-DG. This algorithm benefits from having been trained on an openly-accessible database consisting of high resolution 3T MRI data pertaining to hippocampal subregions (Kulaga-Yoskovitz et al., 2015). The generation of medial surface sheets (*i.e.*, midpoint between pial and white matters) for each subfield is accomplished via a Hamilton-Jacobi approach (Kim et al., 2014), with surficial parameterization based on a spherical harmonics framework with a point distribution model (Styner et al., 2006). Biomarkers of local grey matter, such as columnar volume, can then be calculated for every vertex of each subfield mesh by taking the product of voxel volume and number of inclusive voxels (Kim et al., 2014). HippUnfold is another recently developed toolbox for the automated segmentation of the hippocampus (DeKraker et al., 2022). Unlike the surface-based patch algorithm, HippUnfold automates detailed tissue segmentation by leveraging a U-Net deep convolutional neural network. The resulting "unfolded" hippocampal plane can be used as a subject-specific feature space to map out salient markers, such as gray matter data for each subfield, including the left and right subiculum, CA1, CA2, CA3, CA4, and dentate gyrus. For group-level considerations, subfields can be linearly registered to MNI152

space, a process that corrects for interindividual variability in intracranial volume. Combined with targeted behavioral outcome measures, these morphological indices provide the ideal analytical inputs for addressing interindividual as well as between-group differences in relational cognition.

While sMRI provides a powerful framework for detecting morphological correlates of relational memory, functional MRI (fMRI) offers a complementary platform that instead focuses on spatiotemporal neural dynamics derived from the blood oxygen level-dependent (BOLD) signal. This signal occurs when the magnetic properties of underlying tissues shift as a function of blood flow and oxygen consumption when a region of the brain is upregulated (Buchbinder, 2016). Since its development in 1992 (Kwong et al., 1992; Ogawa et al., 1992), BOLD fMRI has quickly grown into a staple of contemporary cognitive neuroimaging, with task-based and resting-state paradigms constituting platform exemplars. In task-based fMRI, one or more experimental conditions are contrasted against one or more baseline conditions, and the signal change in the BOLD response is averaged across several trials in either blocked or event-related designs (Buchbinder, 2016). Numerous studies have now implemented task-based fMRI to tap into relational processes along episodic (Li et al., 2021; Liu et al., 2022; Vidal-Piñeiro et al., 2021; Whalley et al., 2009; Zhuang et al., 2019), semantic (Rice et al., 2018; Seidenberg et al., 2009; Woodard et al., 2009), and spatial domains (Aguirre & D'Esposito, 1997; Hassabis et al., 2009; Jokeit et al., 2001; Kim & Maguire, 2019; Schindler & Bartels, 2013; Tavakol et al., 2021). Furthermore, online interfaces like Neurosynth can readily tap into large-scale fMRI data and automatically synthesize general patterns of BOLD activation based on user-defined input criteria, making it easier than ever to generate robust meta-analytical inferences. While task activation frameworks have their own merit, the brain at rest offers a different look into neural dynamics. In the absence of active

involvement in higher cognitive tasks, the brain, which only makes up 2% of total body weight, accounts for a staggering 20% of energy metabolism (Attwell & Laughlin, 2001). Interestingly, increases in energy consumption secondary to heightened cognitive load are relatively small, on the order of 2.5% above ground state (Buchbinder, 2016). In resting-state fMRI (rs-fMRI), instead of comparing activation and control conditions, the intrinsic activity of the brain is measured and evaluated, thus exploiting its exceptionally high baseline energetics (Buchbinder, 2016). The most common method of quantifying resting-state neural dynamics is to determine the whole-brain functional connectivity by computing the correlation strength between the BOLD time-series of different brain areas (Biswal et al., 1997; Buckner et al., 2013; Cordes et al., 2000; Fox et al., 2006; Lowe et al., 2000; Smith et al., 2009). Indeed, the intrinsic functional architecture of the cortex represents a tried and tested method of anchoring behavior to the innerworkings of the brain (He et al., 2020; Medea et al., 2018; Smith et al., 2015; Sormaz et al., 2017). Notwithstanding the relatively small increases in energy consumption secondary to heightened cognitive demand, new evidence suggests that functional connectomes derived from task paradigms may provide greater resolution into underlying cognitive processes than the conventional resting-state framework (Cole et al., 2021). Thus, the functional organization of the brain as derived from either intrinsic or task-elicited platforms is especially amenable to the study of substrates of relational memory, especially when it is analytically dovetailed with powerful multivariate associative techniques, such as partial least squares (PLS) (Subramaniapillai et al., 2022). PLS identifies a common feature space of maximal covariance between two different datasets (Kebets et al., 2019; McIntosh & Lobaugh, 2004). As such, it is ideal for uncovering latent associations between various modality inputs, be it behavioral, socio-demographic, morphological, or functional.

The following section presents some classic experimental paradigms performed in animals and humans, where the behavioral, anatomical, and functional correlates of different relational memory domains have been studied.

Radial arm maze

In addition to the contraptions used in the previously described rodent experiments (O'Keefe & Dostrovsky, 1971; O'Keefe & Nadel, 1978; Tolman, 1948), the radial arm maze (RAM) is among the earliest apparatuses used to study spatial memory (Olton & Samuelson, 1976). As the name implies, the RAM consists of radiating paths of equal length that extend out from a central platform, "like spokes on a wheel" (Olton et al., 1978). Usually, there are eight such "spokes", each one terminating in a cylindrical well that can store food pellets. A typical protocol consists of a pre-training phase, where the rodents get acclimated to the experimental environment by freely navigating the maze, a training phase, where rodents learn the locations of food rewards, and a testing phase, where they must find their way to these rewards from different starting locations within the maze. The first lesional rodent study to employ the RAM found that, compared to control and extra-limbic neocortical ablation groups, rats with surgically severed efferent hippocampal fibers were severely impaired on pathfinding trials (Olton et al., 1978). Since then, human analogues of the rodent platform have been extensively used to study a wide range of spatial navigational behaviors, including age- and sex-related phenotypic differences, both in real environments (Bohbot et al., 2002; Foreman et al., 1990; Foreman et al., 1984; Mandolesi et al., 2009; Moraleda Barreno et al., 2013; Serra et al., 2021) as well as virtual ones (Bohbot et al., 2004; Goodrich-Hunsaker & Hopkins, 2010; Iaria et al., 2003; Kim et al., 2018; Levy et al., 2005; Patel et al., 2022; West et al., 2023).

Morris water maze

Developed by Richard G. M. Morris in 1981, the eponymous Morris water maze (MWM) was designed to eliminate confounding navigational factors, such as olfactory and even visual cues (Morris, 1981; Othman et al., 2022). The MWM consists of a water-filled circular pool that sits in the middle of a rectangular room, with distal visual cues on each wall. Inside the pool, a cylindrical platform can be placed at any location, with its circular podium either slightly above the water surface or slightly submerged under it depending on the experimental protocol. While the water significantly reduces the effect of olfactory cues in supporting wayfinding, it can also be rendered opaque by mixing in a small quantity of milk, thus making it difficult to visually locate the podium (Morris, 1981; Othman et al., 2022). In his first study, Morris found that, following the conditioning phase, rodents learned to swim rapidly to the podium from any location along the perimeter of the pool, even though the platform was odorless and visually indiscernible (Morris, 1981). Morris concluded that his findings were in line with the cognitive map theory, since the distal room cues enabled the rats to generate novel pathfinding behaviors. In a follow-up experiment conducted in collaboration with John O'Keefe, Morris discovered prolonged and significant navigational deficits in hippocampally lesioned rats, adding more weight in support of the cognitive map theory and the central role of the structures of the MTL (Morris et al., 1982). In the years since, much like the RAM, the MWM too has been adapted for human studies, with themes spanning hippocampal damage (Astur et al., 2002), sex differences in navigational phenotypes (Astur et al., 2004), hippocampal/parahippocampal theta oscillations (Cornwell et al., 2008), high-resolution spatial binding (Kolarik et al., 2016), and prenatal alcohol exposure (Dodge et al., 2020). In fact, the virtual analogue of the MWM is the most popular virtual reality paradigm for assessing spatial memory in humans today (Thornberry et al., 2021). The MWM also offers

great cross-species utility (Othman et al., 2022; Schoenfeld et al., 2017), with an availability of protocols across different animal models, including mice (Vorhees & Williams, 2006) as well as domestic and wild guinea pigs (Lewejohann et al., 2010).

Four Mountains Task

The Four Mountains Task (FMT) is a computerized delayed match-to-sample protocol with thirty total trials that tests short-delay topographical memory in humans (Chan et al., 2016). It was first used in a small cohort of patients with hippocampal damage and age- and sex-matched controls to ascertain the involvement of the MTL in spatial cognition across relatively small timescales (Hartley et al., 2007). The results showed that while topographical perception is reasonably well preserved in these patients, their short-delay allocentric spatial processing is indeed affected. Moreover, since impairment of hippocampal function typically precedes the onset of Alzheimer's disease, the FMT has additionally been shown to effectively detect the early stages of dementia (Chan et al., 2016). We discuss how this task is administered in Project I of this thesis. Briefly, at each trial, a computer-rendered layout composed of four distinct mountains is presented to the participant for ten seconds. Following this encoding phase, four new landscapes are shown, and the participant must select the one that corresponds to the initial configuration of mountains. To control for visual matching strategies, low feature visual cues in each option are also slightly altered compared with the original layout.

Semantic association tasks

Typical semantic assessment protocols involve the use of trial-by-trial *n*-alternative force choice paradigms where a probe is presented along with *n* number of choices at each trial. While the

modalities of displayed stimuli (*i.e.*, auditory, lexical, and symbolic) may vary across task designs, the general workflow consists of selecting a single target from the presented choices based on the degree of conceptual relatedness with the probe. In (Davey et al., 2015), where the authors examined neocortical contributions to semantic retrieval, two similar word-to-picture matching tasks were administered: identity- and thematic-matching. In the identity-matching module, participants had to choose from a triad of words (*i.e.*, "animal", "tool", and "plant") the category to which a symbolic probe (*i.e.*, the picture of a dog) belongs. Likewise, during the thematic-matching protocol, they were instructed to select from three options (*i.e.*, "zoo", "orchestra", and "driver") the target word that showed the highest association with the probe stimulus (*i.e.*, the image of a tuba). Conceptual association strengths between visual probes and target words were determined in a holdout group of nine individuals who rated each stimulus pair on a 7-point Likert scale, ranging from 0 (*i.e.*, no discernible association) to 7 (*i.e.*, extremely strong link). In a related study that looked at the intrinsic connectivity of the hippocampus with the neocortex (Sormaz et al., 2017), participants performed a lexicon-based 3-alterantive force choice semantic judgment task. At the onset of each trial, a blank screen appeared on the computer monitor for a duration of 500 ms, after which three words were presented at the bottom of the screen for 900 ms. Then, a probe word was displayed above these three options, and participants had to select the word choice that was related in meaning with the probe within 3 s. In another task-based functional MRI study that investigated the role of the ATL in representing semantic knowledge (Rice et al., 2018), participants had to make a nationality judgment (*i.e.*, European *vs.* non-European) across two conditions (*i.e.*, social *vs.* non-social) based on visual or auditory stimuli (*i.e.*, social: a picture of Tom Hanks or the spoken words "Tom Hanks"; non-social: a picture of the Eiffel Tower or the spoken words "The Eiffel Tower"). This task was adapted by (Alam et al., 2021) to assess

hemispheric differences of the ATL in semantic categorization across different stimulus modalities. Here, participants made the same nationality judgment across modality-specific task blocks where corresponding concepts were presented in either symbolic or lexical format (*i.e.*, symbolic block: a picture of Gwyneth Paltrow *vs.* lexical block: the words "Gwyneth Paltrow"). The Intelligenz-Struktur-Test is yet another example of a semantic judgment task, which, unlike the other paradigms, does not actually employ a reference probe (Helmstaedter, 2002). Instead, participants must correctly identify the target word that represents the conceptual outlier among five options (*i.e.*, sitting, lying, *going*, kneeling, standing).

Episodic judgment tasks

In (Sormaz et al., 2017), in addition to the semantic judgment task, the authors also administered a previously established paired-associate recall test (Payne et al., 2012) to examine episodic memory. The protocol consisted of an encoding phase, where participants were presented with a list of forty unrelated word pairs (5 s per trial), an initial retrieval phase, where they had to remember the second word when prompted by the first one (once with, and once without feedback), and a final retrieval phase conducted 1-5 days later, during which they received no feedback. Lexical stimuli were selected from the University of South Florida free association database, which counts 72,000 curated word pairs (Nelson et al., 2004). Other episodic paradigms have employed symbolic stimuli to examine, among other things, sex- and age-related changes in brain dynamics (Ankudowich et al., 2016; Ankudowich et al., 2017; Subramaniapillai et al., 2022; Subramaniapillai et al., 2019). In these studies, participants performed a difficulty-modulated (*i.e.*, easy *vs.* hard) episodic task consisting of separate runs for encoding and retrieval while being scanned in the MRI machine. At the start of each encoding trial, they were prompted to memorize

either the spatial location of black-and-white faces on the screen (*i.e.*, spatial context) or the order in which they were presented (*i.e.*, temporal context). In the easy condition, six faces were serially displayed either to the left or right of a central fixation cross. In the hard condition, twelve faces were shown instead of six. Between encoding and retrieval phases, a distractor task was administered to prevent participants from mentally rehearsing the stimuli. Then, at the onset of each retrieval trial, participants were cued as to the nature of the task (*i.e.*, spatial context *vs.* temporal context). For the spatial context, participants were prompted with two faces and asked to identify the one that was originally presented on the left/right of the monitor during encoding. For the temporal context, they were instead asked to select the face that was seen most/least recently. In the easy condition, three pairs of faces were shown, and in the hard condition, six. Other assessment protocols that arguably afford more ecological validity implement movie viewing as a paradigm for tapping into episodic memory. For example, in a recent study (Liu et al., 2022), the authors investigated patterns of activation and connectivity between the hippocampus and medial prefrontal cortex that underlie memory formation. Here, participants watched a 50-min long movie inside the MRI scanner. Based on transitions in the storyline, the movie was split into 50 events. After viewing, participants produced their own detailed accounts of the story without any cue. These subjective responses were also split into unique events and matched with the reference movie segments. Events that were mentioned were classified as "remembered" and those that were omitted were labeled as "forgotten". Furthermore, events that were recalled in the correct sequential order were designated as "in-order" while those that were remembered in an incorrect succession were categorized as "out-of-order". In this manner, the researchers were able to examine similarities and differences in brain dynamics across well-defined episodic categories.

1.3 Temporal lobe epilepsy as a human model of memory impairment

In what has been described as arguably the single most important case study in the history of neuroscience (Squire, 2009), Brenda Milner discussed the cognitive sequelae that befell Henry Molaison following bilateral MTL resection that included removal of the hippocampal formation and a significant portion of the amygdaloid complex and entorhinal cortex (Neylan, 2000). This radical procedure was carried out by William Scoville to treat Molaison's pharmaco-resistant epilepsy, which presented itself as frequent bouts of incapacitating generalized seizures. In a widely cited report (Scoville & Milner, 1957), the authors stated that while surgical intervention had significantly alleviated Molaison's pre-surgical symptoms, his episodic and spatial memory had become so impaired that he could neither recognize the hospital staff nor find his way to the bathroom. These observations were effectively the first to implicate the structures of the MTL, including the hippocampus, in sustaining different forms of relational memory. Ever since, patients diagnosed with pharmacoresistant temporal lobe epilepsy (TLE), who present with sclerotic lesions of the hippocampus, have become a classic model of mnemonic dysfunction in humans, with ongoing work that spans over sixty years of published work in the scientific literature (Barrett Jones et al., 2022; Breier et al., 1996; Helmstaedter et al., 1995; Li et al., 2021; Mayeux et al., 1980; Penfield & Milner, 1958; Rugg et al., 1991; Scoville & Milner, 1957; Sideman et al., 2018; Voets et al., 2009; Yoo et al., 2006; Zanao et al., 2023).

Epilepsy, in general, is one of the oldest recorded disorders in human history, with the first known case dating back to a 4,000-year-old Mesopotamian account in which it was defined as the "hand of sin" (Magiorkinis et al., 2010). It is among the most prevalent chronic neurologic conditions, with an estimated 30%-40% of patients who do not respond to conventional pharmacological

treatment, a majority of whom are specifically diagnosed with TLE (Engel Jr, 2001; Tavakol et al., 2019). The International League Against Epilepsy (ILAE) outlines two primary forms of TLE: (*i*) medial/mesial TLE (mTLE), which presents with morphological anomalies relating to the hippocampus, parahippocampus, and amygdala; (*ii*) lateral TLE (lTLE), a less common form, which affects the temporal neocortex (Allone et al., 2017). TLE-associated seizures are generally categorized into three forms: (1) simple partial seizures (SPS) or "auras", presenting with minimal perturbations to consciousness, (2) complex partial seizures (CPS), where disturbances to attention are more noticeable, and (3) generalized tonic-clonic seizures or "grand mal", which are associated with greatly impaired awareness and even complete loss of consciousness (Allone et al., 2017). Other forms of extratemporal epilepsies (ETEs) relate to cortical malformations that occur during neural development, such as focal cortical dysplasia (FCD), which, along with mTLE, account for 60%-80% of pre-op patients in tertiary epileptic care (Tavakol et al., 2019). Contemporary experimental platforms have increasingly integrated high resolution multimodal neuroimaging data with macroscale connectomics, thus enabling to bridge the gap between focal and large-scale network anomalies in pharmacoresistant epilepsies (Tavakol et al., 2019). For example, modern studies have shown that the severity of local hippocampal pathology is inversely correlated with measures of structural and functional connectivity of the hippocampus with the default mode network (DMN), with marked sclerotic lesions being associated with lower hippocampal-DMN connectivity, which is a strong biomarker of impaired memory (Bell et al., 2011; Bernhardt et al., 2016; Bernhardt et al., 2019).

Given that TLE patients represent a well-established model of memory impairment in humans, it is no wonder that they have been so thoroughly studied in the context of relational memory using

the previously described neuroimaging and behavioral platforms. Even so, since each cognitive task comes with its own unique set of advantages and limitations, a complete understanding of relational cognition can only be achieved when findings from across a wide range of paradigms are integrated. This endeavour, noble as it is, presents important obstacles for the scientific community, given the large degrees of freedom involved in consolidating results across different experimental designs, which include heterogenous population demographics, incompatible outcome measures, and variable task modalities. Therefore, it stands to reason that an experimental platform that inherently controls for some of these factors can significantly streamline investigations of human relational memory.

Here, we present the integrated Relational Evaluation Paradigm (iREP), a standardized, multidomain, and difficulty-modulated framework specially designed for the MRI environment, which consists of a task battery that taps into the different types of relational processing (*i.e.*, episodic, semantic, and spatial). In Project I (Tavakol et al., 2021), we administered the iREP to a cohort of healthy individuals while they were being scanned, and uncovered integrated structure-function correlates of spatial memory in medial and lateral temporal areas. In Project II (Tavakol et al., 2022), we compared the iREP-derived behavioral phenotypes of a group of TLE patients to those of age- and sex-matched healthy controls, and discovered a graded pattern of TLE-associated cognitive deficits, with episodic memory being most affected, followed by spatial, while semantic memory showed mixed results. Finally in Project III, we extracted task-based functional connectivity patterns for each module of the iREP within the same two groups, and found strong latent associations between demographics/behavioral variables and functional connectome profiles. In addition to establishing the iREP as a valid framework for examining multiple layers

of relational memory within the same individuals across different populations, our studies further speak to both unique as well as shared anatomical, behavioral, and functional markers underlying different relational cognitive domains and neurological diagnostic groups.

In the next section (Project I), first we address the construct validity of the spatial module of the iREP, which we label as the *conformational shift spatial task* (CSST). The CSST represents the true novelty of the iREP as the episodic and semantic modules are pictorial versions of previously established word-based assessment protocols. Here, we evaluate the behavioral association of the CSST with these other iREP modules as well as two additional control tests, namely, the *four mountains task* (FMT), which examines allocentric spatial memory, and the *mnemonic similarity task* (MST), which taps into pattern separation, the capacity to differentiate similar cognitive representations. We then investigate the correspondence between MRI-derived metrics of cortical morphology and CSST performance scores. Furthermore, we acquire meta-analytical whole-brain co-activation maps relevant to spatial processing to functionally constrain additional correlational analyses between behavior and structure. Finally, we conduct exploratory seed-based resting-state connectivity analyses centered on previously defined clusters of finding and evaluate whether their intrinsic whole-brain integration profiles are modulated by CSST accuracies. Overall, we determine that the CSST is construct-valid, showing specificity to spatial processes that overlap with semantic judgment. We also ascertain the presence of integrated structure-function clusters within medial and lateral temporal lobes that underlie interindividual differences in spatial memory capacity, with functionally-relevant cortical regions showing additional brain-behavior associations.

2 PROJECT I: structure-function substrates of spatial memory

This section has been published in Cerebral Cortex.

A Structure–Function Substrate of Memory for Spatial Configurations in Medial and Lateral Temporal Cortices

Shahin Tavakol[1], Qiongling Li[1], Jessica Royer[1], Reinder Vos de Wael[1], Sara Larivière[1], Alex Lowe[1], Casey Paquola[1], Elizabeth Jefferies[2], Tom Hartley[2], Andrea Bernasconi[1], Neda Bernasconi[1], Jonathan Smallwood[2], Veronique Bohbot[3], Lorenzo Caciagli[4,5,†] and Boris Bernhardt[1,†]

[1]McConnell Brain Imaging Centre, Montreal Neurological Institute and Hospital, McGill University, Montreal, Quebec H3A 2B4, Canada, [2]University of York, York YO10 5DD, UK, [3]Douglas Mental Health University Institute, McGill University, Montreal, Quebec H4H 1R3, Canada, [4]Department of Clinical and Experimental Epilepsy, UCL Queen Square Institute of Neurology, WC1N 3BG London, United Kingdom and [5]Department of Bioengineering, University of Pennsylvania, Philadelphia, PA 19104, USA

Address correspondence to Boris Bernhardt, PhD, Multimodal Imaging and Connectome Analysis Lab, McConnell Brain Imaging Centre, Montreal Neurological Institute and Hospital, McGill University, Montreal, Quebec, Canada. Email: boris.bernhardt@mcgill.ca.

†Lorenzo Caciagli and Boris Bernhardt are joint co-authors.

2.1 ABSTRACT

Prior research has shown a role of the medial temporal lobe, particularly the hippocampal–parahippocampal complex, in spatial cognition. Here, we developed a new paradigm, the conformational shift spatial task (CSST), which examines the ability to encode and retrieve spatial relations between unrelated items. This task is short, uses symbolic cues, incorporates two difficulty levels, and can be administered inside the scanner. A cohort of 48 healthy young adults underwent the CSST, together with a set of behavioral measures and multimodal magnetic resonance imaging (MRI). Inter-individual differences in CSST performance correlated with scores on an established spatial memory paradigm, but neither with episodic memory nor mnemonic discrimination, supporting specificity. Analyzing high-resolution structural MRI data, individuals with better spatial memory showed thicker medial and lateral temporal cortices. Functional relevance of these findings was supported by task-based functional MRI analysis in the same participants and ad hoc meta-analysis. Exploratory resting-state functional MRI analyses centered on clusters of morphological effects revealed additional modulation of intrinsic network integration, particularly between lateral and medial temporal structures. Our work presents a novel spatial memory paradigm and supports an integrated structure–function substrate in the human temporal lobe. Task paradigms are programmed in python and made open access.

Key words: spatial memory, neuroimaging, task fMRI, medial temporal lobe

2.2 INTRODUCTION

Spatial memory is characterized by the encoding and retrieval of spatial associations. In rodents, structures of the medial temporal lobe (MTL) have long been recognized as crucial neural substrates of spatial memory (Aggleton et al., 1986; Hafting et al., 2005; Morris et al., 1982; O'Keefe & Dostrovsky, 1971; O'Keefe & Nadel, 1978; Winocur, 1982). In humans, early studies in patients with temporal lobe epilepsy revealed a direct correlation between the severity of MTL lesions and deficits in spatial cognition (Milner, 1965; Rains & Milner, 1994; Smith & Milner, 1981, 1989). Ensuing neuroimaging and lesion experiments in neurological patients reinforced the significance of the MTL as a critical brain structure in spatial memory processing, but also pointed to an involvement of other brain regions and the broader conceptualization of spatial memory as a network phenomenon (Aguirre et al., 1996; Ghaem et al., 1997; Maguire et al., 1998). The role of the MTL as a spatial processing hub was further supported by the discovery of human place cells and grid cells, specialized neurons believed to instantiate a scalable and navigable mental representation of space (Ekstrom et al., 2003; Jacobs et al., 2013).

The structural organization of spatial memory relies on the interplay between brain morphology and relevant cognitive phenotypes. For instance, the association between the volume of the MTL and behavioral measures of spatial cognition has been reported since the earliest structural magnetic resonance imaging (sMRI) studies (Abrahams et al., 1999; Hartley & Harlow, 2012; Maguire et al., 2000). Today, state-of-the-art automated segmentation tools can generate surface-wide representations of the brain, sampling morphological markers such as neocortical thickness and volume of hippocampal subregions with unprecedented resolution (Bernhardt et al., 2016; Caldairou et al., 2016; Fischl, 2012; Goubran et al., 2020; Kim et al., 2014; Kim et al., 2005; Romero et al., 2017; Wang et al., 2012). These millimetric anatomical indices are ideal for

investigating the link between morphological and behavioral variability across individuals. Complementing sMRI studies, a large body of research has focused on the analysis of functional MRI (fMRI) acquisitions. Task-based fMRI studies have shown consistent MTL involvement during spatial memory tasks, together with activations in neocortical areas (Aguirre & D'Esposito, 1997; Hassabis et al., 2009; Jokeit et al., 2001; Schindler & Bartels, 2013). Complementing these paradigms, resting-state fMRI (rs-fMRI) enables to interrogate intrinsic functional networks (Biswal et al., 1997; Buckner et al., 2013; Cordes et al., 2000; Fox et al., 2006; Lowe et al., 2000; Smith et al., 2009). An increasing body of rs-fMRI studies has also assessed intrinsic functional network substrates underlying interindividual differences in cognitive capacities (He et al., 2020; Medea et al., 2018; Smith et al., 2015; Sormaz et al., 2017).

The current study devised a new and open-access paradigm to assess spatial memory in humans and to elucidate the functional anatomy of spatial memory processing via structural and functional MRI analyses. We developed the conformational shift spatial task (CSST), a short, easy-to-use assessment that taps into the capacity to encode and retrieve spatial interdependencies between three conceptually unrelated objects. We administered the CSST to 48 healthy individuals inside a 3 T Siemens Magnetom Prisma scanner as part of a broader task-based fMRI battery, which included additional testing probes for semantic memory, episodic memory, and mnemonic discrimination. Together with the semantic and episodic memory tasks, the CSST constitutes an integral part of a relational memory fMRI battery that can address structural and functional convergence and divergence across relational mnemonic domains. All three tests were homogenized by (*i*) implementing comparable visual stimuli, (*ii*) incorporating task difficulty modulation across two conditions (*i.e.*, 28 easy trials and 28 difficult trials), (*iii*) using a three-alternative forced choice trial-by-trial paradigm. Given that these tasks are designed to probe

different domains of relational memory, we hypothesized that behavioral scores on the CSST would correlate with performances on the semantic and episodic association tasks, with greater association observed between spatial and semantic domains (Bellmund et al., 2018; Constantinescu et al., 2016; McNaughton et al., 2006; Mok & Love, 2019; Moscovitch et al., 2005; Nadel & Moscovitch, 1997). We also evaluated participants with supplementary assessment tools outside the scanner, including the four mountains task (FMT), an established spatial memory paradigm that uses scenes rather than symbolic stimuli, and which does not have varying difficulty levels (Hartley et al., 2007). We further hypothesized that CSST performance would show strongest correlations with performance on the FMT, as both tasks are devised to assess the same relational domain, that is, spatial processing. In addition to its task-based section, our protocol encompassed structural MRI as well as rs-fMRI acquisitions. We used these to assess associations between spatial memory scores and variations in MRI-derived morphological measures of cortical thickness and hippocampal volume across participants. Although surface-based analyses were regionally unconstrained, based on prior literature in humans and animals studying spatial memory (Abrahams et al., 1999; Aguirre & D'Esposito, 1997; Hafting et al., 2005; Hartley & Harlow, 2012; Hassabis et al., 2009; Jokeit et al., 2001; Maguire et al., 2000; Morris et al., 1982; O'Keefe & Nadel, 1978; Rains & Milner, 1994; Schindler & Bartels, 2013; Smith & Milner, 1989), we expected to observe structure–function substrates in the medial temporal lobe regions, such as the parahippocampal gyrus. Results were contextualized against task-based fMRI findings in the same participants and ad hoc meta-analytical inference. Structural imaging observations were further used for post hoc explorations of rs-fMRI connectivity modulations by interindividual differences in task performance.

2.3 METHODS

Participants

A total of 48 healthy adults (16 women, mean age ± SD = 29.71 ± 6.55 years, range: 19 to 44 years, four left-handed), recruited in 2018 and 2019, participated in our study and had normal or corrected-to-normal vision. Control participants did not have any neurological or psychiatric diagnosis. Our study was approved by the Research Ethics Committee of the McGill University and participants gave written and informed consent upon arrival at the Montreal Neurological Institute.

Conformational Shift Spatial Task

In the CSST, the participant discriminated the spatial arrangement of three semantically unrelated items (*i.e.*, a brick, a tire, a bucket) from two additional foil configurations of the same items (Fig. 1a). At each trial, following a jittered inter-trial interval (1.5–2.5 s), the participant encoded the salient features of an original trio arrangement for a duration of 4 s. Following a jittered inter-stimulus interval (0.5–1.5 s), three distinct versions of the trio were displayed. All three conformations had undergone an equal rotation about the trio center of mass between 45° clockwise to 45° counterclockwise. The correct conformation had not undergone any additional transformation unlike the other two foils.

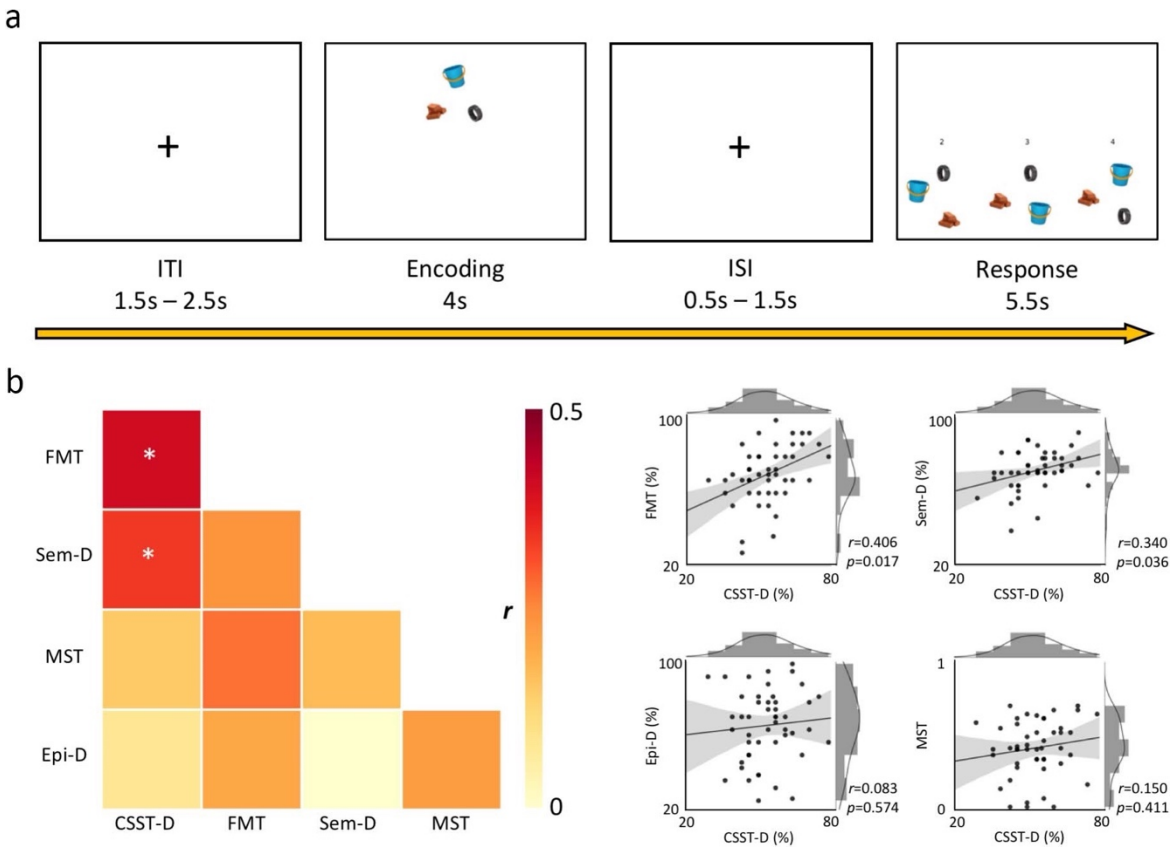

Figure 1. Task design and behavioral associations. (a) Following a jittered inter-trial interval (ITI), the participant had to encode the spatial configuration of the stimulus trio for 4 s. After a jittered inter-stimulus interval (ISI), the participant had 5.5 s to choose the original spatial conformation among two foil options. (b) left panel: correlation heat map of performance across all tasks. CSST-D shows significant associations with FMT and Sem-D following adjustment for false discovery rate (∗pFDR < 0.05). Right panel: joint-plot of CSST-D associations with other tasks (CSST-D: conformational shift spatial task-difficult, FMT: four mountains task, Sem-D: semantic task-difficult, MST: mnemonic similarity/discrimination task, Epi-D: episodic difficult).

In the "difficult" condition (*i.e.*, CSST-D), the two distractor layouts had been subjected to "one" specific additional transformation each: the spacing between the three items had changed with respect to the original configuration. In the "easy" condition (*i.e.*, CSST-E), the foil configurations had undergone "two" specific additional transformations each: (1) the spacing between the three items had changed with respect to the original configuration; (2) the relative positions of trio items had been swapped. The participant was allowed up to 5.5 s to select the correct response. Thus, distractors in "difficult" trials varied from the original configuration by 2 degrees of separation (*i.e.*, rotation about the center of mass and spacing alteration), whereas distractors in "easy" trials

comprised 3 degrees (*i.e.*, rotation about the center of mass, spacing alteration, and item positional swap).

The entire task was composed of 56 pseudo-randomized trials (*i.e.*, 28 easy, 28 difficult). The semantic inter-relatedness of the trio items was computed via the UMBC Phrase Similarity Service (Han et al., 2013). Based on the frequency with which two nouns representing the presented visual symbols co-occur within the Refined Stanford WebBase Corpus, which contains 100 million web pages from over 50 000 websites, this algorithm computed a conceptual relatedness index. We implemented prototypical visual stimuli as proxies for selected lexical entries whose similarity indices were inferior to 0.3 (range: 0–1).

Additional Cognitive Tasks

Four Mountains Task (Hartley et al., 2007). The FMT is an established spatial cognition paradigm. In this version, 15 trials were administered in total. At each trial, the participant had 10 s to encode the spatially relevant stimuli within a computer-rendered landscape composed of four distinct mountains varying in shape and size. After the encoding phase, participants had to select the correct landscape in a four- alternative-forced-choice paradigm. The correct answer corresponded to the originally encoded landscape albeit depicted from a different first-person perspective, whereas the three incorrect options showed renderings of four mountains with different characteristics and configurations. All choices were additionally modified along lighting, weather, and vegetation texture to control for visual matching strategies. There was no time limit, but participants were instructed to respond as quickly and as accurately as possible. Following each trial, participants had to report how certain they were about their response (*i.e.*, certain or uncertain).

Semantic Task. We used a symbolic variant of a previously used lexicon-based semantic association paradigm (Sormaz et al., 2017; Wang et al., 2018). Consisting of 56 pseudo-randomized trials, the task implements a three-alternative-forced-choice paradigm and is modulated for difficulty across conditions with equal number of trials (*i.e.*, 28 difficult: Sem-D; 28 Easy: Sem-E). At each trial, a target object appeared at the top of the monitor (*i.e.*, apple) with three objects below (*i.e.*, desk, banana, kettle). Participants had to select the bottom item that was conceptually the most similar to the target. The semantic relatedness of items was measured via the UMBC similarity index (see above description regarding CSST). In difficult trials, the correct response and the target shared an index greater or equal to 0.7, whereas the foils shared a similarity index between 0.3 and strictly smaller than 0.7 with the target. In easy trials, the indices were greater than or equal to 0.7 between correct response and target, and 0 to strictly smaller than 0.3 between any given foil and target.

Episodic Task. We used a symbolic variant of a previously used lexicon-based paradigm (Payne et al., 2012; Sormaz et al., 2017) that involves two phases. In the encoding phase, participants had to memorize pairs of images shown simultaneously. Each pair was corrected for conceptual relatedness using the UMBC similarity algorithm (see above) with an index smaller than 0.3. The encoding phase was modulated for difficulty across conditions: some trials were shown only once throughout the session, whereas others were displayed twice to ensure more stable encoding. Following a 10 min delay, the retrieval phase was administered. At each trial, participants had to identify the object that was originally paired with the target object from the encoding phase in a three-alternative-forced-choice paradigm, similar to the one described in the semantic task. There were 56 pseudo-randomized trials in total with 28 corresponding to pairs of images encoded only once (*i.e.*, Epi-D) and 28 to pairs of images encoded twice (*i.e.*, Epi-E).

Mnemonic Similarity (Discrimination) Task (Stark et al., 2013). The MST assessed the capacity to discriminate between stimuli with overlapping features. It comprised two phases: encoding and recall, administered ~8 min apart. The encoding phase consisted of 64 trials in which the participant had to choose whether the displayed item belonged "indoors" or "outdoors." The recall phase was based on a three-alternative-forced-choice paradigm. At this stage, the participant had to select whether the presented item was an exact duplicate from the encoding phase (*i.e.*, "old"), an inaccurate duplicate (*i.e.*, "similar"), or an altogether novel stimulus (*i.e.*, "new"). This phase consisted of 32 trials per condition for a total of 96 trials.

MRI Acquisition

MRI data were acquired on a 3 T Siemens Magnetom Prisma-Fit with a 64-channel head coil. Two T1-weighted (T1w) scans with identical parameters were acquired with a 3D-MPRAGE sequence (0.8 mm isotropic voxels, matrix = 320 × 320, 224 sagittal slices, TR = 2300 ms, TE = 3.14 ms, TI = 900 ms, flip angle = 9°, iPAT = 2). Task and resting-state fMRI time series were acquired using a 2D echo planar imaging sequence (3.0 mm isotropic voxels, matrix = 80 × 80, 48 slices oriented to AC-PC-30 degrees, TR = 600 ms, TE = 30 ms, flip angle = 50°, multiband factor = 6). The CSST task was approximately 15 min long and presented via a back-projection system to the participants. During the 7 min- long rs-fMRI scan, participants were instructed to fixate a cross displayed in the center of the screen and to clear their mind.

Structural MRI Processing

Generation of Neocortical Surfaces. To generate models of the cortical surface and to measure cortical thickness, native T1w images were processed using FreeSurfer 6.0 (http://surfer.nmr.mgh.harvard.edu). Previous work has cross-validated FreeSurfer with

histological analysis (Cardinale et al., 2014; Rosas et al., 2002) and manual measurements (Kuperberg et al., 2003). Processing steps have been described in detail elsewhere (Dale et al., 1999; Fischl et al., 1999). In short, the pipeline includes brain extraction, tissue segmentation, pial and white matter surface generation, and registration of individual cortical surfaces to the fsaverage template. This aligns cortical thickness measurement locations among participants, while minimizing geometric distortions. Cortical thickness was calculated as the closest distance from the gray/white matter boundary to the gray matter/cerebrospinal fluid boundary at each vertex. Thickness data underwent spatial smoothing using a surface-based diffusion kernel (FWHM = 10 mm). As in prior work (Valk et al., 2016), data underwent manual quality control and potential correction for segmentation inaccuracies.

Functional MRI Processing

(a) Task-based fMRI data were preprocessed using SPM12 (https://www.fil.ion.ucl.ac.uk/spm/). Steps included image realignment, distortion correction using AP-PA blip pairs, structural and functional co-registration, as well as functional data normalization and spatial smoothing (FWHM = 6 mm). Of the originally acquired fMRI scans, data for four participants were omitted due to artifacts caused by field inhomogeneity. For the remaining participants (n=44), first-level mass-univariate analyses were performed by modeling all task regressors into the SPM design matrix, which included trial onsets and durations/reaction times for ITIs, encoding phases, ISIs, retrieval phases, and post-retrieval rest periods, in addition to six standard motion parameters as well as a constant term. Regressors were convolved with the built-in SPM canonical hemodynamic response function without temporal nor dispersion derivatives. Following mass-univariate model estimations, first-level contrast maps from weighted comparisons between retrieval and encoding (*i.e.*, when the participant chooses a specific stimulus configuration vs. when the participant is

passively encoding the original stimulus conformation) were used to generate a single group-level activation map, which was thresholded (pFWE = 0.05) and mapped onto fsaverage template using FreeSurfer.

(b) The rs-fMRI scans were preprocessed using a combination of FSL, available at https://fsl.fmrib.ox.ac.uk/fsl/fslwiki (Jenkinson et al., 2012), and AFNI, available at https://afni.nimh. nih.gov/afni (Cox, 1996), and included removal of the first five volumes from each time series to ensure magnetization equilibrium, distortion correction based on AP-PA blip pairs, reorientation, motion correction, skull stripping, grand mean scaling, and detrending. Prior to connectivity analysis, time series were statistically corrected for effects of head motion, white matter signal, and CSF signal. They were also band-pass filtered to be within 0.01 to 0.1 Hz. All participants had overall low head motion and mean frame-wise displace. Following rs-fMRI preprocessing in native space, a boundary-based registration technique (Greve & Fischl, 2009) mapped the functional time series to each participant's structural scan and subsequently, to the neocortical and hippocampal surface models. Surface-based fMRI data also underwent spatial smoothing (FWHM = 10 mm).

Statistical Analysis

Analyses were performed using SurfStat for Matlab (MathWorks, R2019b) available at http://math.mcgill.ca/keith/surfstat (Worsley et al., 2009).

(A) Behavioral Task Correlation

To assess the sensitivity and specificity of the newly developed protocol for spatial cognition, we cross-correlated the CSST-D with the FMT, Sem-D, Epi-D, and MST. Given that all participants

were high functioning healthy individuals, we only incorporated performance scores on the difficult conditions where applicable, which additionally precluded ceiling effects.

(B) Cortical Thickness Analysis

Surface-wide linear models evaluated associations between task scores and cortical thickness:

$$T_i = \beta_0 + \beta_1 * Age + \beta_2 * Sex + \beta_3 * Score + \varepsilon$$

where T_i is the thickness measure at vertex i for a total of 327,684 vertices. "Age," "Sex," and "Score" are model terms, β_0, β_1, β_2, and β_3, the estimated model parameters, and ε is the error coefficient.

We then regressed out the effects of Age and Sex from cortical thickness measures:

$$T_i = \beta_0 + \beta_1 * Age + \beta_2 * Sex + \varepsilon$$
$$rT_i = T_i - (\beta_0 + \beta 1 * Age + \beta_2 * Sex)$$

where rT_i is the residual thickness measure at vertex i, corrected for "Age" and "Sex." To assess whether the brain-behavioral correlations were generalizable to another spatial task, we correlated residual thickness from clusters of findings with FMT scores obtained outside the scanner.

(C) Hippocampal Analysis

A multi-template surface-patch algorithm was implemented to segment the hippocampus into its subfields (Bernhardt et al., 2016; Caldairou et al., 2016; Kim et al., 2014; Styner et al., 2006). The product of voxel volume and number of inclusive voxels was computed for each subfield. Next, total hippocampal volume was measured as the sum of all subregional volumes. Volume-based models were then used to assess effects of task scores on the whole hippocampus:

$$V = \beta_0 + \beta_1 * Age + \beta_2 * Sex + \beta_3 * Score + \varepsilon$$

where V is the total volume of the hippocampus. A similar model was run for vertex-wise hippocampal columnar data derived from subfield surface mapping (see Supplementary Methods).

(D) Functional Contextualization

Task-based second-level functional activation maps were obtained from 44 participants and thresholded ($pFWE$ =0.05) before being mapped to fsaverage. Average residual (*i.e.*, age- and sex-corrected) cortical thickness across all vertices within regions of activation was then correlated with task scores. Furthermore, Neurosynth-based meta-analysis was used to perform a search for the term "navigation," which resulted in 77 studies with a total of 3,908 activations. The generated association map was thresholded ($pFDR$ = 0.01) and mapped onto fsaverage. Once more, average residual thickness was computed and correlated with task results.

(E) Resting-State Connectivity Analysis

Surface-wide linear models assessed the modulatory effect of task performance on rs-fMRI connectivity between clusters of structural imaging findings (see B) and resting-state data:

$$Z_i = \beta_0 + \beta_1 * \text{Age} + \beta_2 * \text{Sex} + \beta_3 * \text{Score} + \varepsilon$$

where Z_i is the Fisher Z-transformed correlation coefficient between mean resting-state intensity for a given cluster in (B) and whole brain data at vertex i.

We performed a similar analysis to (j) to evaluate the effect of task score on functional connectivity between clusters in (B) and resting-state data mapped on the hippocampal template.

(F) Correction for Multiple Comparisons

We used random field theory for non-isotropic images to correct for multiple comparisons ($pFWE$ = 0.05). Main structural MRI findings were based on a stringent cluster-defining threshold of P =

0.001. For more exploratory rs-fMRI connectivity analyses, we used a more liberal cluster-defining threshold of P = 0.025.

2.4 RESULTS

Behavioral Findings

We examined the association between the newly-developed CSST and other tasks from our experimental protocol (Fig. 1b, Supplemental Table 1). We excluded scores obtained on easy conditions across all difficulty-modulated tasks to prevent ceiling effects, as our cohort composed of high functioning healthy adults (18.13 ± 4.26 years of education; 47 currently employed/studying). Our participants indeed performed close to ceiling for the easy condition (CSST-E), but not the difficult condition (CSST-D) ($t = 16.8$, $P < 0.001$; Supplemental Fig. 1). Furthermore, no sex differences were observed in CSST-D scores (Supplemental Fig. 2). To ensure that the CSST is sensitive to spatial processing, we first cross-referenced it against the well-established FMT paradigm that was administered outside the scanner (Hartley et al., 2007). FMT scores correlated strongly with performances in both the CSST-E ($r = 0.419$, $P = 0.003$; Supplemental Fig. 3) and the CSST-D ($r = 0.406$, $P = 0.004$; Supplemental Fig. 3). Intra-CSST association was also significant ($r = 0.386$; $P = 0.007$; Supplemental Fig. 3). CSST-D and FMT correlations were reproduced when analyzing women and men separately (Supplemental Fig. 4).

Several analyses supported specificity of CSST-D to spatial processing while also noting overlap with relational memory more generally (Fig.1b). Specifically, CSST-D correlated with Sem-D ($r = 0.340$; $P = 0.018$) while showing neither an association with MST ($r = 0.150$; $P = 0.308$) nor with Epi-D ($r = 0.083$; $P = 0.574$). CSST-D also correlated with Sem-E ($r = 0.301$; $P = 0.038$), but

not with Epi-E (r = 0.205, P = 0.161; Supplemental Fig. 3). As expected, CSST-D showed no meaningful associations with MST, Epi-D, and Epi-E when analyzing women and men separately, but only in men did CSST-D significantly correlate with Sem-D (Supplemental Fig. 4).

Structural Substrates of Spatial Memory Performance in Neocortical Regions

Controlling for age and sex, we observed positive correlations between CSST-D scores and thickness of bilateral superior temporal, left temporo-polar, bilateral parahippocampal, and left posterior cingulate cortices (Fig. 2a, see Supplemental Fig. 5 for right-handed participants only). Following correction for multiple comparisons ($pFWE < 0.05$), findings were significant in the left superior temporal sulcus (r = 0.597), left anteromedial superior temporal gyrus (r = 0.609), right posterior parahippocampal gyrus (r = 0.610), and the left inferior temporo-occipital junction (r = 0.591; Fig. 2b). CSST-D associations were consistent across clusters when separately analyzing both biological sexes (r- values women/men; cluster 1: 0.59/0.62; cluster 2: 0.41/0.72; cluster 3: 0.66/0.62; cluster 4: 0.62/0.63; Supplemental Fig. 6). Notably, average thickness of these four clusters also positively correlated with performance on the FMT (r = 0.353; P = 0.014; Fig. 2c) and Sem-D (r = 0.373; P = 0.009; Fig. 2c). Cluster-wise associations ranged between r = 0.233–0.326 for FMT, and between r = 0.217– 0.369 for Sem-D (Supplemental Fig. 7). Although surface-based associations between thickness and FMT were not significant after multiple comparisons correction, effect size maps were significantly similar to those from the correlation between thickness and CSST-D after correction for age and sex (r = 0.472, non-parametric P < 0.001: (Alexander-Bloch et al., 2018), Supplemental Fig. 8). Cortical thickness did not correlate with scores in other tasks for the same significance criteria, indicating specificity of the observed brain-behavior correlations. These findings implicate local regions within the left temporal lobe as well

as the right MTL as cortical substrates underlying interindividual differences in aptitude on the CSST-D.

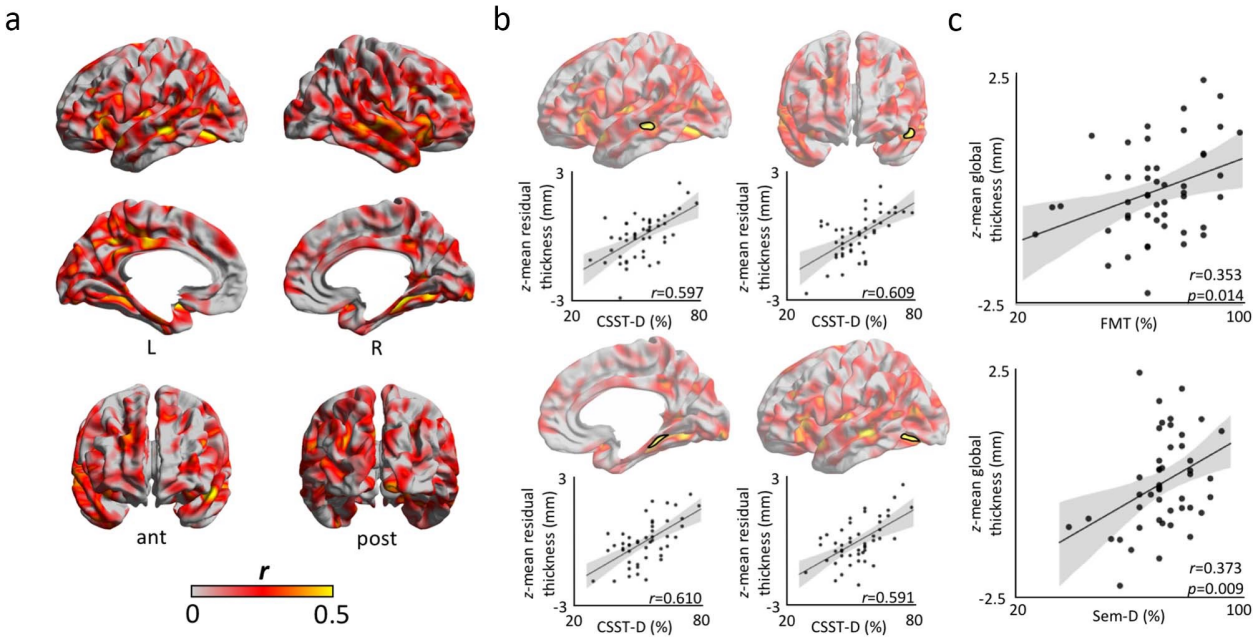

Figure 2. Cortical substrates of the CSST. (a) Product–moment correlation coefficients of CSST-D performance on cortical thickness after regressing out age and sex. (b) Findings corrected for multiple comparisons (pFWE <0.05; cluster-defining threshold of CDT=0.001) highlight clusters in the left superior temporal sulcus, left anteromedial superior temporal gyrus, right posterior parahippocampal gyrus, and left inferior temporo-occipital junction. (c) Correcting for age and sex, average cortical thickness across clusters of finding showed robust correlations with performance on FMT (r = 0.353; P = 0.014) and Sem-D (r = 0.373; P = 0.009).

Structural Substrates of Spatial Memory Performance in Hippocampal Subregions

Controlling for effects of age and sex, we observed a trend between CSST-D scores and total hippocampal volume (r = 0.234, one-tailed P = 0.052). While no surface-wide association passed stringent criteria for multiple comparisons corrections (*i.e.*, pFWE < 0.05; CDT = 0.001), we observed uncorrected associations between CSST-D and hippocampal columnar volumes along the long axis of each subfield (Supplemental Fig. 9).

Functional Contextualization

We contextualized the structural imaging findings with respect to areas relevant for spatial cognition, using task-based fMRI activation maps obtained from the same participants and Neurosynth-based meta-analysis. We contrasted estimated parameters for retrieval and encoding within each participant to control for visual processes common to both phases for the same trial. This subtraction contrast also allowed us to separate the cognitive processes believed to be implicated in CSST performance. Specifically, we expected the retrieval phase to require both successful encoding and successful delayed matching of the given spatial configuration. Thus, contrasting both trial phases can capture neural mechanisms specific to topographical memory recall. We pooled data across CSST-E and CSST-D trials (Supplemental Table 2) as one-tailed t-tests failed to ascertain significant group-level activation differences between conditions. We then mapped the volumetric second-level activations (Supplemental Fig. 10, Supplemental Table 3) to fsaverage and computed average cortical thickness in highlighted regions, which showed no correlation with CSST- D scores ($r = 0.189$, one-tailed $P = 0.110$; Fig. 3a, Supplemental Fig. 11a). An additional ad hoc meta-analysis was also performed (Fig. 3b, Supplemental Fig. 11b); here, the Neurosynth-derived map was similarly mapped to fsaverage and average cortical thickness in activated areas was computed. We observed a significant association between CSST-D behavioral performance and average thickness across Neurosynth-derived regions ($r = 0.319$, one-tailed $P = 0.014$).

Modulatory Effect of Task Performance on Functional Connectivity Profile

We conducted exploratory seed-based connectivity analyses centered on clusters of findings from the structural analyses (*i.e.*, left superior temporal sulcus, left anteromedial superior temporal gyrus, right posterior parahippocampal gyrus, and the left inferior temporo-occipital junction) (Fig.

4). Accounting for age and sex, we observed a marginal association between CSST-D score and the connectivity strength of the right parahippocampal cluster (seed 3; Fig. 4a) and a region encompassed by the left middle frontal and precentral gyri extending medially via the paracentral lobule into the anterior cingulate ($p_{FWE} = 0.052$; outlined cortical surface on third row; Fig. 4b). Here, individuals with higher scores on CSST-D presented with higher functional connectivity between these nodes. We also found that CSST-D performance positively modulated connectivity between the left superior temporal sulcus (seed 1; Fig. 4a) and left CA1–3 ($p_{FWE} = 0.014$; outlined hippocampal surface on first row; Fig. 4b). A similar modulation was seen for the cluster in the left inferior temporo-occipital junction (seed 4; Fig. 4a), which showed connectivity modulation to right CA1–3 by CSST-D ($p_{FWE} = 0.036$; outlined hippocampal surface on fourth row; Fig. 4b).

2.5 DISCUSSION

Our goal was to design a novel cognitive task to evaluate the ability to encode and retrieve spatial relationships between unrelated objects in humans and to identify the neural substrates of such spatial processing via structural and functional connectivity analyses. To this end, we developed and administered the new CSST to 48 healthy young adults as part of a larger task-based fMRI battery and conducted structural and resting-state fMRI (rs-fMRI) analyses. In addition to the CSST, our battery also included a semantic association task and an episodic memory task that were developed in concert with the CSST to address questions pertaining to relational memory more generally. All three tasks were homogenized in terms of visual stimuli, task difficulty and duration, as well as in terms of response paradigm (*i.e.*, three-alternative forced choice). These tests were further optimized for administration outside as well as inside the scanner and are made openly available. An additional test for assessing mnemonic discrimination was also included. Behavioral

correlations with additional memory metrics supported relative sensitivity and specificity of the CSST to spatial memory, and some overlap with relational memory more generally. Studying in vivo measures of cortical morphology, we identified substrates underlying interindividual differences in CSST performance comprising a network of lateral and medial temporal lobe regions. Complementary explorations of rs-fMRI data indicated a stronger functional connectivity of these areas in individuals with higher scores on the CSST. Structural MRI findings could be functionally contextualized by showing overlaps to task-based fMRI activations from the CSST paradigm itself as well as ad hoc meta-analysis. In this work, we present a new paradigm that taps into spatial memory processing, and our multimodal MRI results offer new insights into integrated structure–function substrates of human spatial cognition.

The CSST is an openly accessible (https://github.com/MICA-MNI/micaopen) and convenient python-based protocol that can be administered inside or outside the scanner in less than 15 min. It implements symbolic stimuli in a three-alternative-forced-choice paradigm and consists of two experimental conditions modulated for difficulty (easy: CSST-E; difficult: CSST-D), which is suitable for the study of interindividual variations and between-group differences in the context of healthy and clinical cohorts. The CSST encompasses 56 pseudo-randomized trials (28 per condition) with four equivalent iterations, which can be leveraged to perform multiple probes while controlling for habituation. In addition to paradigm development, we assessed behavioral associations between CSST performance to measures obtained from tasks tapping into spatial, semantic, and episodic dimensions of memory. As this study analyzed high functioning healthy adults, we restricted the analyses to scores obtained on the difficult condition, CSST-D. The CSST-E scores, where our healthy individuals perform close to ceiling, may be more suitable for phenotyping individuals with deficits in spatial cognition, including older adults (Bohbot et al.,

2012; Perlmutter et al., 1981; Pezdek, 1983) and those with neurological disorders (Bird et al., 2010). In our cohort, CSST-D results correlated with FMT scores measured outside the scanner, suggesting that the task is sensitive to topographic memory. Interestingly, behavioral outcome on the CSST-D was neither correlated with scores on an episodic paired-associates task nor with performance on a mnemonic discrimination task. However, we did observe a correlation with a semantic decision-making task, and in a prior study we had also found that the spatial and semantic aspects of memory were associated via the organization of connectivity between the hippocampus and the lateral temporo-parietal cortex (Sormaz et al., 2017).

Following these behavioral explorations, we utilized the CSST to determine potential structural correlates of interindividual differences in spatial cognition. We examined whether interindividual differences in CSST-D scores correlated to MRI-derived neocortical thickness and hippocampal columnar volume measures. Accounting for variance explained by age and sex, we observed associations with the thickness of bilateral superior temporal, left temporo-polar, bilateral parahippocampal, and left posterior cingulate areas. Following multiple comparisons correction, findings clustered within left lateral temporal and right medial temporal lobe areas, notably the right posterior parahippocampus. As a primary relay between the allocortical subregions of the hippocampal formation and the isocortex, the parahippocampal cortex plays an essential role in different forms of spatial processing, including memory for scenes and configuration of objects (Abrahams et al., 1999; Aguirre et al., 1996; Bohbot et al., 2015; Bohbot et al., 2000; Bohbot et al., 1998; Epstein & Kanwisher, 1998). Increased gray matter volume of the entorhinal cortex has previously been associated with improved performance on games that rely on geometric relationships, such as Tetris and Minesweeper, as well as platform games, such as Super Mario 64 (Kühn & Gallinat, 2014). One study also found an increase in gray matter thickness of bilateral

parahippocampal cortex following 15 daily gaming sessions on a first-person shooter platform, with long-lasting changes in the left parahippocampal cortex (Momi et al., 2018). The authors argued that detailed environmental mapping of the virtual arena conferred a competitive advantage as evidenced by continued navigation during episodes of virtual blindness (*i.e.*, when hit by smoke or flashbang grenades). However, too great a reliance on the response strategy mediated by the caudate nucleus, which is the most favored spontaneous navigational behavior in first-person shooter paradigms, has instead been shown to shrink the hippocampus (West et al., 2018). Functional neuroimaging paradigms have further implicated the parahippocampal gyrus in object-location retrieval (Owen et al., 1996), local geometry encoding (Epstein & Kanwisher, 1998; Epstein, 2008), fine-grained spatial judgment (Hirshhorn et al., 2012), and 3D space representation (Kim & Maguire, 2018). In line with previous findings, our observations suggest that measures of parahippocampal gray matter could serve as a proxy for cortico-hippocampal information coherence, with greater efficiency of the system translating into better spatial cognition skills. Although their core microstructural changes are incompletely understood, it has been suggested that variations in cortical thickness may, nonetheless, capture underlying variations in cytoarchitecture. For example, while thickness measurements may be anti-correlated to neuronal density, regions of relatively high thickness with reduced density may instead present with more complex dendritic arborization, which could facilitate integrative information processing (Cahalane et al., 2012; Collins et al., 2010; la Fougère et al., 2011; Wagstyl et al., 2015).

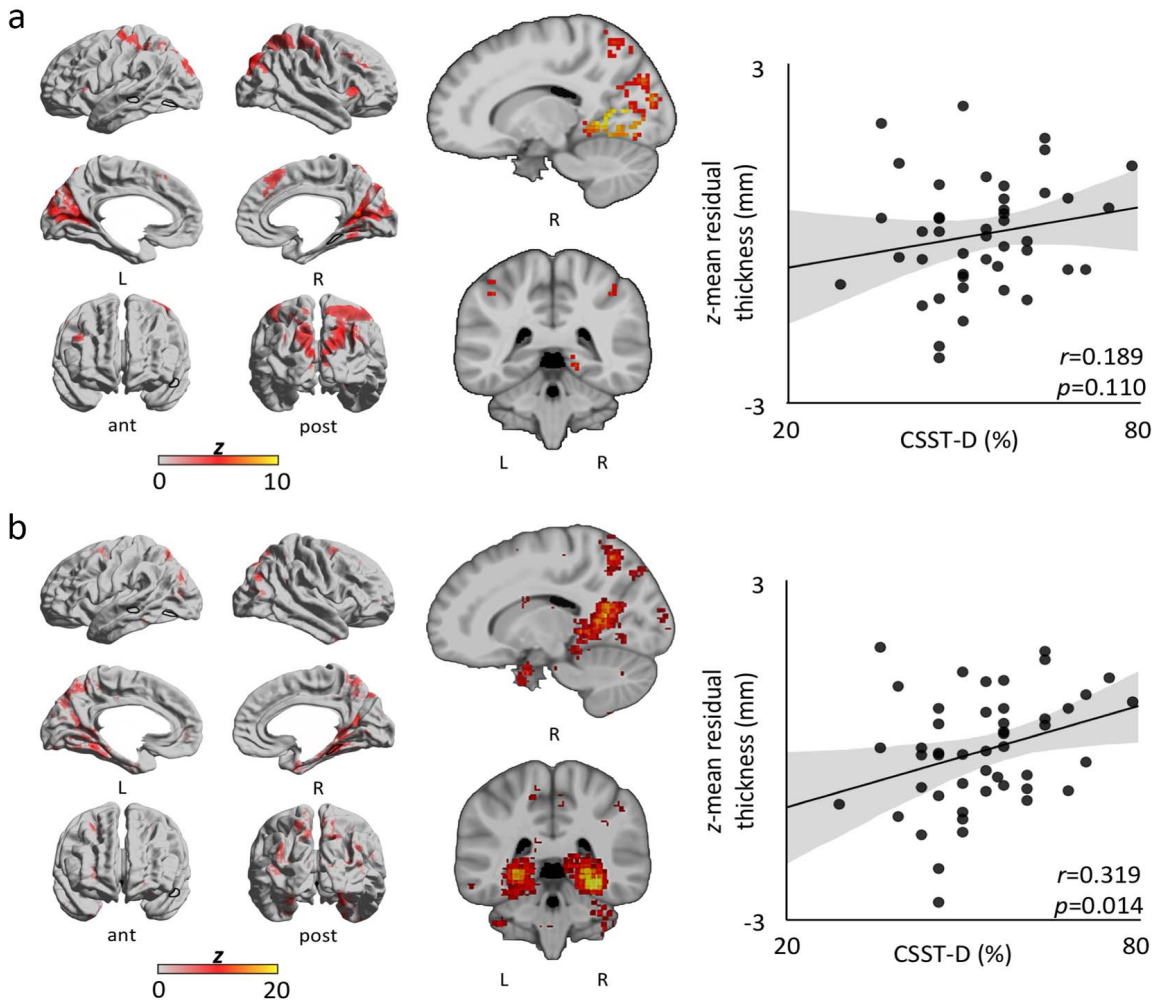

Figure 3. Functional contextualization. To further address task validity, CSST-D scores were correlated with average cortical thickness across regions of activation from CSST- and Neurosynth-derived maps. (a) Left column: Group level (n = 44) CSST surface-wide activation for "retrieval-versus-encoding" weighted contrast. Notably, the right PHG shows significant activation. Dark outlines correspond to structural clusters. Middle column: volumetric activation (MNI coordinates: 15, −40). Right column: Trend between average cortical thickness across regions of activation and CSST-D score (r = 0.189, one-tailed P = 0.110). (b) Left column: Neurosynth-derived surface-wide coactivations for the term "navigation." Dark outlines correspond to structural clusters. Middle column: volumetric activation (MNI coordinates: 15, −40). Right column: Significant association between average cortical thickness across coactivated areas and CSST-D performance (r = 0.319, one-tailed P = 0.014).

Regarding the hippocampus, we observed a positive trend between CSST-D scores and total hippocampal volume. The hippocampus has long been associated with spatial processing in experimental work in animals (Aggleton et al., 1986; Burgess et al., 2007; O'Keefe & Nadel, 1978; Sargolini et al., 2006), as well as in lesional patients (Milner, 1965; Rains & Milner, 1994; Smith & Milner, 1981, 1989) and human neuroimaging studies (Abrahams et al., 1999; Aguirre et al.,

1996; Ghaem et al., 1997; Hassabis et al., 2009; Kim & Maguire, 2018; Maguire et al., 1998; Maguire et al., 2000; Robin et al., 2018). Furthermore, task-based fMRI analysis of the CSST paradigm and ad hoc meta-analysis via Neurosynth confirmed consistent activations in the hippocampus-parahippocampus complex, particularly in its posterior divisions. It is worth noting that while our result pertaining to the whole hippocampal volume corroborates prior evidence, our analytical approach may not have been sensitive enough to identify subregional effects. Further analyses with larger cohorts and/or higher resolution imaging of the hippocampus are required to more robustly explore subregional substrates in the hippocampus; such approaches may benefit from methodologies that tap into hippocampal longitudinal and medio-lateral axes (Paquola et al., 2020; Plachti et al., 2019; Przeździk et al., 2019; Vos de Wael et al., 2018).

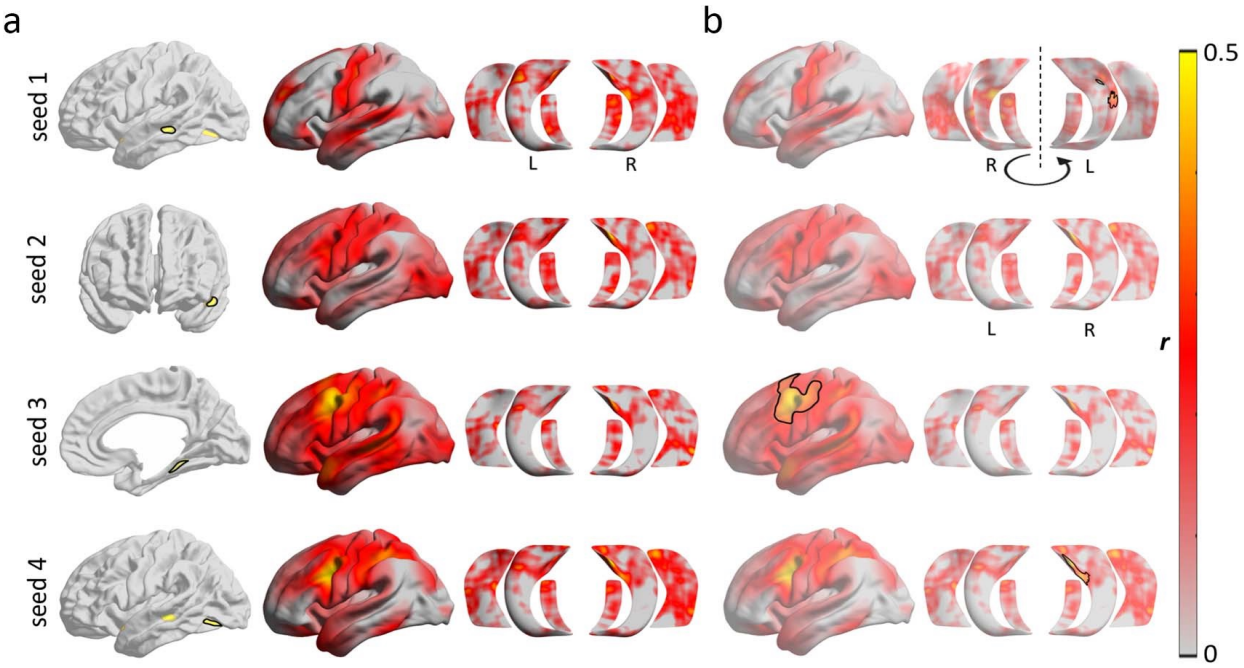

Figure 4. **Seed-based resting-state functional connectivity analysis.** Analyses focused on clusters of significant structural modulations (see Fig. 2; presented in rows). (a) Left column: seeds; Middle and right columns: whole-brain and hippocampal functional connectivity for each seed. (b) Associations between CSST-D and connectivity profiles.

Our choice of task-related functional contrasts was informed by the overlap between whole-brain findings for the retrieval-versus-encoding comparison and Neurosynth-based meta-analytical results obtained for the term "navigation". Other contrasts (*i.e.*, easy-vs.-difficult and successful-vs.-unsuccessful trials) failed to yield voxel-wise findings after correction for multiple comparisons. These negative observations mandate in-depth analyses using multivariate approaches in addition to classical univariate methodologies, especially when investigating associations between interindividual variations in functional activation and behavioral outcome measures on the CSST. We will address these questions and more in follow-up studies.

In addition to results pertaining to the MTL, we observed structural MRI effects in lateral temporal areas whose role is less well defined in spatial cognition. Within-sample fMRI and ad hoc meta-analysis results did not support any functional relevance of lateral temporal regions to spatial memory processing and navigation. Several studies have already pointed to contributions from extra-MTL structures such as the posterior cingulate, retrosplenial, dorsolateral prefrontal, and posterior parietal cortices (Aguirre et al., 1996; Byrne et al., 2007; Ghaem et al., 1997; Maguire et al., 1998; Whitlock et al., 2008), but none explicitly to lateral temporal areas. In one virtual-reality fMRI study in which participants navigated a circular platform, grid-cell firing patterns were consistently observed in the lateral temporal cortices, in addition to MTL findings (Doeller et al., 2010). Another experiment showed that movement-onset periods in a square virtual environment were linked to increases in theta frequency power mainly within the hippocampus, but also across the lateral temporal lobes, with greater changes in theta power for relatively longer path lengths (Bush et al., 2017). A meta-analytic review also found that bilateral lateral temporal cortices participated in the processing of familiar as opposed to recently learned virtual environments (Boccia et al., 2014). Interestingly, the same review also reported greater involvement of the right

parahippocampus in recently learned virtual settings when compared with familiar ones. Our observation that measurements of cortical thickness across disparate clusters within the left lateral temporal lobe correlate with performance on the CSST-D corroborates previous findings regarding a complementary role of lateral temporal areas to medial regions in spatial processing.

To provide network-level context for these structural findings, we implemented seed-based rs-fMRI connectivity analyses centered on lateral and medial temporal clusters where morphological associations to CSST-D performance were seen. Using more exploratory thresholding, we observed a positive association between CSST-D scores and the connectivity strength between components of this network, specifically between medial and lateral temporal regions, together with a region denoted laterally by the middle frontal and precentral gyri, and medially by the paracentral lobule and superior anterior cingulate. Significant connectivity modulations were obtained for three out of four clusters that showed main effects of CSST-D on cortical thickness; such a combined effect on morphology and functional connectivity speaks to intracortical and network level substrates underlying spatial cognition. Since the discovery of rodent place cells (O'Keefe & Dostrovsky, 1971) and the formulation of the cognitive map theory (O'Keefe & Nadel, 1978), which primarily focused on the hippocampus, the neural landscape of spatial cognition has increasingly been conceptualized as a network that encompasses widespread brain areas that perform complementary operations. One leading model posits a vast circuit involving MTL and extra-MTL regions that participate in the reciprocal transformation of body-centered and subject-invariant spatial representations (Bicanski & Burgess, 2018; Byrne et al., 2007; Dhindsa et al., 2014). An at times overlooked assumption is that regions involved in specific neural processes may be recruited in various other cognitive domains. Given that the human brain is a finite organ capable of multiple mental functions, it is not surprising that many neural operations show

anatomical convergence. In fact, some of the regions discussed herein in the context of spatial memory may apply equally as well to other related cognitive faculties (Bellmund et al., 2018; Constantinescu et al., 2016; Epstein et al., 2017; Mok & Love, 2019).

Thus, the behavioral correlation that we observed between spatial and semantic memory scores could point to shared mechanisms across different mnemonic domains. This finding is in line with prior literature suggesting such functional versatility of the hippocampus, which is likely predicated on its structural connectivity to other brain systems (Moscovitch et al., 2005; Nadel & Moscovitch, 1997). Notably, associations between semantic and spatial processing also paralleled our recent study of individual differences in different types of memory (Sormaz et al., 2017). In this study, we found that both semantic and spatial memory were related through their association between hippocampal and lateral parietal connectivity at rest. It has been proposed that the brain may organize semantic information as a navigable conceptual mental space, a mechanism not unlike the encoding of spatial information into a cognitive map via the concerted activity of hippocampal place cells and entorhinal grid cells (Constantinescu et al., 2016; Hafting et al., 2005; McNaughton et al., 2006; O'Keefe & Dostrovsky, 1971). New evidence further indicates that these cell populations are in fact functionally more flexible than previously believed. For example, it has been argued that the neural mechanisms that encode for Euclidean space may also eventuate a multitude of orthogonally stable cognitive spaces, each representing a unique dimension of experience, such as conceptual knowledge (Bellmund et al., 2018). Recent findings support the involvement of domain-invariant learning algorithms that apply to the neural organization of both spatial and semantic information (Mok & Love, 2019). By implementing our newly developed CSST in conjunction with stimulus-matched episodic and semantic memory paradigms, it may be

possible to efficiently explore the degree of structural and functional convergence across relational memory domains both in healthy as well diseased populations.

2.6 Funding

Faculty of Medicine studentship from McGill University (to S.T.); China Scholarship Council (CSC) (to Q.L.); fellowship from the Canadian Open Neuroscience Platform (CONP) and CIHR (to J.R.); studentships from the Savoy foundation for Epilepsy and the Richard and Ann Sievers award (to R.V.d.W.); Canadian Institutes of Health Research (CIHR) (to S.L.); postdoctoral fellowship of the Fonds de la Recherche du Quebec—Santé (FRQ- S) (to C.P.); European Research Council (Project ID: 771863— FLEXSEM to E.J.); FRQ-S and CIHR (MOP-57840, MOP-123520 to A.B. and N.B.); European Research Council (WANDERINGMINDS- ERC646927 to J.S.); CIHR (Grant Number 274766 to V.B.); PhD Scholarship from Brain Research UK (award 14181) to L.C.; Berkeley Fellowship (UCL and Gonville and Caius College, Cambridge to L.C.); National Science and Engineering Research Council of Canada (NSERC Discovery-1304413 to B.B.); Canadian Institutes of Health Research (CIHR FDN-154298 to B.B.); SickKids Foundation (NI17–039 to B.B.), Azrieli Center for Autism Research (ACAR- TACC to B.B.); BrainCanada (to B.B.); Tier-2 Canada Research Chairs program (to B.B.).

2.7 Notes

The authors would like to express their gratitude to the MRI technicians at the Montreal Neurological Institute.

2.8 SUPPLEMENTARY METHODS

Structural MRI processing

Hippocampal subfield surface mapping. We harnessed a validated approach for the segmentation of hippocampal subfields, generation of surfaces running through the core of each subfield, and surface-based "unfolding" of hippocampal features (Bernhardt et al., 2016; Caldairou et al., 2016; Vos de Wael et al., 2018). In brief, each participant's native-space T1w image underwent automated correction for intensity non-uniformity, intensity standardization, and linear registration to the MNI152 template. Images were subsequently processed using a multi-template surface-patch algorithm (Caldairou et al., 2016), which automatically segments the left and right hippocampal formation into subiculum, CA1-3, and CA4-DG. An open-access database of manual subfield segmentations and corresponding high resolution 3T MRI data (Kulaga-Yoskovitz et al., 2015) was used for algorithm training. A Hamilton-Jacobi approach (Kim et al., 2014) generated a medial surface sheet representation running along the central path of each subfield and surfaces were parameterized using a spherical harmonics framework with a point distribution model (Styner et al., 2006). For each subfield surface vertex, we then calculated columnar volume as a marker of local grey matter (Kim et al., 2014). During data analysis, vertex-wise projections of hippocampal columnar volume underwent surface-wide smoothing (FWHM=10) using SurfStat for Matlab (MathWorks, R2019b).

2.9 SUPPLEMENTARY FIGURES

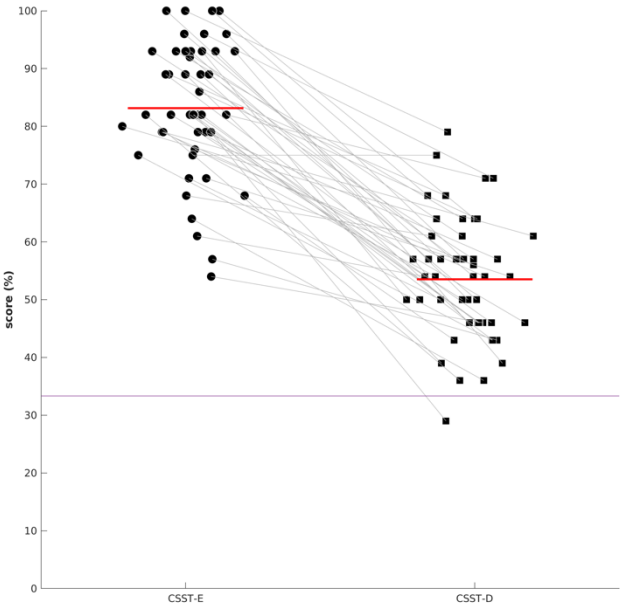

Supplemental Figure 1 | Participants scored significantly higher on the CSST-E (83.1±11.3%) compared to the CSST-D (53.5±10.7) as evidenced by a two-tailed paired student t-test (t=16.8, p<0.001). Red horizontal lines show distribution means. Chance level performance is depicted as a horizontal line (33.33%). Participants scored significantly higher than chance level on each condition (CSST-E: t=30.4, p<0.001; CSST-D: t=13.1, p<0.001).

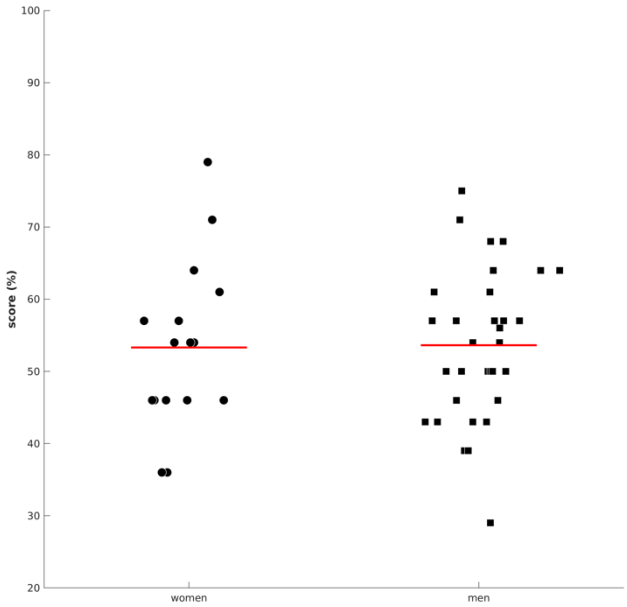

Supplemental Figure 2 | In order to assess whether variability in the results is driven by middle-aged participants, we assessed whether individuals above 35 years of age performed similarly to younger adults. No age-related differences were observed in either sex group (older women: 54.5±14.4%, young women: 52.9±11.3%, t=0.227, p=0.823; older men: 50.4±7.5%, young men: 54.5±11.0%, t=0.918, p=0.366). Thus, we combined data across age strata in each group and compared scores. We observed no sex differences in CSST-D performance (women: 53.3±11.7%; men: 53.6±10.4%; t=0.094, p=0.925).

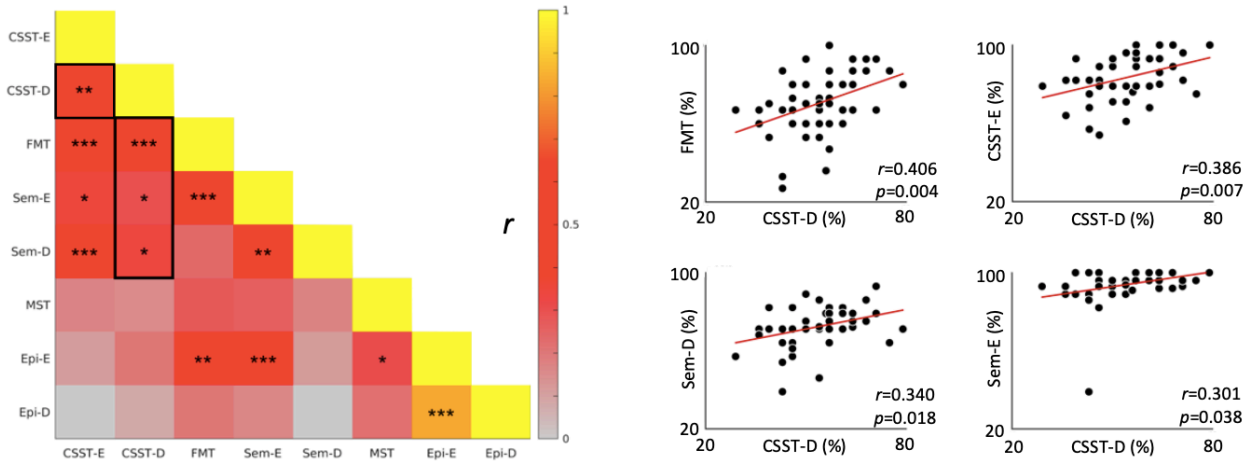

Supplemental Figure 3 | *left*: correlation matrix of performance across all tasks, including easy conditions. Outlined area shows tasks with which CSST-D shows significant associations (*p<0.05; **p<0.01; ***p<0.005). *right*: scatter plot of most significant associations with other tasks (FMT: Four Mountains Task; CSST-D/E: Conformational Shift Spatial Task-Difficult/Easy; Sem-D/E: Semantic Task-Difficult/Easy; Epi- D/E: Episodic Difficult/Easy; MST: Mnemonic Similarity/Discrimination Task)

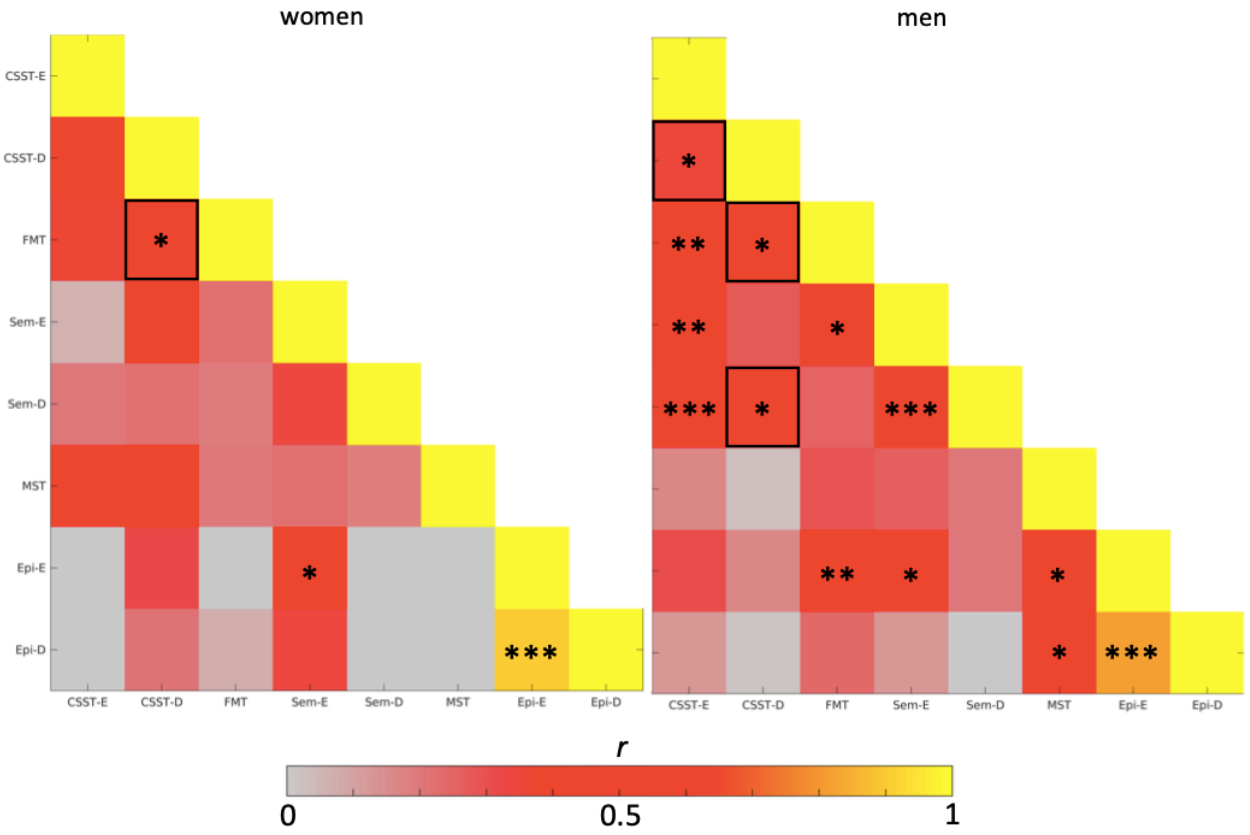

Supplemental Figure 4 | Correlation matrix of performance across all tasks for women and men. Outlined areas show tasks with which CSST-D shows significant associations (*p<0.05; **p<0.01; ***p<0.005). (FMT: Four Mountains Task; CSST-D/E: Conformational Shift Spatial Task-Difficult/Easy; Sem-D/E: Semantic Task-Difficult/Easy; Epi-D/E: Episodic Difficult/Easy; MST: Mnemonic Similarity/Discrimination Task)

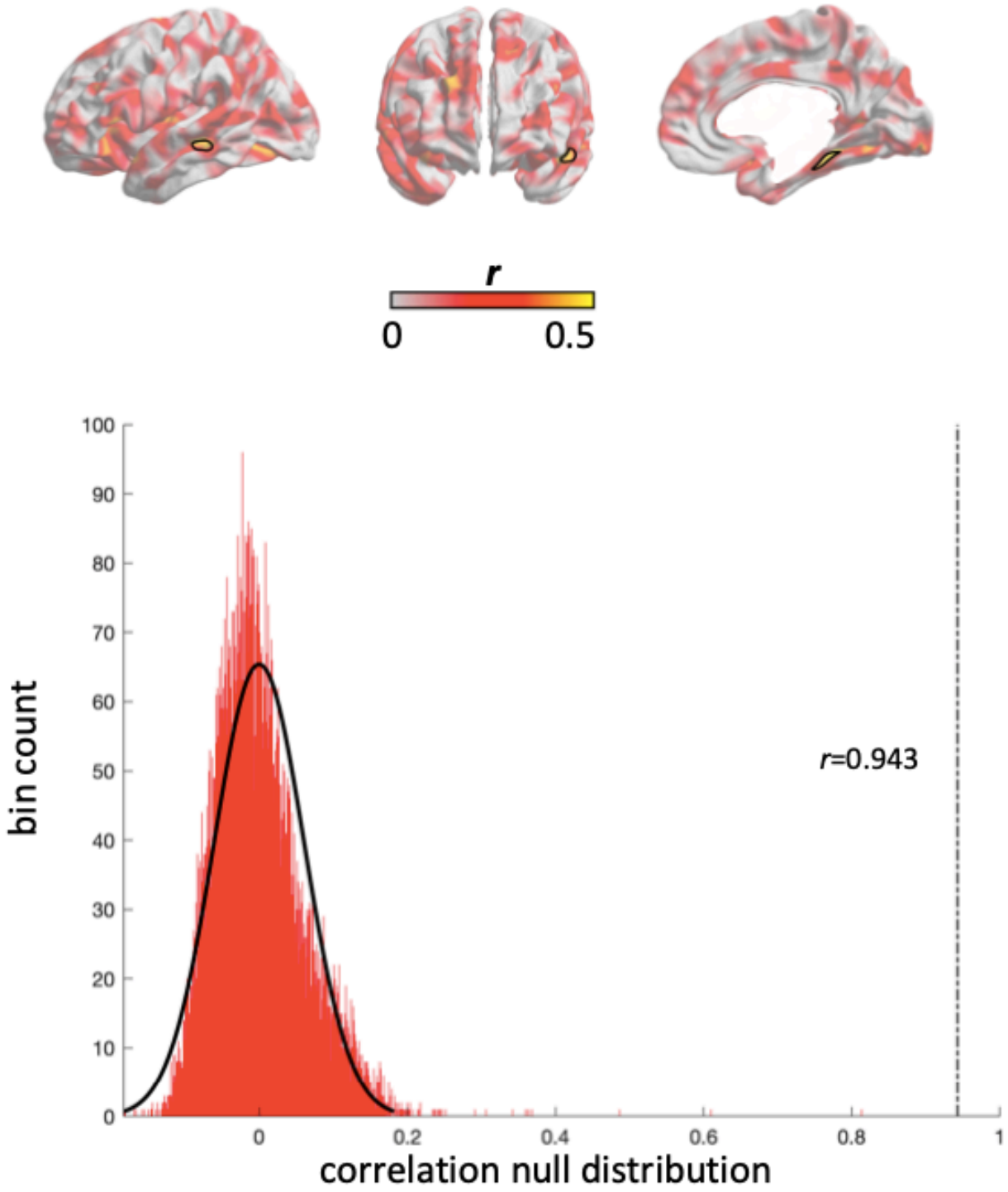

Supplemental Figure 5 | top panel: Product-moment correlation coefficients of CSST-D performance on cortical thickness after regressing out age and sex for right-handed participants (n=44). Highlighted clusters denote regions of significant association after multiple comparisons correction (p_{FWE}<0.05). **bottom panel:** a non-parametric null distribution was generated by correlating the *CSST-D x cortical thickness* statistical *t* map with 10,000 permutated *t* maps of *right-handed only CSST-D x cortical thickness*. Actual correlation between original maps is shown by the dashdotted line (*r*=0.943, non-parametric *p*<0.001).

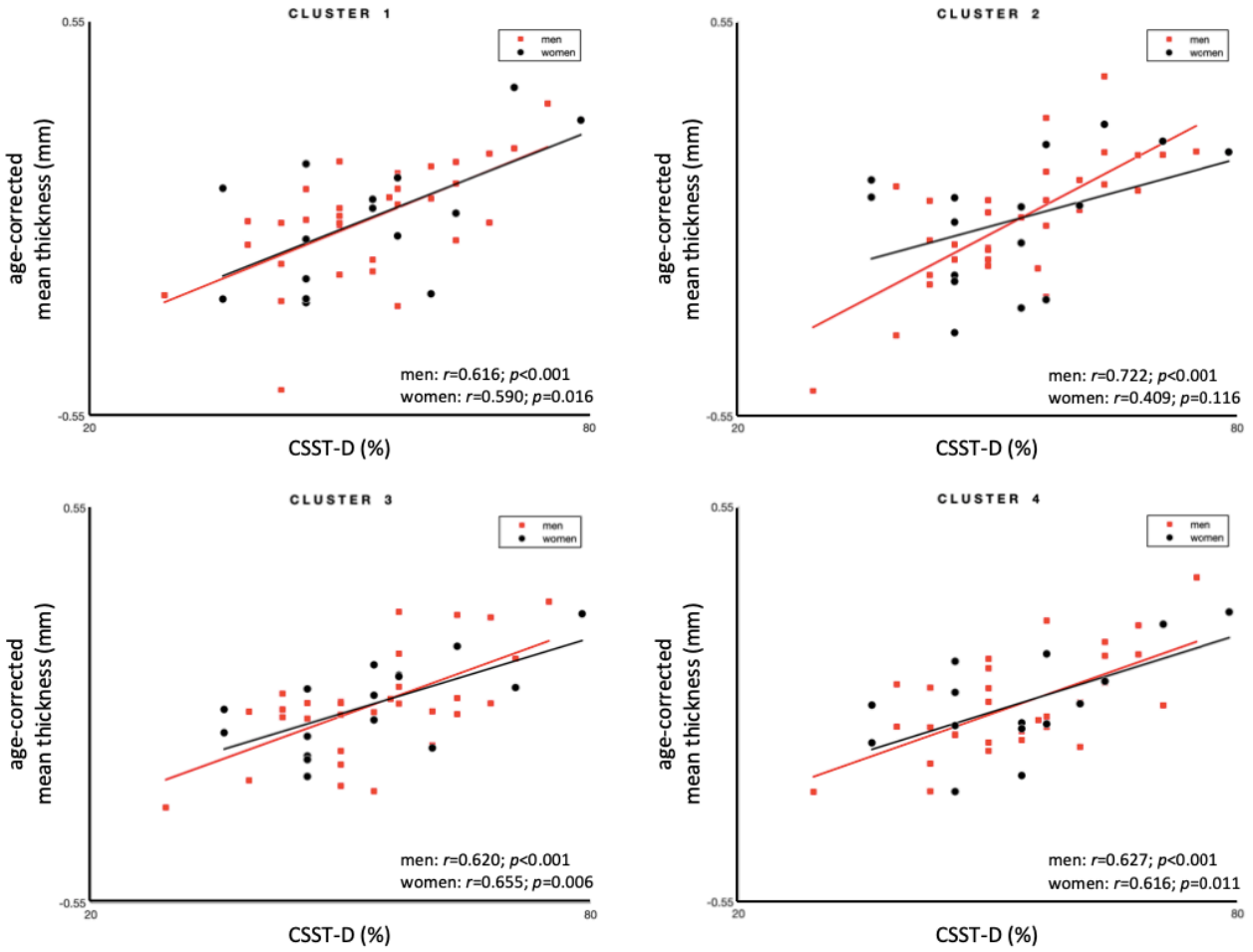

Supplemental Figure 6 | Controlling for age, we observed moderate-to-high associations between average cortical thickness and CSST-D scores for all clusters in men and women.

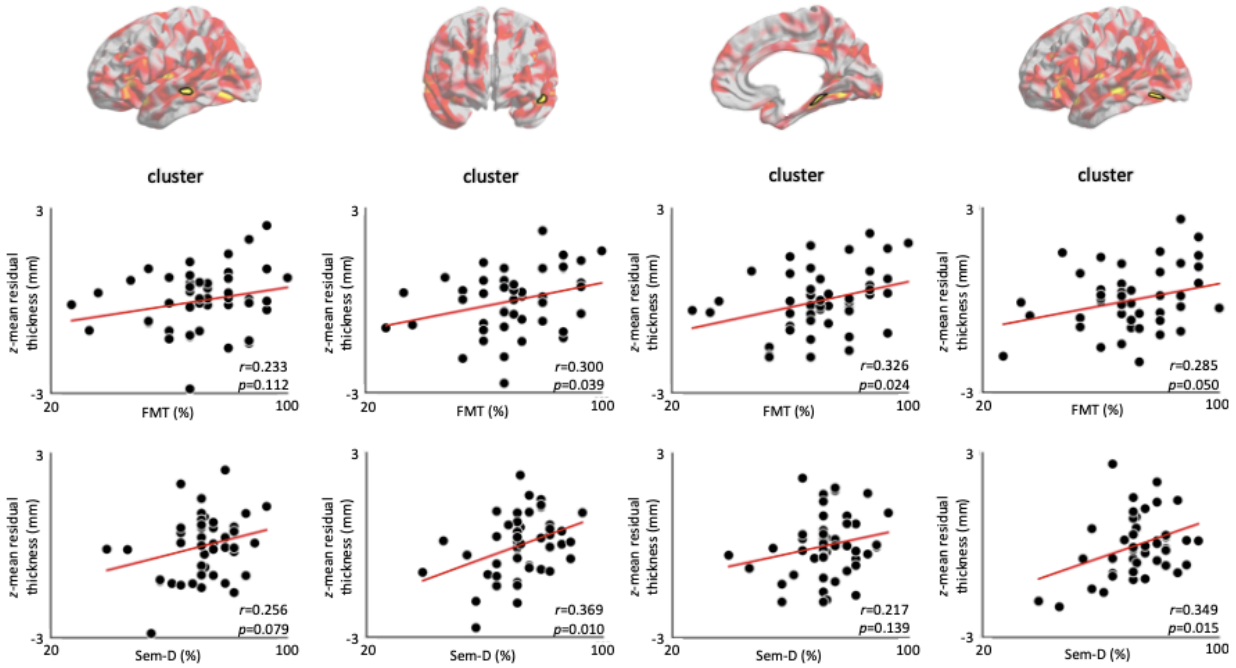

Supplemental Figure 7 | Cluster-wise associations between cortical thickness and scores for FMT (top row scatterplots) and Sem-D (bottom row scatterplots). Correlation coefficients ranged between r=0.233-0.326 for FMT (mean effect of 0.353), and between r=0.217-0.369 for Sem-D (mean effect of 0.373).

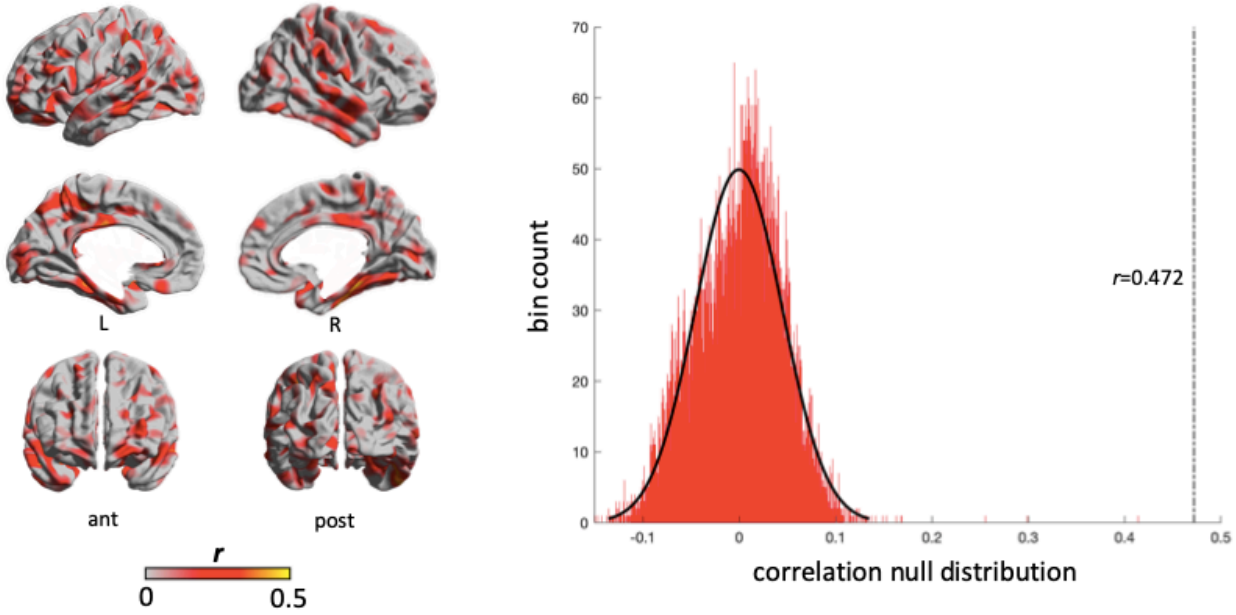

Supplemental Figure 8 | left panel: Product-moment correlation coefficients of FMT performance on cortical thickness after regressing out age and sex. **right panel:** a non-parametric null distribution was generated by correlating the *CSST-D x cortical thickness* statistical *t* map with 10,000 permutated *t* maps of *FMT x cortical thickness*. Actual correlation between original maps is shown by the dashdotted line (r=0.472, non-parametric p<0.001).

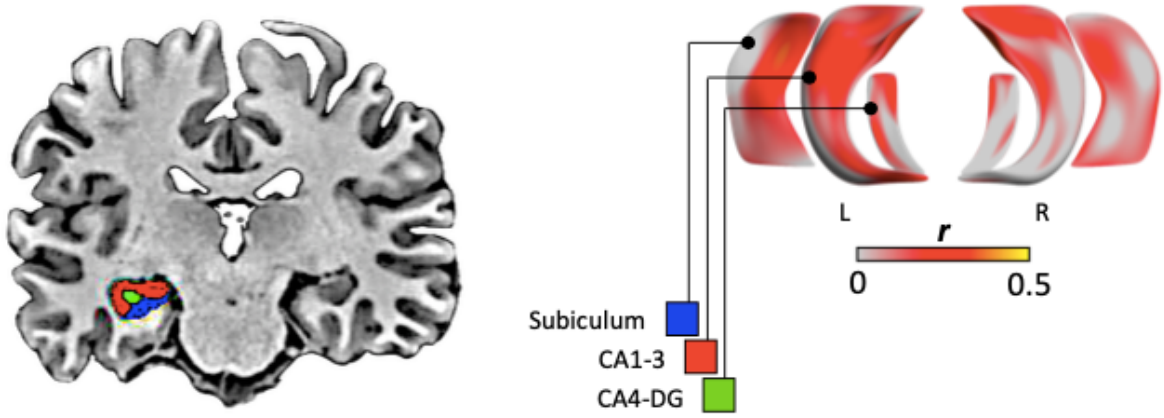

Supplemental Figure 9 | left panel: coronal section of the brain showing the hippocampal subfields. **right panel:** uncorrected associations between CSST-D score and columnar volume shown on hippocampal subfield surfaces after regressing out age and sex.

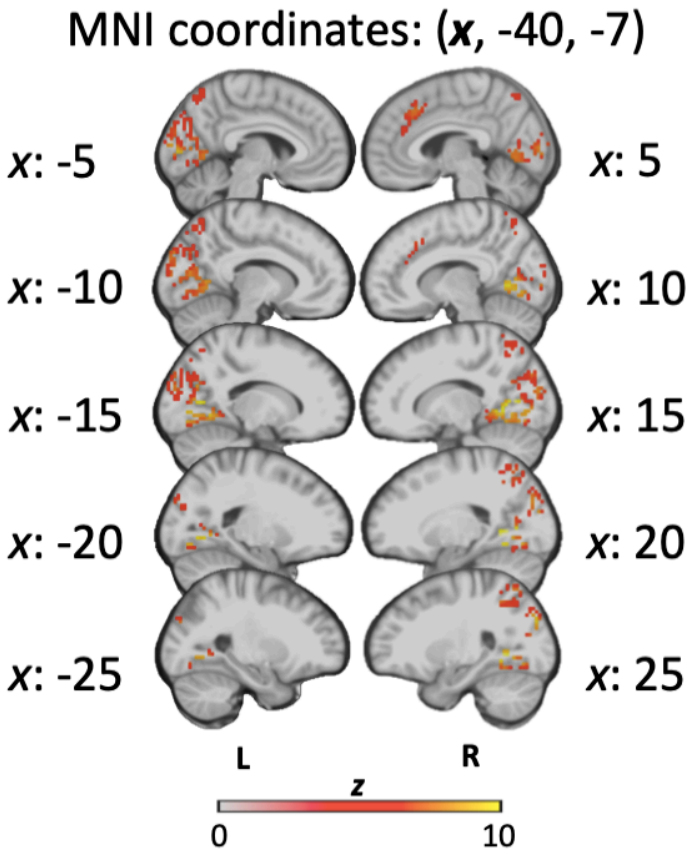

Supplemental Figure 10 | Group-level volumetric activation map for the contrast between retrieval and encoding.

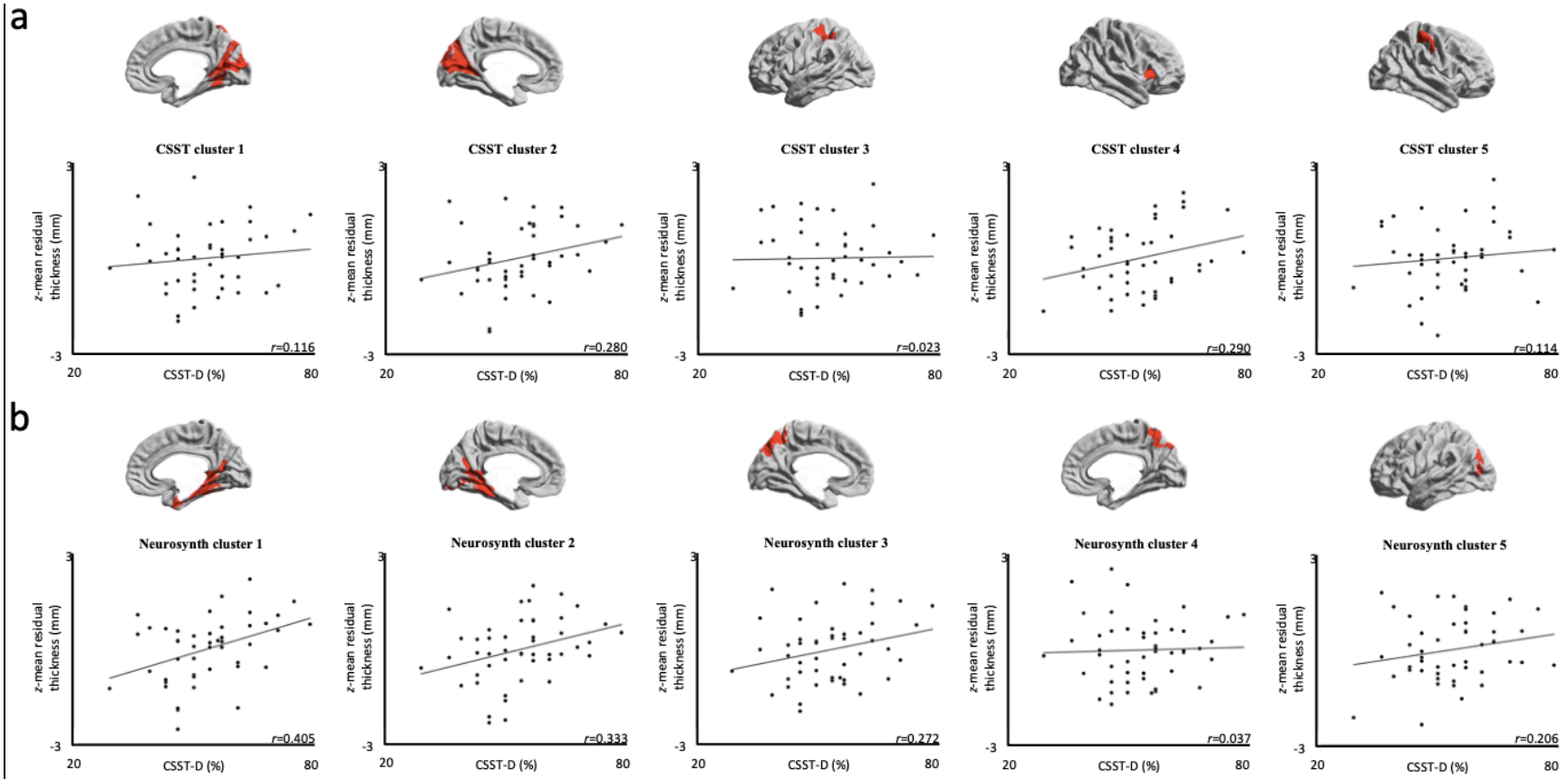

Supplemental Figure 11 | Associations between cortical thickness and CSST-D performance for functionally-defined clusters after controlling for age and sex. a) Top 5 largest clusters for group level (n=44) CSST activation for *retrieval-vs.-encoding* weighted contrast (r=0.023-0.290). **b)** Top 5 largest clusters for Neurosynth-derived coactivations for the term *"navigation"* (r=0.037-0.405).

FMT	0.406			
Sem-D	0.340	0.237		
MST	0.150	0.278	0.172	
Epi-D	0.083	0.206	-0.058	0.224
	CSST-D	FMT	Sem-D	MST

Supplemental Table1 | Product-moment correlation coefficients of task performance scores (see **Figure 1b**)

	successful	unsuccessful
CSST-E	23 ± 3 (15-28)	5 ± 3 (0-13)
CSST-D	15 ± 3 (8-22)	13 ± 3 (6-20)
Total	38 ± 5 (28-50)	18 ± 5 (6-28)

Supplemental Table 2 | Number of successful and unsuccessful trials in the each condition of the CSST reported as the mean ± SD (range) .

MNI x,y,z {mm}	peak T	peak p(unc)	peak p(FWE-corr)
18 -64 5	14.87	<0.001	<0.001
21 -58 -1	14.52	<0.001	<0.001
12 -58 2	11.74	<0.001	<0.001
-15 -67 8	11.24	<0.001	<0.001
-18 -76 -4	11.16	<0.001	<0.001
-21 -64 -4	10.7	<0.001	<0.001
33 23 2	9.68	<0.001	<0.001
39 20 -13	7.13	<0.001	0.001
-39 -22 59	9.54	<0.001	<0.001
-39 -37 41	7.99	<0.001	<0.001
-33 -16 65	7.97	<0.001	<0.001
36 -49 50	9.17	<0.001	<0.001
27 -52 47	9.01	<0.001	<0.001
24 -67 59	8.2	<0.001	<0.001
6 26 41	8.46	<0.001	<0.001
6 38 23	6.37	<0.001	0.008
45 -28 47	8.19	<0.001	<0.001
42 -37 47	7.91	<0.001	<0.001
51 -19 44	7.19	<0.001	0.001
45 32 23	8.05	<0.001	<0.001
-9 -70 53	7.14	<0.001	0.001
-12 -76 47	6.52	<0.001	0.005

Supplemental Table 3 | Group-level volumetric statistics for contrast between retrieval and encoding across pooled CSST-E and CSST-D trials.

With the establishment of the construct-validity of the spatial iREP within healthy individuals in the previous section, in the next one (Project II), we aim to behaviorally phenotype a group of TLE patients as well as age- and sex-matched healthy controls (HC) on the full gamut of the iREP. Here, we want to investigate phenotypic variations across relational memory domains and different population cohorts. To this end, we conduct complementary omnibus and multivariate associative analyses to first address interactive associations in behavioral performance across groups and iREP measurements, and then to identify multivariate profiles of maximal covariance between iREP measurements and salient demographic variables, including age, sex, diagnostic group, and hippocampal volume. We show that compared to HC, TLE patients appear to be significantly affected on all relational memory domains, with between-group differences persisting along episodic and spatial components even when accounting for underlying socio-demographic and cognitive presentations. We additionally confirm the presence of latent multivariate links between relational memory behavioral phenotypes that scale commensurately with changes in age, diagnostic group status, and hippocampal volume. Overall, we reveal a graded pattern of behavioral deficits in older, TLE patients, with relatively smaller hippocampi for whom the episodic system is severely affected, with additional impairments seen in the spatial system, while the semantic system presents with mixed results.

3 PROJECT II: relational memory deficits in temporal lobe epilepsy

This section has been preprinted and is currently under review at Epilepsy & Behavior.

DIFFERENTIAL RELATIONAL MEMORY IMPAIRMENT IN TEMPORAL LOBE EPILEPSY

Shahin Tavakol[*], Valeria Kebets[*], Jessica Royer[*], Qiongling Li[*], Hans Auer[*], Jordan DeKraker[*], Elizabeth Jefferies[&], Neda Bernasconi[*], Andrea Bernasconi[*], Christoph Helmstaedter[°], Jorge Armony[%], R. Nathan Spreng[*#], Lorenzo Caciagli[†], Birgit Frauscher[Ψ], Jonathan Smallwood[+], and Boris Bernhardt[*#]

[*]*McConnell Brain Imaging Centre, Montreal Neurological Institute and Hospital, McGill University, Montreal, Canada*
[&]*University of York, York, United Kingdom*
[°]*Department of Neuropsychology, University of Bonn, Bonn Germany*
[†] *Department of Bioengineering, University of Pennsylvania, Philadelphia, USA and UCL Queen Square Institute of Neurology, London, United Kingdom*
[Ψ]*ANPHY lab, Montreal Neurological Institute and Hospital, McGill University, Montreal, Canada*
[+]*University of Queens, Kingston, Ontario, Canada*
[%]*Department of Psychiatry, McGill University, Montreal, Canada*
[#]*Department of Neurology and Neurosurgery, Montreal Neurological Institute and Hospital, McGill University, Montreal, Canada*

CORRESPONDENCE TO:
Boris Bernhardt, PhD
Associate Professor of Neurology and Neurosurgery
Montreal Neurological Institute and Hospital, McGill University
Email: boris.bernhardt@mcgill.ca

Shahin Tavakol, PhD candidate
Email: shahin.tavakol@mail.mcgill.ca

3.1 ABSTRACT

OBJECTIVE. Temporal lobe epilepsy (TLE) is typically associated with pathology of the hippocampus, a key structure involved in relational memory, including episodic, semantic, and spatial memory processes. While it is widely accepted that TLE-associated hippocampal alterations underlie memory deficits, it remains unclear whether impairments relate to a specific cognitive domain or multiple ones.

METHODS. We administered a recently validated task paradigm to evaluate episodic, semantic, and spatial memory in 24 pharmacoresistant TLE patients and 50 age- and sex-matched healthy controls. We carried out two-way analyses of variance to identify memory deficits in individuals with TLE relative to controls across different relational memory domains, and used partial least squares correlation to identify factors contributing to variations in relational memory performance across both cohorts.

RESULTS. Compared to controls, TLE patients showed marked impairments in episodic and spatial memory, with mixed findings in semantic memory. Even when additionally controlling for socio-demographic variables and overall cognitive/executive function, between-group differences persisted along episodic and spatial domains. Moreover, age, diagnostic group, and hippocampal volume were all associated with relational memory behavioral phenotypes.

SIGNIFICANCE. Our behavioral findings show graded deficits across relational memory domains in people with TLE, which provides further insights into the complex pattern of cognitive impairment in the condition.

Key words: relational memory, temporal lobe epilepsy, hippocampus

3.2 INTRODUCTION

Temporal lobe epilepsy (TLE) is the most common pharmacoresistant epilepsy in adults, and typically associated with pathology of the hippocampus (Spiers et al., 2001; Tavakol et al., 2019; Thom, 2014), a key structure involved in the formation and retrieval of memories. Hippocampal lesions are believed to disrupt mnemonic functions in individuals with TLE, which can sometimes impact their quality of life more than seizures (Hoppe et al., 2007; Viskontas et al., 2000). To improve patient care, it is crucial to understand the full scope of TLE deficits by recognizing how hippocampal damage impacts various cognitive processes.

Relational memory encompasses several faculties that synthesize the elements of subjective experience into a coherent mental representation (Bellmund et al., 2018; Eichenbaum & Cohen, 2001; Olsen et al., 2012). Relational memory domains include episodic, semantic, and spatial memory. Episodic memory integrates contiguous spatiotemporal events (Tulving, 1983; Tulving, 2002) into a self-referential abstraction known as an episode (Eichenbaum, 2018; Eichenbaum et al., 1999). Semantic memory amalgamates notions and facts into a mental hierarchy of conceptual categories (Cutler et al., 2019; Helmstaedter et al., 1997; Solomon & Schapiro, 2020). Spatial memory maps out and binds the locations of ambient objects into a mental feature space of the physical environment, also referred to as a cognitive map (O'Keefe & Nadel, 1978). Recent studies point to some convergence of these relational domains in healthy individuals, both at the behavioral and neural level, generally supporting a key involvement of the hippocampus and associated neocortical networks (Aguirre & D'Esposito, 1997; Binder & Desai, 2011; Binder et al., 2009; Hassabis et al., 2009; Jefferies, 2013; Jokeit et al., 2001; Moscovitch et al., 2016; Rugg & Vilberg, 2013; Schindler & Bartels, 2013). In healthy controls (HC), we previously showed an

association between semantic and spatial cognition based on behavioral performance scores obtained on different cognitive tests (Tavakol et al., 2021), which was reflected in similar profiles of intrinsic functional connectivity between the hippocampus and neocortex (Sormaz et al., 2017). Other task-based investigations have uncovered patterns of brain activity that are compatible with neural representations for both semantic concepts as well as physical space (Constantinescu et al., 2016; Mok & Love, 2019).

Episodic memory impairment is well-established in TLE, backed up by ample behavioral (Barrett Jones et al., 2022; Phuong et al., 2021; Viskontas et al., 2000) and neuroimaging (McCormick et al., 2014; Sepeta et al., 2018; Sidhu et al., 2013) findings. On the other hand, and surprisingly, the literature on other relational memory domains remains scarce. With respect to spatial memory, findings are relatively limited, but suggest atypical behavioral phenotypes and neural representations (Schmidbauer et al., 2022; Tallarita et al., 2019). Likewise, despite well-recognized impairments in language and naming performance in TLE (Barrett Jones et al., 2022; Bell et al., 2001; Giovagnoli et al., 2005), relational semantic memory has only sporadically been studied in TLE (Helmstaedter et al., 1997; Lambon Ralph et al., 2012). Notably, there have not been any integrated assessments of episodic, semantic, and spatial memory in the same patients. Examining patients and HC using a multidomain memory paradigm can help address the specificity of TLE-associated behavioral impairments across these different cognitive domains.

The current study investigated episodic, semantic, and spatial memory in TLE patients as well as HC using a recently developed, open-access behavioral battery (*integrated Relational Evaluation Paradigm*, iREP). The iREP combines three computerized and domain-specific modules (*i.e.*,

Episodic, Semantic, and Spatial), each of which incorporates visual stimuli representing ordinary items, two levels of difficulty (Easy *vs.* Difficult), and a 3-alternative forced choice design. We first ran independent analyses in each cohort to confirm the difficulty manipulation across modules, and then performed an analysis of variance (ANOVA) to identify between-group behavioral differences in episodic, semantic, and spatial memory performance on the iREP. Finally, we implemented partial least squares (PLS) analysis, a multivariate associative technique, to identify how variations in clinical/demographic factors contribute to shared mnemonic phenotypes across memory domains.

3.3 METHODS

Participants

We studied 74 adult participants recruited between 2018 and 2022 at the Montreal Neurological Institute and Hospital, including a cohort of 24 pharmacoresistant TLE patients (12 women, mean age ± SD: 35.0 ± 11.5 years, range: 18–57, 2 ambidextrous) referred to our hospital for presurgical investigation, and 50 age- and sex-matched HC recruited via advertisement (20 women, 32.0 ± 7.8 years, range: 19-57 years, 5 left-handed). Epilepsy diagnosis and seizure focus lateralization were established following a comprehensive multidisciplinary assessment based on medical history, neurological and neuropsychological evaluation, video-electroencephalography telemetry, and magnetic resonance imaging (MRI). Fifteen patients had a left-sided seizure focus, and 9 had a right-sided focus. Based on quantitative hippocampal MRI volumetry (DeKraker et al., 2022), 15 patients (62.5%) showed hippocampal atrophy ipsilateral to the focus (*i.e.*, absolute ipsilateral-contralateral asymmetry index > 1.5 and/or ipsilateral volume z-score < -1.5). Average age at

seizure onset was 21.1 ± 10.8 years (range: 2-49 years), and average duration of epilepsy was 13.8 ± 10.9 years (range: 1-39 years). At the time of study, no patient had undergone resective surgery. Following an average time of 147 ± 98 days post-study, 9 patients underwent surgery, and 5 were rendered seizure free after a mean follow-up of 372 ± 329 days post-op. All participants had normal or corrected-to-normal vision. Our study was approved by the Research Ethics Committee of the Montreal Neurological Institute and Hospital, and all participants provided written and informed consent.

Relational memory phenotyping

The *integrated Relational Evaluation Paradigm* (iREP) is a recently developed, open access, python-based relational memory assessment tool (https://github.com/MICA-MNI/micaopen/task-fMRI) (Tavakol et al., 2021). It incorporates three memory domain specific modules: Episodic, Semantic, and Spatial. iREP administration is flexible. Modules can be completed in the laboratory or within varied neuroimaging platforms (*i.e.*, MRI scanner environment). Task instructions require verbal comprehension, but the task execution is non-verbal and homogenized via *(i)* the use of similar visual stimuli taken from a pooled custom-made and semantically-indexed library, *(ii)* the modulation of cognitive load across two conditions (*i.e.*, Easy *vs.* Difficult) with a pseudo-randomized trial presentation order, and *(iii)* the implementation of a 3-alternative forced choice trial-by-trial paradigm. Each module contains four distinct stimulus lists (*i.e.*, A, B, C, and D) for inter-individual counterbalancing and/or longitudinal administration. This allows for a combined evaluation of different forms of relational memory across two difficultly levels using a matched stimulus set and task structure. In the current study, all participants were tested on the iREP inside the MRI scanner, as part of a multimodal neuroimaging protocol described elsewhere (Tavakol et

al., 2021). Participants used an MRI-compatible response box to provide their answers. The neural responses recorded with functional MRI are outside the scope of this study, but will be the focus of forthcoming projects.

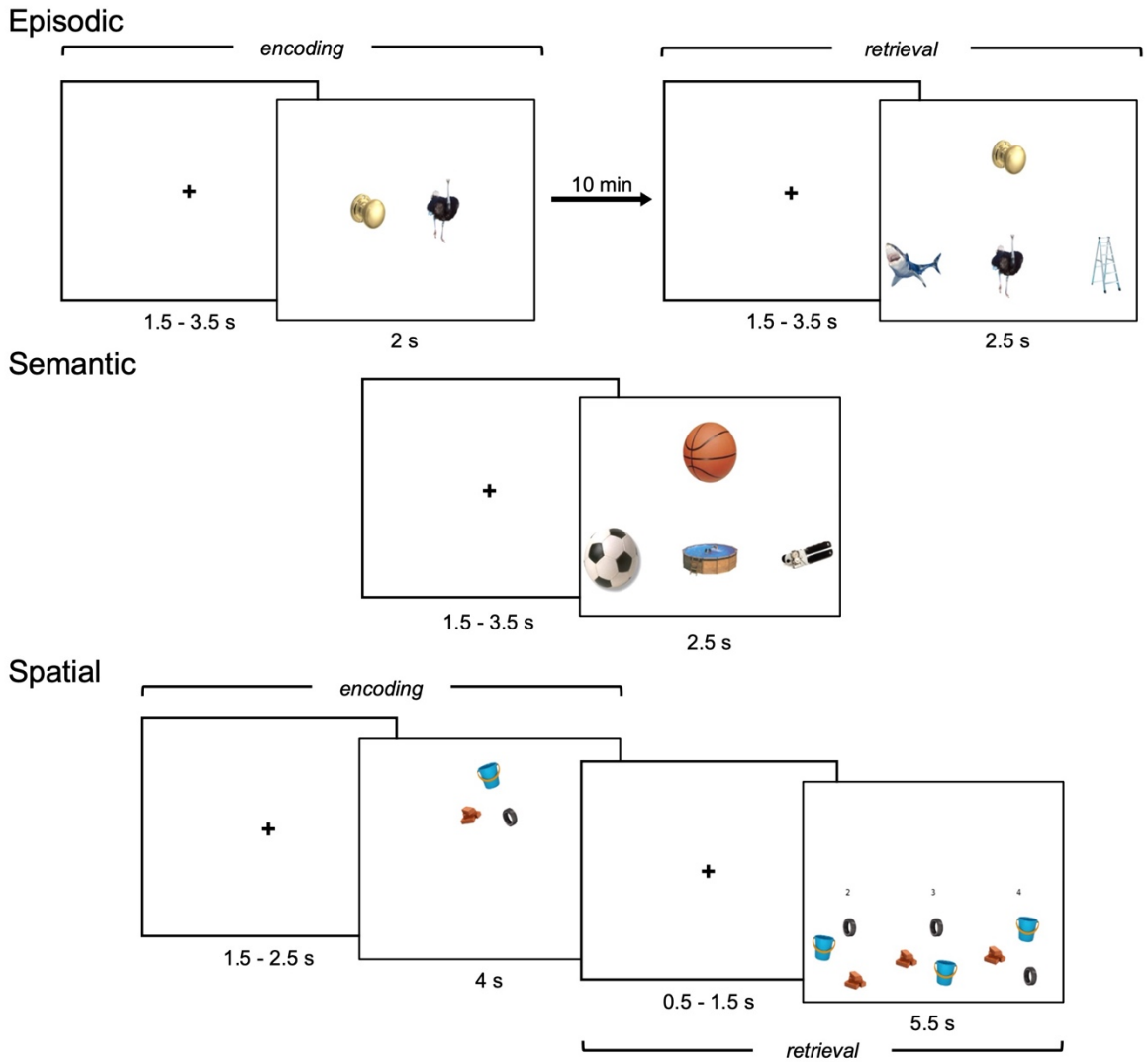

Figure 1. Trial design for each iREP module. *(top row)* The Episodic task consists of two separate runs. During Encoding, object pairs must be memorized. After a 10-minute break during Retrieval, the item that was originally paired with the top image must be recalled among three options. *(middle row)* In the Semantic task, the item that is the most conceptually congruent with the top object must be selected out of three choices. *(bottom row)* During the Spatial task, the configuration of three items must initially be encoded (*encoding*). Within the same trial, the original spatial arrangement must be chosen out of three options (*retrieval*). Numbers are there to visually aid participants on which response key to press. Overall durations for stimuli and inter-stimulus intervals are shown for each module.

(i) Episodic module. The episodic module is a symbolic version of an established lexicon-based episodic memory paradigm (Payne et al., 2012; Sormaz et al., 2017) that involves an encoding and a retrieval phase (**Fig. 1: top row**). In the encoding phase (~6 minutes), the participant memorizes a pair of unrelated objects presented simultaneously at each trial (*i.e.*, doorknob and ostrich). Half of the stimulus pairs is shown only once throughout the run for a total of 28 trials (*i.e.*, Difficult condition), and the other half is displayed twice to ensure more stable encoding for a combined 56 trials (*i.e.*, Easy condition), with a total of 84 trials for the entire task. The retrieval phase (~4.5 minutes) is administered after a 10-min interval. During each trial, one item is displayed at the top of the monitor (*i.e.*, doorknob) and three others, at the bottom (*i.e.*, shark, ostrich, and ladder). From the latter three options, the participant selects the object that was paired with the top item during the encoding phase. There are 56 pseudo-randomized trials in total with equal number of trials per condition (*i.e.*, 28 Difficult: Epi-D; 28 Easy: Epi-E).

(ii) Semantic module. The semantic module is a symbolic variant of an established lexicon-based semantic association protocol (Sormaz et al., 2017; Wang et al., 2018) (**Fig. 1: middle row**). This task consists of 56 pseudo-randomized trials (~4.5 minutes), with two conditions of equal length (*i.e.*, 28 Difficult: Sem-D; 28 Easy: Sem-E). At each trial, a reference item appears at the top of the monitor (*i.e.*, basketball) with three stimuli below (*i.e*., soccer ball, above ground pool, can opener), exactly as described in the retrieval phase of the Episodic module. The participant selects the option that is conceptually most alike to the object presented at the top. Pairwise conceptual affinity indices (*cai*) were calculated using an algorithm that leverages internet-based lexical corpora (Han et al., 2013), ranging from 0 to 1. In Sem-E trials, the correct response (*i.e.*, soccer ball) and the top image (*i.e.*, basketball) are related by $cai > 0.66$; in Sem-D trials, the similarity

index is given by $0.33 \leq cai \leq 0.66$. Regardless of condition, the conceptual relatedness of the top stimulus and the foils (*i.e.*, above ground pool, can opener) is always $cai < 0.33$. Thus, the level of difficulty across conditions is a function of the semantic relationship between the top object and the correct response.

(iii) Spatial module. Spatial memory was assessed using a recently validated paradigm (Tavakol et al., 2021) (**Fig. 1: bottom row**). This module consists of 56 pseudo-randomized trials (~12.5 minutes), with two conditions (*i.e.*, 28 Difficult: Spa-D; 28 Easy: Spa-E). At each trial, the participant first memorizes the spatial configuration of three objects, and then selects the same arrangement among three options in a delayed-onset design. In Spa-D trials, the two distractor layouts are very similar to the target configuration as only the spacing between the objects has changed. In the Spa-E trials, in addition to the spacing, the relative position of each item within the configuration is also changed, thus making it easier to differentiate the correct arrangement from the two foils.

iREP scoring

For each participant, we computed six iREP accuracy scores (*i.e.*, Epi-E, Epi-D, Sem-E, Sem-D, Spa-E, and Spa-D): $accuracy = \frac{n_{Correct}}{n_{Trial}} * 100$, where $n_{Correct}$ is the number of correct responses and n_{Trial} is the number of trials, which is always 28.

Parallel assessment of executive and overall cognitive function

In addition to the iREP, we administered the EpiTrack and the Montreal Cognitive Assessment (MoCA) protocols to our participants to account for factors that could potentially affect the

relationship between study cohorts and iREP outcome measures. Both tools are behavioral screening protocols for cognitive impairment. The EpiTrack is commonly used in patients with epilepsy to identify and monitor impairments in processing speed and attention (Lähde et al., 2021; Lutz & Helmstaedter, 2005), while the MoCA is used to detect mild cognitive impairment and dementia (Nasreddine et al., 2005).

Hippocampal atrophy determination

We acquired MRI data on a 3 T Siemens Magnetom Prisma-Fit with a 64-channel head coil. Two T1-weighted scans with identical parameters were performed with a 3D-MPRAGE sequence (0.8 mm isotropic voxels, matrix = 320 × 320, 224 sagittal slices, TR = 2300 ms, TE = 3.14 ms, TI = 900 ms, flip angle = 9°, iPAT = 2). We used HippUnfold (DeKraker et al., 2022) to segment the left and right hippocampi in each participant, and to estimate their volumes. HippUnfold implements a U-Net deep convolutional neural network to automate detailed hippocampal tissue segmentations. Grey matter data are then mapped onto the resulting "unfolded" hippocampal space, with distinct subregional features. In the current work, we only examined whole hippocampal grey matter volumes, restricting analyses to MNI152-derived metrics to account for interindividual variability in intracranial volume. To compute the absolute ipsilateral-contralateral asymmetry index, we first calculated non-normalized left-right asymmetry scores for controls and patients as follows: $\frac{Hipp_L - Hipp_R}{(Hipp_L + Hipp_R)/2}$, where $Hipp_L$ ($Hipp_R$) is the volumes of the left (right) hippocampus in MNI152 space. We normalized patient asymmetry scores with respect to those of controls, and thresholded indices at *abs(index)* > 1.5. To calculate patient ipsilateral volume z-scores, we normalized left and right volumes for patients with respect to corresponding volumes

for controls, and thresholded ipsilateral values at z_{ipsi} < -1.5. Criteria for atrophy were met if either measure was satisfied.

Statistical Analysis

(i) Analysis of variance (ANOVA). We ran a 2x6 repeated measures mixed ANOVA which comprised one between-group factor with two levels (*i.e.*, group: HC, TLE) and one within-group factor with six levels (*i.e.*, iREP: Epi-E, Epi-D, Sem-E, Sem-D, Spa-E, Spa-D), with individual identifiers for each participant (*i.e.*, id):

$$(1)\ accuracy \sim 1 + group * iREP + Error(id/iREP)$$

(ii) Control analyses. To assess whether significant between-group differences in relational memory performance were seen above and beyond differences in socio-demographic factors (age, sex) and impairments in executive function and overall cognitive ability (EpiTrack, MoCA), we regressed out the effects of covariates of interest and refit the model using the residual scores:

$$(2)\ accuracy \sim 1 + covariate + Error \rightarrow\ residual\ accuracy$$

$$(3)\ residual\ accuracy \sim 1 + group * iREP + Error(id/iREP)$$

(iii) Partial least squares (PLS). We also used multivariate models to complement the above case-control method from a data-driven perspective. PLS is a multivariate associative technique that maximizes the covariance between two datasets by decomposing their cross-correlation matrix and deriving optimal linear combinations of the original datasets known as latent variables (LV) (Kebets et al., 2019; McIntosh & Lobaugh, 2004). Unlike the factorial nature of ANOVA, which seeks to detect significant effects among the various levels of predetermined variables, PLS aims to generate a lower-dimensional manifold of these factors that effectively recapitulates their raw

information content. In this way, PLS offers a flexible and complementary mode of analysis. We computed the cross-correlation matrix between five clinical/demographic features (*i.e.*, age, sex, group, hippocampal volume) and six iREP measurements (*i.e.*, Epi-E, Epi-D, Sem-E, Sem-D, Spa-E, Spa-D). Hippocampal volume was normalized with respect to healthy controls, averaged across hemispheres in HC, and ipsilateral to epileptogenic focus in TLE patients. We decomposed the cross-correlation matrix via singular value decomposition, which resulted in a vector of left singular values (*i.e.*, clinical saliences) characterizing a distinct phenotypic pattern for each LV, a diagonal eigenvalue (*i.e.*, singular value) matrix reflecting the covariance explained by each LV, and a vector of right singular values (*i.e.*, iREP saliences) describing a particular iREP pattern for each LV. Subject-specific composite scores were computed by projecting their original clinical and iREP data onto their respective saliences. To test for the significance of each LV, we ran 5,000 permutation tests by resampling the iREP dataset *without* replacement while iteratively realigning permuted saliences to the original ones using Procrustes rotation to obtain a distribution of null singular values. We interpreted LVs by calculating clinical and iREP loadings, which are product moment correlation coefficients between original clinical or iREP values with their corresponding composite scores (*i.e.*, linear projections of original values onto corresponding saliences). To assess the reliability of significant LVs' loadings, we applied a bootstrapping procedure with 5,000 iterations by resampling the iREP dataset *with* replacement and realigning bootstrapped saliences to the originals using Procrustes transform. We then computed *z*-scores for each variable loading by dividing the loading coefficient by its estimated standard error, which is the standard deviation of the bootstrapped distribution. Finally, we converted *z*-scores into FDR-adjusted (Benjamini & Hochberg, 1995) *p*-values ($\alpha_{FDR} = 0.05$) to determine coefficient significance.

All data and codes used in this work are openly available at:

https://github.com/MICA-MNI/micaopen/tree/master/tle_memory_manuscript_codes

3.4 RESULTS

The structure of relational memory in HC and TLE patients: ANOVA findings

First, we evaluated the Easy versus Difficult manipulation by conducting three paired sample t-tests within each cohort. In both groups, within each module, accuracy scores were significantly higher for the Easy compared to the Difficult condition (ts > 7.0, $p_{FDR} < 0.0001$, **Figure 2a**). Next, we compared accuracy on the iREP measurements between HC and TLE groups in a 2x6 repeated measures mixed ANOVA (**Figure 2b**), where we observed that performance scores on the iREP were modulated by group ($F_{2.6, 186.7} = 4.86$, $p < 0.01$, $\eta_p^2 = 0.063$). Decomposing the *group × iREP* interaction using simple main effects tests, we confirmed that HC scored significantly higher than TLE patients on nearly all measurements: Epi-E ($F_{1, 72} = 7.76$, $p < 0.01$), Epi-D ($F_{1, 72} = 15.18$, $p < 0.001$), Sem-D ($F_{1, 72} = 6.52$, $p < 0.05$), Spa-E ($F_{1, 72} = 6.16$, $p < 0.05$), and Spa-D ($F_{1, 72} = 8.02$, $p < 0.01$). In the Sem-E condition, TLE patient scores did not differ from HC ($F_{1, 72} = 0.07$, ns). Two additional control analyses in which we accounted for the effects of socio-demographics (*i.e.*, age & sex) and executive/cognitive functions (*i.e.*, MoCA & EpiTrack) confirmed the robustness of group differences in relational memory, especially along episodic and spatial domains. As in the baseline analysis, *group × iREP* interactions were significant for both covariate models (socio-demographics: $F_{2.6, 186.7} = 4.86$, $p < 0.01$; executive functions: $F_{2.5, 165.0} = 3.47$, $p < 0.05$). Of note, MoCA and EpiTrack scores were available for only a subset of the original cohort (nHC = 48/50, nTLE = 19/24). Across both control regimens, between-group differences persisted for Epi-D ($F_{1, 72} = 14.10$, $F_{1, 65} = 9.30$; ps < 0.01) and Spa-D ($F_{1, 72} = 6.54$, $F_{1, 65} = 5.62$; ps < 0.05). Findings for

Epi-E and Spa-E were significant when controlling for socio-demographics ($F_{1, 72} = 7.02$, $F_{1, 72} = 5.09$; ps < 0.05), but not when accounting for executive/cognitive functions ($F_{1, 65} = 3.30$, $F_{1, 65} = 1.74$; ps ns). Neither covariate analysis found significant between-group differences in Sem-E ($F_{1, 72} = 0.29$, $F_{1, 65} = 3.45$; ps ns).

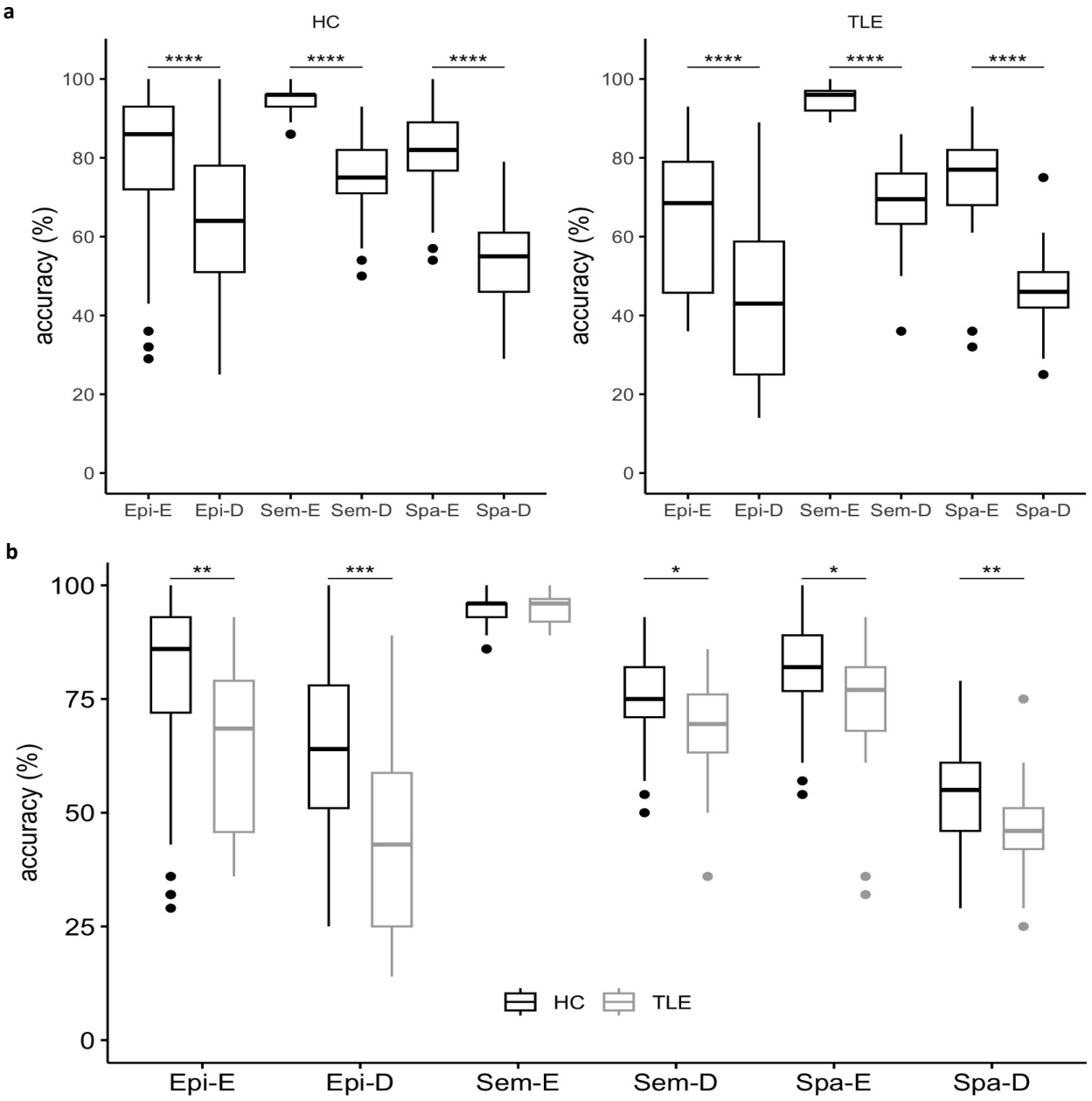

Figure 2. iREP performance. *(a)* For each group, we ran three paired sample t-tests to validate the Easy *vs*. Difficult manipulation (ts > 7.0, **** $p_{FDR} < 0.0001$). *(b)* Results from the repeated measures mixed ANOVA showed a significant *group × iREP* interaction effect ($F_{2.6, 186.7} = 4.86$, $p < 0.01$). Simple main effects tests confirmed that HC performed significantly better than TLE on Epi-E ($F_{1, 72} = 7.76$, ** $p < 0.01$), Epi-D ($F_{1, 72} = 15.18$, *** $p < 0.001$), Sem-D ($F_{1, 72} = 6.52$, * $p < 0.05$), Spa-E ($F_{1, 72} = 6.16$, * $p < 0.05$), and Spa-D ($F_{1, 72} = 8.02$, ** $p < 0.01$). There was no group difference in Sem-E ($F_{1, 72} = 0.07$, ns).

The structure of relational memory in individuals with TLE and controls: PLS findings

ANOVA findings were complemented by our PLS results, which revealed that age, group, and hippocampal volume contributed to relational memory performance. The first latent variable (LV1) obtained via the decomposition of the cross-correlation matrix between clinical phenotypes and iREP accuracies accounted for 86% of total covariance (**Figure 3a, left**). The correlation between corresponding clinical and behavioral composite scores along LV1 was also significant, as attested by permutation tests ($r = 0.46$, $p_{perm} < 0.001$, **Figure 3a, right**).

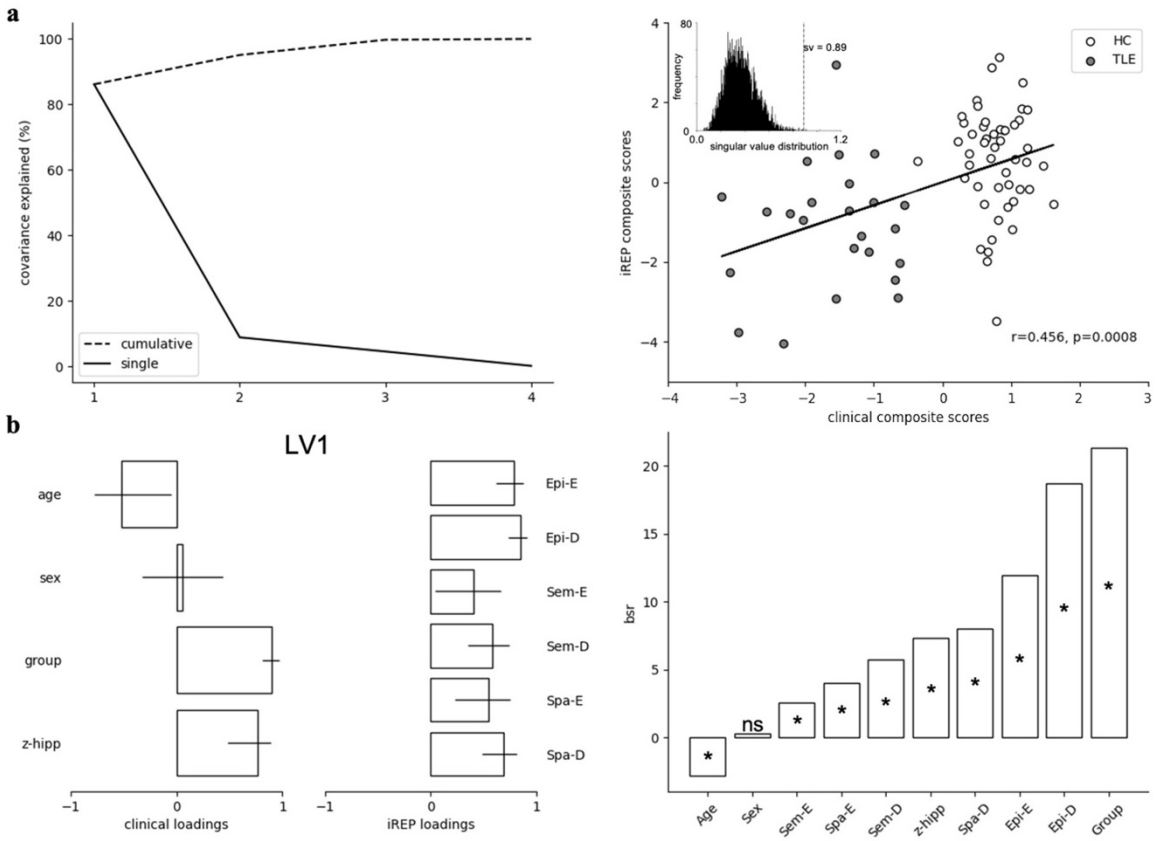

Figure 3. PLS. *(a) left:* the first latent variable (LV1) accounted for 86% of the covariance between four clinical features (*i.e.*, age, sex, group, and hippocampal volume) and six iREP measurements (*i.e.*, Epi-E, Epi-D, Sem-E, Sem-D, Spa-E, and Spa-D). *right:* the association between clinical and iREP composite scores along LV1 was significant ($r = 0.46$, $p_{perm} < 0.001$) as attested by 5,000 permutations (inset: dashed line "sv" represents the actual singular value). *(b) left:* clinical and iREP loadings (95% CIs calculated by bootstrapping). *right:* loading reliabilities were determined by *z* score estimation via bootstrapped ratios (bsr) for each variable by dividing loading coefficients by the estimated standard error derived from 5,000 bootstraps. *Z* scores were adjusted for FDR (* $p_{FDR} < 0.05$).

Additional bootstrapping evaluated the robustness of loadings along LV1 (age: -0.52, sex: 0.05, group: 0.90, normalized hippocampal volume: 0.77, Epi-E: 0.79, Epi-D: 0.85, Sem-E: 0.40, Sem-D: 0.58, Spa-E: 0.55, Spa-D: 0.69, **Figure 3b, left**). Except for sex (z = 0.29, p_{FDR} ns), all other variables presented with significantly reliable loadings (age: z = -2.72, group: z = 21.17, normalized hippocampal volume: z = 7.39, Epi-E: 11.87, Epi-D: 18.81, Sem-E: 2.56, Sem-D: 5.79, Spa-E: 4.18, Spa-D: 8.04, all $p_{FDR} < 0.05$, **Figure 3b, right**). Thus, younger age, allocation to the HC cohort, and larger total hippocampal volumes were associated with better performance across all tasks, and while the iREP pattern was shared across modules, episodic accuracies showed highest contributions, followed by spatial, and finally semantic, validating our ANOVA findings. Overall, diagnostic group and episodic scores were the most important features of LV1.

3.5 DISCUSSION

Our objective was to analyze the pattern of behavioral impairments across relational memory domains in patients with TLE, the most common pharmacoresistant epilepsy in adults and a human disease model of memory dysfunction. We compared the performances of TLE patients to those of age- and sex-matched healthy controls on the different modules of the iREP, a recently developed cognitive assessment tool. The iREP is a comprehensive battery that includes three complementary and homogenous tasks that collectively tap into the episodic, semantic, and spatial memory systems. Modules are further stratified into two conditions that correspond to levels of difficulty, thus offering two degrees of probing resolution into each cognitive domain. In addition to verifying the task difficulty manipulation via paired student t-tests, we applied a repeated measures ANOVA in conjunction with PLS analysis to identify module-specific associations in

behavioral scores across groups and iREP measurements, and to discern latent associative patterns between clinical features and performance scores.

Our ANOVA results confirmed that TLE patients were considerably impaired on the episodic module, a finding that expands on an already well-established scientific corpus (Hoppe et al., 2007; Spiers et al., 2001; Tavakol et al., 2019; Thom, 2014; Viskontas et al., 2000). Also, PLS analysis revealed that group allocation and performance scores on both conditions of the episodic task were the strongest contributors to the first PLS latent variable, further validating the notion of episodic deficits in TLE. We identified additional contributions from the volume of the hippocampus, supporting a potential link between the integrity of the hippocampi and relational cognition in general, and episodic memory specifically. Age was another important contributor to overall relational memory capacities. The decline in hippocampal contributions to relational memory performance in TLE is related to many factors, including subregional structural pathology (Bernhardt et al., 2015), disruptions in connectivity patterns (Bernhardt et al., 2016), and functional reorganization (Postma et al., 2020). Overall, our PLS findings confirmed a relationship between clinical presentation and general mnemonic ability, where younger age, lower hippocampal volume, and TLE diagnosis were associated with poor behavioral performance, especially on the episodic module. We were also interested in whether socio-demographic factors such as age and sex and more general impairments in cognitive and executive function, attention, and processing speed might have contributed to the observed between-group differences in episodic memory (Höller et al., 2020; Xiao et al., 2021). Thus, we ran additional control analyses that accounted for these covariates. In addition to controlling for age and sex, we also administered supplemental behavioral screening tools to ensure that group disparities were not driven solely by

neurobehavioral differences in other domains. Specifically, we used the EpiTrack and MoCA (Lähde et al., 2021; Lutz & Helmstaedter, 2005; Nasreddine et al., 2005), which are designed to track deficits in executive function and attention as well as mild cognitive impairment and dementia, respectively. Group differences in episodic memory persisted even after controlling for these covariates, suggesting that TLE-associated impairments in this domain are not uniquely mediated by socio-demographic variables or non-relational cognitive processes.

In addition to episodic memory deficiency, we identified impaired spatial cognition in our TLE group. Simulation models of spatial processing in conjunction with findings in healthy controls and individuals with focal hippocampal damage, including TLE patients, point to a fundamental role of the hippocampus in allocentric spatial memory, which involves the three-dimensional relations between objects in an environment independent of the subjective viewpoint (Bicanski & Burgess, 2018; Byrne et al., 2007; Dhindsa et al., 2014; Hartley et al., 2007), with the volume of the hippocampus further associated with proficiency in this allocentric domain (Abrahams et al., 1999; Hartley & Harlow, 2012; Maguire et al., 2000). We had previously shown that in a group of healthy individuals, performance on the Difficult condition of the spatial task (Spa-D) correlated with the Four Mountains Task (Tavakol et al., 2021), an established protocol for examining allocentric spatial memory in clinical populations that present with localized hippocampal pathology and mild cognitive impairment (Chan et al., 2016; Hartley et al., 2007). Therefore, we were expecting to see indications of spatial deficits in our TLE cohort. Indeed, our ANOVA findings showed that TLE patients clearly underperformed on the spatial module compared to controls. Specifically, results seemed to have been driven primarily by Spa-D accuracies, given how strongly they contributed to the first PLS latent variable, in addition to the absence of cross-

cohort differences in Spa-E when accounting for EpiTrack and MoCA scores. These observations indicate that the Difficult condition of the spatial task is well adapted for identifying behavioral impairments in spatial cognition. Moreover, they build upon findings in kindling models of epilepsy, where interictal epileptiform discharges are mimicked via successive electrically induced seizures, whereby disruptions of physiological sharp-wave ripples (100-200 Hz) in the hippocampus have been shown to compromise spatial memory consolidation (Ego-Stengel & Wilson, 2009; Gelinas et al., 2016; Girardeau et al., 2009). Our results are also in agreement with previous observations made in pre- and post-surgical TLE patients, where low IQ, age of onset, and epilepsy duration were associated with poor navigational skills on the Hidden Goal Task, a human analogue of the rodent Morris Water Maze (Amlerova et al., 2013). Additional evidence for spatial impairment in individuals with TLE has been reported using virtual reality paradigms, such as the Boxes Room, where patients committed more errors and travelled longer distances to a goal location than did controls (Cánovas et al., 2011; Glikmann-Johnston et al., 2008; Rosas et al., 2013). While TLE-related spatial deficits are not as well documented as episodic memory impairments, the findings we have presented here expand on these previous observations and provide support for the notion that atypical behavioral phenotypes in spatial memory may present an intermediary feature between those associated with episodic and semantic memory.

Group differences were less well defined on the semantic module, as HC scored higher than TLE patients on the difficult condition only, and even then, group differences vanished when controlling for socio-demographic or other cognitive covariates. Unlike the episodic and spatial tasks, which encompass built-in phases for stimulus encoding and retrieval, the semantic protocol consists of retrieval only. Presumably, the underlying conceptual associations between objects required to

complete this module successfully were incidentally and repeatedly encoded throughout the participant's lifetime, implicating long-term memory consolidation, which benefits not only from hippocampal but also non-hippocampal neocortical contributions (Klinzing et al., 2019), with further evidence suggesting that the neocortex can rapidly form conceptual associations independent of the hippocampus (Sharon et al., 2011). Indeed, where TLE patients have been shown to present with semantic deficits, faulty encoding of novel conceptual relations has been suggested as a potential cause (Helmstaedter et al., 1997). This consideration is in line with the complementary learning systems framework, which posits a division of labour underlying memory and learning, whereby the hippocampus rapidly encodes non-overlapping episodic representations that are gradually consolidated into a latent semantic structure across the neocortex through interleaved reinstatement of episodic engrams (McClelland et al., 1995; O'Reilly et al., 2014). Likewise, the multiple trace theory stipulates a resilience of the semantic memory system to lesions of the hippocampus, a structure, which, in contrast to its recurrent involvement in binding disparate neocortical patterns that code for either episodic or spatial information, is surmised to be only transiently active in the context of semantic cognition (Nadel et al., 2000). In addition, we also note that semantic impairments in people with TLE are typically measured using visual confrontation naming tasks like the Boston Naming Test, which, while suitable for identifying dysnomia, do not necessarily tap into semantic association processes *per s*e (Bell et al., 2001; Giovagnoli et al., 2005). In fact, TLE patients seem to be relatively intact on semantic assessment protocols similar to our own where conceptual judgment is required (Giovagnoli et al., 2005; Lambon Ralph et al., 2010), such as the Intelligenz-Struktur-Test, where an outlier must be selected out of five lexical alternatives (*i.e.*, sitting, lying, *going*, kneeling, standing) (Helmstaedter, 2002). While research is ongoing to elucidate the network dynamics involved in verbal deficiencies

associated with TLE (Trimmel et al., 2018), behavioral divergence across verbal and non-verbal domains may offer an avenue for mapping out phenotypic differences between TLE and other similar neurological conditions, such as semantic dementia, in which patients appear to be impaired on both domains (Bozeat et al., 2000). Even though the semantic module of the iREP is a valid test of general conceptual knowledge (Sormaz et al., 2017; Tavakol et al., 2021; Wang et al., 2018), the absence of a significant between-group difference on Sem-E in the current work does not necessarily entail that TLE patients might be unaffected on more sensitive measures of semantic cognition, as it has been shown that impairments may emerge if tasks are sufficiently difficult (Lambon Ralph et al., 2012), which is also supported by our findings on Sem-D. Based on these considerations, we can conclude that TLE-related impairments in memory of general associations between everyday items only become observable when these associations are sufficiently weak, with socio-demographic variables such as age and sex as well as impairments in other more general cognitive areas further compacting semantic deficits.

Collectively, our results demonstrate atypical behavioral patterns of relational memory in TLE patients. They point to impairments in episodic and spatial memory that are associated with variations in age and hippocampal volume, with memory for general semantic associations remaining relatively intact. These findings imply a hierarchical pattern of relational memory dysfunction related to medial temporal lobe pathology, with the episodic domain being more affected than the spatial domain, and the semantic system being the least affected. We acknowledge a range of limitations of the current work, however. First, given stringent diagnostic criteria for inclusion in our TLE cohort, we studied only a relatively modest sample of 24 pharmacoresistant patients. Seizure onset, seizure laterality, and hemispheric dominance are likely important

contributors to behavioral outcomes, yet we needed to omit them from our study because of sample size constraints. With ongoing expansion of our patient cohort, we hope to eventually account for these factors. Furthermore, our task was administered in a controlled laboratory experiment (in our case in the MRI scanner). This might have, at least in part, contributed to reduced behavioral performance, a finding to be verified using ecologically more valid tasks in future work. Even so, our initial observations already provide novel and detailed insights into differential impairments across relational memory domains accompanying hippocampal damage in TLE patients, warranting complementary investigations into underlying neural substrates. Notably, task paradigm and analysis scripts are openly available, with the hope of facilitating adoption of our assessment as well as independent replication of our findings.

3.6 SUPPLEMENTARY FIGURE

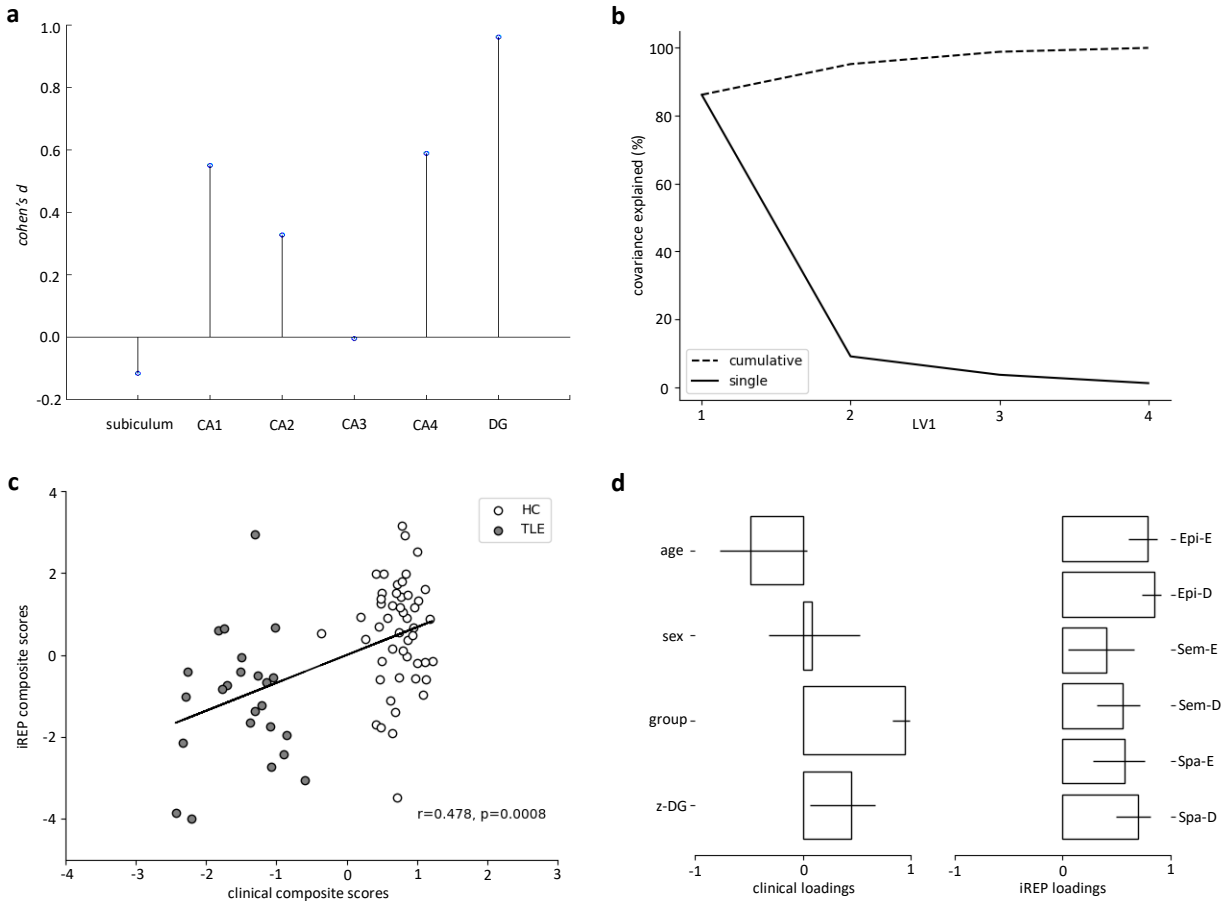

Supplemental figure. *(a)* Between-group *cohen's d* metrics were computed for normalized hippocampal subfield volumes when controlling for age and sex. The largest effect size was observed for the dentate gyrus. *(b)* We ran the same PLS analysis as in the main study using normalized DG volumes instead of total hippocampal volume. LV1 accounted for nearly 90% of the covariance explained in this regimen. *(c)* Composite scores were significantly correlated along LV1. *(d)* The multivariate pattern of loadings along LV1 closely mirrored original findings.

In the previous two sections, we leveraged the iREP to identify consolidated structure-function substrates of relational memory in healthy individuals in addition to establishing the presence of a hierarchical pattern of TLE-associated cognitive impairments across domains, with the episodic being most affected, the semantic being least affected, and the spatial system showing an intermediary phenotype. In the next and final section (Project III), we aim to uncover functional brain organizations that may underlie domain and group differences in relational memory capacity. We additionally seek to identify a lower-dimensional functional motif that may be conserved across relational components. Thus, we conduct a series of iREP module-specific multivariate investigations that analyze the covariation between hidden features of task-based functional connectivity and behavioral-demographic phenotypes. We run supplementary cross-module hybrid analyses to uncover the level of convergence/divergence across relational domains. First, we identify module-specific latent connectivity patterns that are associated with variations in age, diagnostic group, and performance scores, harkening back to Project II findings. Next, we confirm the existence of a lower-dimensional functional topography within the limbic network that is linked to a multivariate profile consisting of younger, healthy individuals who present with relatively high behavioral scores across all iREP measurements. Moreover, we detect altered whole-brain functional integration of the default mode network (DMN) in older, TLE patients who perform relatively poorly on the iREP, which may reflect underlying TLE-associated structural-functional pathology.

4 PROJECT III: multivariate profiles of relational memory

This section presents preliminary results pertaining to task-based functional connectivity.

MULTIVARIATE BEHAVIORAL AND FUNCTIONAL PATTERNS OF RELATIONAL MEMORY

Shahin Tavakol[*], Valeria Kebets[*], Jessica Royer[*], Qiongling Li[*], Hans Auer[*], Elizabeth Jefferies[&], Lorenzo Caciagli[†], Birgit Frauscher[Ψ], Jonathan Smallwood[+], and Boris Bernhardt[*#]

[*]*McConnell Brain Imaging Centre, Montreal Neurological Institute and Hospital, McGill University, Montreal, Canada*
[&]*University of York, York, United Kingdom*
[†] *Department of Bioengineering, University of Pennsylvania, Philadelphia, USA and UCL Queen Square Institute of Neurology, London, United Kingdom*
[Ψ]*ANPHY lab, Montreal Neurological Institute and Hospital, McGill University, Montreal, Canada*
[+]*University of Queens, Kingston, Ontario, Canada*
[#]*Department of Neurology and Neurosurgery, Montreal Neurological Institute and Hospital, McGill University, Montreal, Canada*

CORRESPONDENCE TO:
Boris Bernhardt, PhD
Associate Professor of Neurology and Neurosurgery
Montreal Neurological Institute and Hospital, McGill University
Email: boris.bernhardt@mcgill.ca

Shahin Tavakol, PhD candidate
Email: shahin.tavakol@mail.mcgill.ca

4.1 ABSTRACT

OBJECTIVE. Prior work has shown a graded pattern of behavioral impairments in relational memory in temporal lobe epilepsy (TLE). The underlying network-level functional dynamics of these behavioral presentations are unclear. The aim of this study was to examine the convergence of functional topographies across relational memory domains in TLE patients and controls.

METHODS. We administered a novel relational memory paradigm to evaluate episodic, semantic, and spatial memory in 24 pharmacoresistant TLE patients and 50 age- and sex-matched healthy controls while they underwent scanning. We conducted separate partial least squares (PLS) correlation analyses in each memory domain to ascertain associations between behavioral accuracies and task-based functional connectomes. We additionally ran hybrid analyses in which we used PLS-derived functional connectivity saliences in one domain to predict latent patterns of behavioral-functional association in the other two domains.

RESULTS. Across episodic, semantic, and spatial dimensions, TLE patients presented with patterns of functional connectivity that differed from controls, who exhibited latent connectivity topographies that converged within the limbic system. TLE patients displayed heightened whole-brain DMN functional integration, especially during episodic processing, and presented with cortical patterns that may indicate compensatory functional mechanisms for underlying MTL alterations.

SIGNIFICANCE. Our findings show altered functional dynamics in TLE that are associated with poor relational memory performance. They further shed light on common as well as domain-specific cortical topographies in healthy controls that underlie better behavioral outcomes.

Key words: relational memory, temporal lobe epilepsy, hippocampus, functional connectivity

4.2 INTRODUCTION

Relational memory consists of different types of associative mental faculties that generally fall into three main categories: episodic, semantic, and spatial. Each domain is defined by the capacity to bind singular elements of subjective experience into an integrated cognitive model that can inform subsequent thoughts and behaviors (Bellmund et al., 2018; Eichenbaum & Cohen, 2001; Olsen et al., 2012). In episodic memory, distinct spatiotemporal events combine to form a continuous thematic narrative known as an episode (Tulving, 1983; Tulving, 2002). In semantic memory, separate concepts merge into superordinate categories of meaning (Cutler et al., 2019; Helmstaedter et al., 1997; Solomon & Schapiro, 2020), whereas in spatial memory, the locations of distinct items consolidate into a broad mental construct known as a cognitive map (O'Keefe & Nadel, 1978). Since the late 1950s, the study of relational memory in humans has gone hand in hand with investigations specific to temporal lobe epilepsy (TLE), which is the most common pharmacoresistant form of the condition that presents with sclerotic lesions of the hippocampus (Tavakol et al., 2019). With over six decades of ongoing scientific work dedicated to disease-associated impairments in relational memory, TLE is widely regarded as the leading human model of memory dysfunction (Barrett Jones et al., 2022; Breier et al., 1996; Helmstaedter et al., 1995; Li et al., 2021; Mayeux et al., 1980; Penfield & Milner, 1958; Rugg et al., 1991; Scoville & Milner, 1957; Sideman et al., 2018; Voets et al., 2009; Yoo et al., 2006; Zanao et al., 2023).

A common methodological approach for studying cognition is to anchor behavioral phenotypes to whole-brain markers derived from the intrinsic functional architecture of the brain as measured by resting-state functional MRI (rs-fMRI) (He et al., 2020; Medea et al., 2018; Smith et al., 2015; Sormaz et al., 2017). Despite the relative stability of intrinsic networks against task-elicited

perturbations, new evidence suggests that active state neural dynamics may offer superior resolution into cognitive processes (Cole et al., 2021), which is why recent efforts have capitalized on functional connectomics derived from task-based fMRI paradigms to study relational memory (Subramaniapillai et al., 2022). Coupled with multivariate associative techniques, such as partial least squares (PLS), which identifies a common manifold of maximal covariance between different datasets (Kebets et al., 2019; McIntosh & Lobaugh, 2004), task-based functional connectivity can provide great insights into shared and unique multivariate substrates of relational memory. Currently, findings from contemporary neuroimaging studies point to a wide range of neural markers that sometimes overlap across relational domains. For instance, the ventromedial prefrontal cortex (vmPFC) and anterior temporal lobe (ATL) play an important role in the consolidation of episodic memory traces by virtue of connections with the anterior hippocampus (Eichenbaum, 2017; Moscovitch et al., 2016). In fact, the ATL is believed to be especially critical in semantic cognition along with the inferior frontal gyrus (IFG), with specific contributions to word processing from the left hemisphere, and bilateral involvement for pictorial stimuli (Hoffman & Morcom, 2018; Jackson, 2021; Rice et al., 2015). In spatial processing, the evidence points to a major engagement of the retrosplenial, parahippocampal, and posterior parietal cortices (Baumann & Mattingley, 2021; Qiu et al., 2019). Moreover, the underlying structures of the medial temporal lobes (MTL), including the hippocampal-entorhinal complex, are consistently recruited to sustain domain-invariant relational processes, a common feature across memory types (Aguirre & D'Esposito, 1997; Binder & Desai, 2011; Binder et al., 2009; Hassabis et al., 2009; Jefferies, 2013; Jokeit et al., 2001; Moscovitch et al., 2016; Rugg & Vilberg, 2013; Schindler & Bartels, 2013). While efforts are ongoing to further understand shared and unique neural correlates of relational

memory, a neuroimaging platform that can tap into all three domains within the same individuals could significantly enhance cross-cohort multivariate analyses of behavior, structure, and function.

In previous works, we implemented the integrated Relational Evaluation Paradigm (iREP) to detect multimodal markers of spatial cognition within medial and lateral temporal cortices in the healthy brain (Tavakol et al., 2021) in addition to uncovering a graded pattern of behavioral deficits across relational domains in patients diagnosed with TLE (Tavakol et al., 2022). The iREP is a recently developed and open-access multidomain task battery that is optimized for administration inside the MRI environment. It consists of three modules that collectively assess episodic (*i.e.*, Epi), semantic (*i.e.*, Sem), and spatial (*i.e.*, Spa) memory. Each task is further modulated for difficulty across Easy and Difficult conditions (*i.e.*, E *vs.* D). Thus, the iREP comprises six outcome measures (*i.e.*, Epi-E, Epi-D, Sem-E, Sem-D, Spa-E, and Spa-D) that can be leveraged to perform graded multidomain cross-cohort analyses of relational cognitive processes. In the current study, we aimed to identify multivariate substrates specific to each cognitive domain of relational memory, in addition to elucidating how these markers vary as a function of neurological status. To this end, we studied a group of TLE patients presenting with lesions to the structures of the medial temporal lobe and age- and sex-matched healthy controls. We conducted a series of PLS correlational analyses based on participant demographics, iREP behavioral scores, and functional connectomes derived from iREP task-fMRI data. We hypothesize that each type of relational memory will display its own unique multivariate profile, where younger age, better task performance, and absence of TLE diagnosis will be associated with domain-specific patterns of neocortical connectivity.

4.3 METHODS

Participants

We studied the same subjects as in (Tavakol et al., 2022). In short, the clinical cohort consisted of 24 pharmacoresistant TLE patients (12 women, mean age ± SD: 35.0 ± 11.5 years, range: 18–57, 2 ambidextrous), and the control group comprised 50 age- and sex-matched HC (20 women, 32.0 ± 7.8 years, range: 19-57 years, 5 left-handed). All participants had normal or corrected-to-normal vision, and had provided written and informed consent to partake in our study, which was approved by the Research Ethics Committee of the Montreal Neurological Institute and Hospital.

Relational memory phenotyping

The *integrated Relational Evaluation Paradigm* (iREP) is a relational memory assessment framework (https://github.com/MICA-MNI/micaopen/task-fMRI) (Tavakol et al., 2022; Tavakol et al., 2021). It comprises three domain specific modules (Episodic, Semantic, and Spatial) that can be completed in the laboratory or inside the MRI scanner environment. All tasks are homogenized via *(i)* the use of pictorial stimuli taken from a pooled custom-made and semantically-indexed library, *(ii)* the modulation of task difficulty across two conditions (*i.e.*, Easy *vs.* Difficult) with a pseudo-randomized trial presentation order, and *(iii)* the implementation of a 3-alternative forced choice trial-by-trial design. Each module contains four stimulus lists (*i.e.*, A, B, C, and D) for inter-individual counterbalancing and/or longitudinal administration. All participants were evaluated on the iREP inside the MRI scanner and manipulated an MRI-compatible response box to provide their answers.

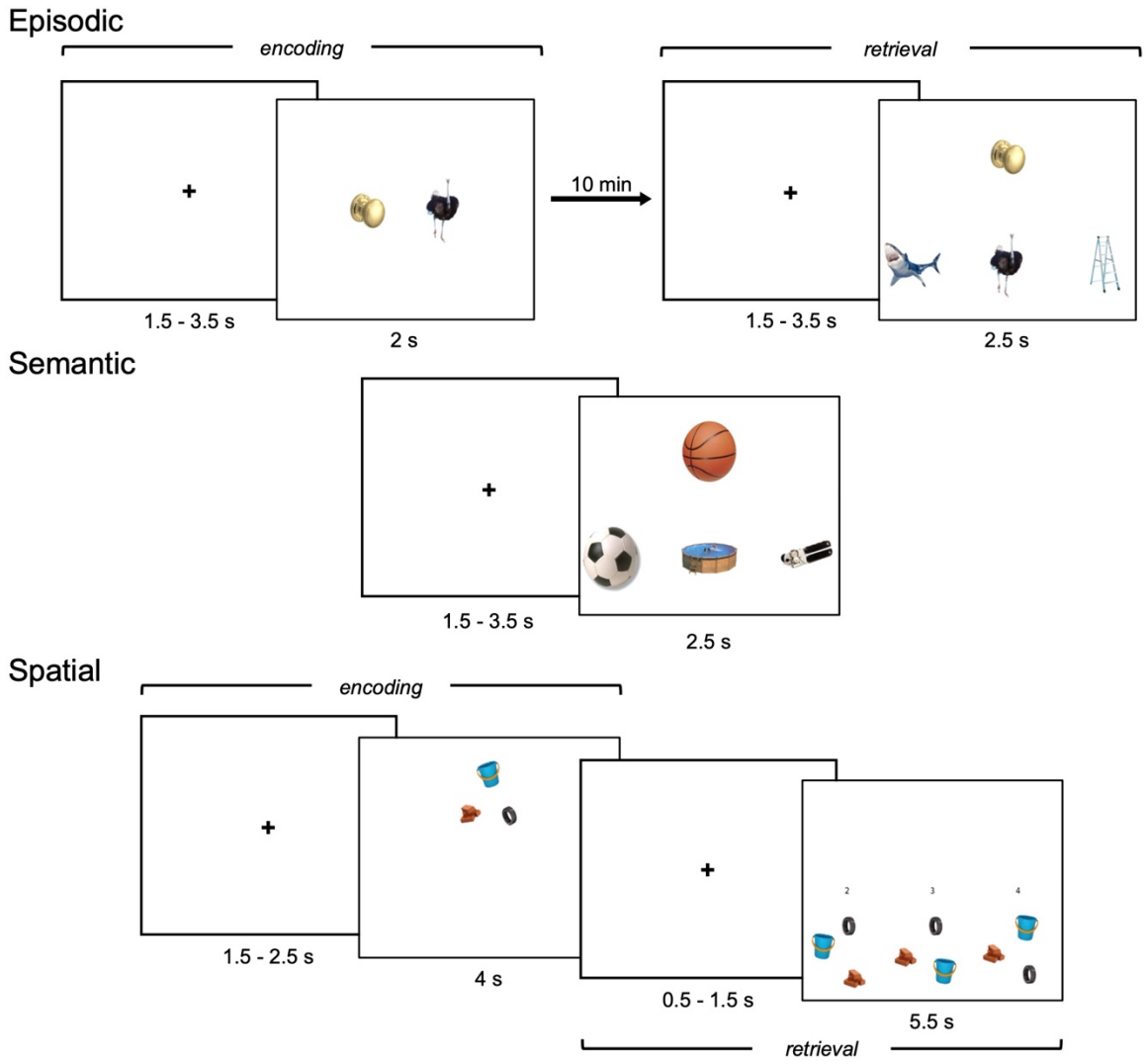

Figure 1. Trial design for each iREP module. *(top row)* The Episodic task consists of two separate runs. During Encoding, object pairs must be memorized. After a 10-minute break during Retrieval, the item that was originally paired with the top image must be recalled among three options. *(middle row)* In the Semantic task, the item that is the most conceptually congruent with the top object must be selected out of three choices. *(bottom row)* During the Spatial task, the configuration of three items must initially be encoded (*encoding*). Within the same trial, the original spatial arrangement must be chosen out of three options (*retrieval*). Numbers are there to visually aid participants on which response key to press. Overall durations for stimuli and inter-stimulus intervals are shown for each module.

(i) Episodic module. This task uses pictorial stimuli and is based on an established lexicon-based episodic memory paradigm (Payne et al., 2012; Sormaz et al., 2017), which includes an encoding and a retrieval phase (**Fig. 1: top row**). During encoding (~6 minutes), participants memorize pairs of unrelated items (*i.e.*, doorknob and ostrich), with half of the stimuli displayed once throughout

the run for a total of 28 trials (*i.e.*, Difficult condition), and the other half, twice for a combined 56 trials (*i.e.*, Easy condition). Following a 10-min interval, the retrieval phase (~4.5 minutes) is administered during which, at each trial, one item is displayed at the top of the screen (*i.e.*, doorknob) and three others, at the bottom (*i.e.*, shark, ostrich, and ladder). Participants must then select the object that was originally paired with the top item during encoding.

(ii) Semantic module. The task implements symbolic stimuli and is modeled on an established lexicon-based semantic association protocol (Sormaz et al., 2017; Wang et al., 2018) (**Fig. 1: middle row**), consisting of 56 pseudo-randomized trials (~4.5 minutes) with two conditions of equal length (*i.e.*, 28 Difficult: Sem-D; 28 Easy: Sem-E). At each trial, a reference object appears at the top of the monitor (*i.e.*, basketball) with three stimuli below (*i.e*., soccer ball, above ground pool, can opener). Participants must choose the option that is semantically most related to the object displayed at the top. Pairwise conceptual affinity indices (*cai*) were computed (range: 0-1) based on internet-based lexical corpora (Han et al., 2013). In Sem-E trials, the correct response (*i.e.*, soccer ball) and the top image (*i.e.*, basketball) are related by $cai > 0.66$; in Sem-D trials, the similarity index is given by $0.33 \leq cai \leq 0.66$. Regardless of condition, the conceptual relatedness of the top stimulus and the foils (*i.e.*, above ground pool, can opener) is always $cai < 0.33$.

(iii) Spatial module. Spatial memory was assessed using a recently validated symbolic-based test, referred to elsewhere as the Conformational Shift Spatial Task (Tavakol et al., 2021) (**Fig. 1: bottom row**). This module consists of 56 pseudo-randomized trials (~12.5 minutes), with two conditions (*i.e.*, 28 Difficult: Spa-D; 28 Easy: Spa-E). At each trial, participants first encode the spatial arrangements of three items, and then select the same configuration among three options in

a delayed-onset design. In Spa-D trials, the two distractor layouts are very similar to the target conformation as only the spacings between objects differ. In the Spa-E trials, the relative position of each item within the configuration is additionally modified.

MRI Acquisition

We described our MRI data acquisition protocol in (Tavakol et al., 2022; Tavakol et al., 2021). Briefly, all data were acquired on a 3 T Siemens Magnetom Prisma-Fit with a 64-channel head coil. Two identical T1-weighted (T1w) scans were obtained with a 3D-MPRAGE sequence (0.8 mm isotropic voxels, matrix = 320 × 320, 224 sagittal slices, TR = 2300 ms, TE = 3.14 ms, TI = 900 ms, flip angle = 9°, iPAT = 2). The three modules of the iREP were administered inside the scanner to participants, and task-based fMRI time series were collected using a 2D echo planar imaging sequence (3.0 mm isotropic voxels, matrix = 80 × 80, 48 slices oriented to AC-PC-30 degrees, TR = 600 ms, TE = 30 ms, flip angle = 50°, multiband factor = 6).

Functional MRI Processing

Functional MRI data were processed using micapipe, the details of which have been described elsewhere (Cruces et al., 2022). In brief, steps include the omission of the first five volumes to allow for magnetic field saturation, realignment of remaining volumes to the first scan, distortion correction using main phase and reverse phase field maps, high-pass filter, and nuisance variable signal removal via ICA-FIX. A boundary-based registration is then applied to average volumetric time series for registration to native FreeSurfer space. Finally, native cortical time series are mapped onto standard surface templates (*i.e.*, fsaverage5 and conte69) via trilinear interpolation before undergoing spatial smoothing (Gaussian kernel, FWHM = 10 mm).

Statistical Analysis

Task-based functional connectome computation. Each participant had three cortical time series registered to conte69 surface template, one for each iREP task. Of note, since the Episodic module comprised two separate runs, one for encoding and one for retrieval, and given that we were interested in subjective responses, only the retrieval phase was used for our analyses. Due to computational overhead, we downsampled the conte69 time series, which counted more than 64K vertices, to the Schaefer parcellation scheme with only 400 cortical regions. For each task, we generated mean functional connectivity profiles by cross correlating all parcel-wise time series and then averaging the resulting pairwise correlation coefficients within each parcel, yielding a 1 x 400 matrix. Lastly, we applied a Fisher Z-transform to the mean functional connectivity coefficients.

Partial least squares (PLS). In this study, we implemented PLS correlation analysis to uncover latent variables (LVs) derived from two distinct datasets that maximize their shared variance (Kebets et al., 2019; McIntosh & Lobaugh, 2004; Tavakol et al., 2022). We ran three separate PLS analyses, one for each iREP module, in which we examined task-specific demographic/behavioral and mean functional connectivity data. For example, in the scheme pertaining to the Semantic module, the first dataset included subject-specific information on age, sex, group, and performance scores for Sem-E and Sem-D, while the second dataset contained the corresponding parcellated mean functional connectivity profiles computed for the Semantic task. After cross correlating both datasets, we decomposed the resulting matrix via singular value decomposition, which yielded a vector of left singular values (*i.e.*, demographic/behavioral saliences) that describe a particular pattern of demographic and task performance observations for each LV, a diagonal output of scaled eigenvalues that recapitulate the covariance explained by each LV, and a vector of right singular

values (*i.e.*, mean functional connectivity saliences) that define specific task-based functional connectome motifs for each LV. We then computed composite scores for all variables by projecting values from the original two datasets onto their corresponding saliences (*i.e.*, calculating the dot product). We assessed the statistical significance of associations along each LV by comparing its actual singular value to a null distribution generated via 10,000 permutations (*i.e.*, resampling demographic/behavioral variables *without* replacement). For every demographic/behavioral and functional connectome variable, we calculated a loading factor, which is the product moment correlation coefficient between its original value and its computed composite score. We assessed loading reliability along LVs showing significance by applying a bootstrapping regimen with 10,000 iterations (*i.e.*, resampling *with* replacement). Specifically, we calculated 95% confidence intervals for each loading based on the bootstrapped samples. If the interval did not cross zero, then the variable in question was deemed to be a robust contributor to the overall pattern observed along the given LV. Procrustes transforms were applied to permuted singular values and bootstrapped saliences to ensure proper alignment with the original observations.

Complementary cross-module comparative analyses. We conducted additional procedures in which we integrated results obtained across the separate task-specific PLS regimens. To determine the degree of convergence between the different task-derived connectivity loadings, we calculated the product-moment correlation coefficient of every task pair and evaluated the levels of significance by running 10,000 permutations in which task loadings were resampled without replacement. We also accounted for multiple comparisons, further adjusting permutation-derived p-values by controlling for the false discovery rate (FDR) (Benjamini & Hochberg, 1995). For visual inspection of cortical patterns, task loadings were stratified according to the 17 Yeo

networks (Yeo et al., 2011) by averaging values across parcels within each network region. Moreover, to establish the existence of shared information between connectivity manifolds across tasks, we computed cross-module latent correlations where we first projected the connectivity profiles of one task onto the connectivity saliences of another, and then correlated the resulting hybrid scores with corresponding demographic/behavioral scores derived in the previous section. For example, to determine whether semantic functional connectivity can explain hidden multivariate episodic features, we (1) generated hybrid "epi x *sem*" connectome scores by computing the dot product between episodic mean connectivity profiles and semantic connectivity saliences obtained via singular value decomposition (see previous section), (2) calculated the product-moment correlation coefficient between hybrid connectome scores and demographic/behavioral scores derived during the episodic PLS scheme, and (3) executed 10,000 permutation tests to assess the significance of the association between latent composite scores. In this case, each permutation was conducted by resampling (without replacement) the episodic demographic/behavioral scores before correlating them with the hybrid functional connectivity scores. For each cross-module scheme, the resulting permutation p-values were additionally FDR-adjusted. Of note, hybrid analyses were performed along latent variables that were deemed significant as per the previous PLS procedures.

4.4 RESULTS

PLS analyses

Episodic regimen

In the analytical scheme pertaining to the episodic module, the first PLS latent variable (epi-LV1) accounted for 55.8% of the total covariance between demographic/behavioral and episodic mean

functional connectome observations (**Figure 2a**). Permutation tests also confirmed the significance of the latent association between epi-LV1 composite scores ($r = 0.66$, $p_{perm} < 0.05$, **Figure 2b**).

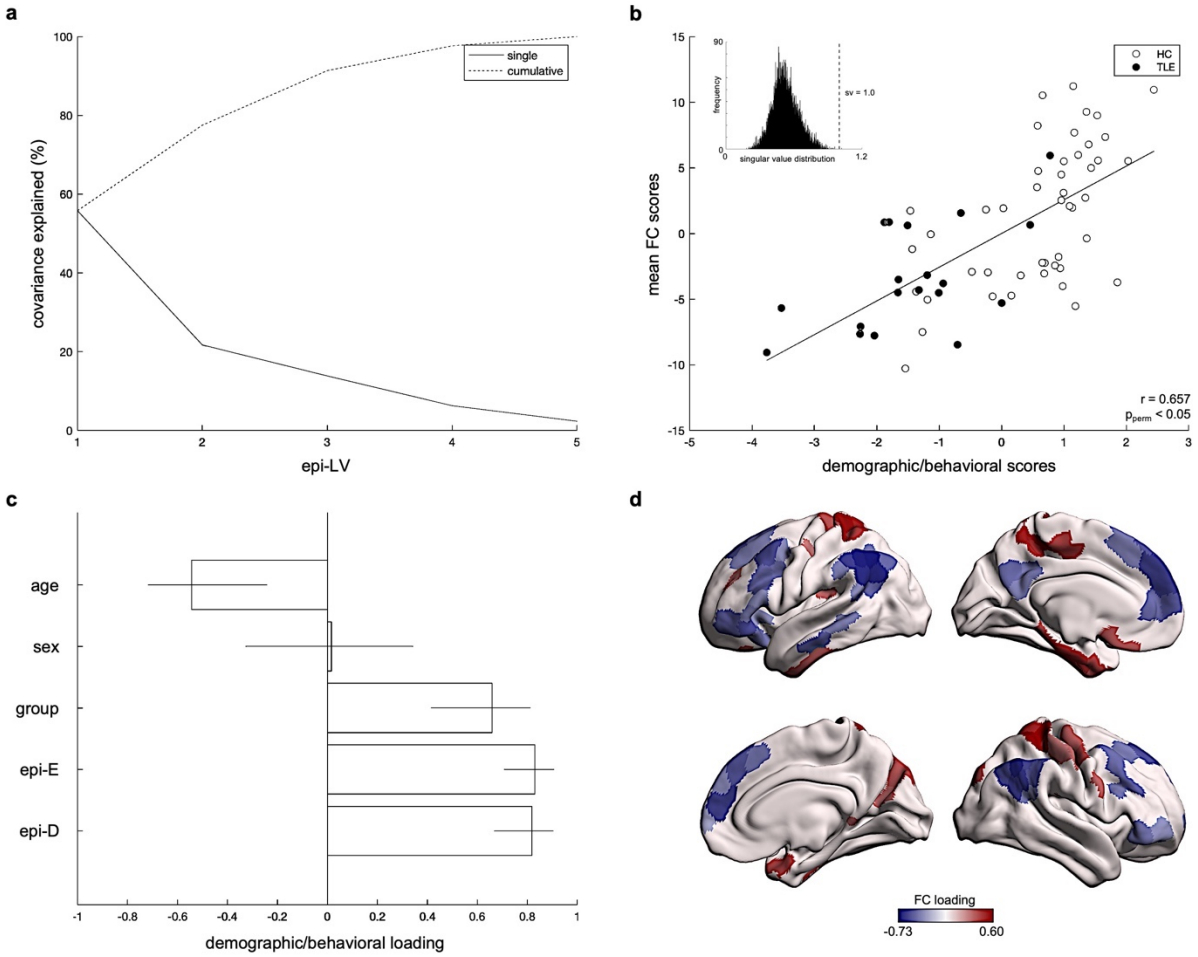

Figure 2. PLS results for Episodic. *(a)* epi-LV1 accounted for 55.8% of the total covariance between demographic/behavioral measurements and mean FC profiles. *(b)* the correlation between composite scores along epi-LV1 was significant ($r = 0.66$, $p_{perm} < 0.05$) as attested by 10,000 permutations (inset: dashed line "sv" represents the actual singular value). *(c)* age, group, epi-E, and epi-D (but not sex) showed robust contributions to epi-LV1. *(d)* whole-brain pattern of reliable mean FC loadings along epi-LV1. Note: the reliability of loading coefficients was determined via 95% CIs calculated over 10,000 bootstraps.

Except for sex, all other demographic/behavioral loadings along epi-LV1 were deemed reliable as attested by 95% CIs derived from the bootstrap resampling regimen (age: -0.54 [-0.72, -0.24], sex: 0.02 [-0.33, 0.34], group: 0.66 [0.41, 0.81], epi-E: 0.83 [0.71, 0.91], epi-D: 0.82 [0.67, 0.90], **Figure 2c**). Similarly, mean functional connectivity loadings revealed robust bidirectional

contributions to epi-LV1 across the cortex at 95% CIs. We observed reliable positive loadings from bilateral pre- and postcentral gyri with intervening central sulci, left anterior middle frontal gyrus, left lateral inferior temporal gyrus, left insula, left parahippocampal gyrus, left orbito-frontal cortex, left paracentral lobule, right medial temporal pole, right medial inferior temporal gyrus, right parieto-occipital fissure, and isthmus of the right cingulate cortex, while negative contributions were found for bilateral pars orbitalis, bilateral superior frontal and posterior middle frontal gyri, bilateral supramarginal and angular gyri, bilateral medial prefrontal cortices, left posterior cingulate cortex, and left retrosplenial cortex, **Figure 2d**).

Semantic regimen

The first latent variable obtained within in the semantic scheme (sem-LV1) described nearly 33.3% of the shared variance between demographic/behavioral factors and mean functional connectivity measurements (**Figure 3a**). The latent correlation between corresponding composite scores along sem-LV1 was significant as determined by permutation tests ($r = 0.73$, $p_{perm} < 0.05$, **Figure 3b**). Apart from sex and sem-E performance, loadings for the remaining demographic/behavioral variables showed reliable contributions to sem-LV1 as confirmed by bootstrapping-derived 95% CIs (age: -0.51 [-0.74, -0.08], sex: 0.02 [-0.36, 0.42], group: 0.77 [0.61, 0.86], sem-E: 0.42 [0.00, 0.69], sem-D: 0.61 [0.30, 0.79], **Figure 3c**). CIs were also computed for whole-brain loading patterns obtained from the mean functional connectomes, with bilateral superior/middle frontal gyri and superior frontal sulcus exhibiting reliable positive contributions to sem-LV1, whereas left postcentral gyrus, left angular gyrus, and left parieto-occipital fissure displayed strong negative loadings (**Figure 3d**).

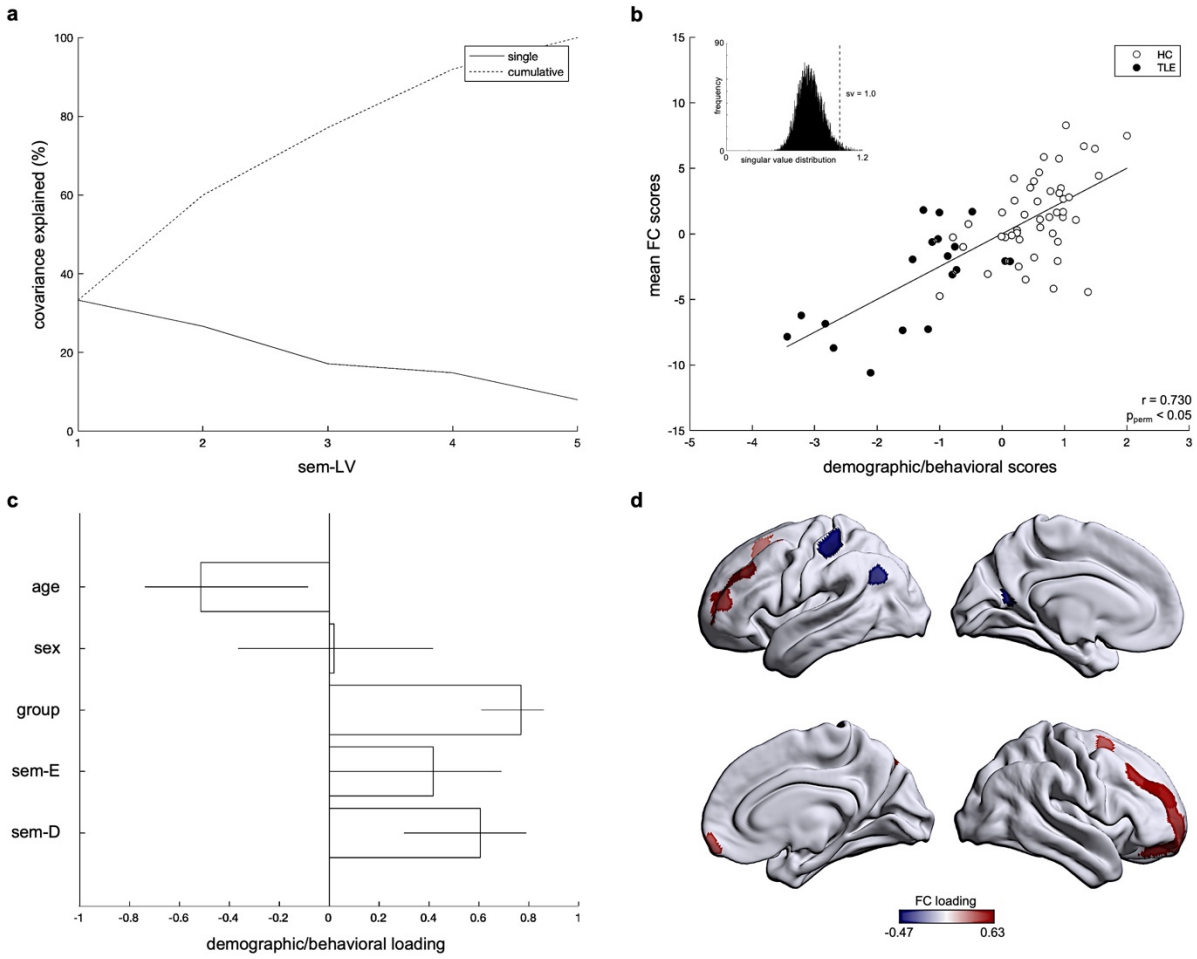

Figure 3. PLS results for Semantic. *(a)* sem-LV1 accounted for 33.3% of the total covariance between demographic/behavioral measurements and mean FC profiles. *(b)* the correlation between composite scores along sem-LV1 was significant (r = 0.73, $p_{perm} < 0.05$) as attested by 10,000 permutations (inset: dashed line "sv" represents the actual singular value). *(c)* age, group, and sem-D (but neither sex nor sem-E) showed robust contributions to epi-LV1. *(d)* whole-brain pattern of reliable mean FC loadings along epi-LV1. Note: the reliability of loading coefficients was determined via 95% CIs calculated over 10,000 bootstraps.

Spatial regimen

The first latent variable extracted from the PLS regimen involving the spatial module (spa-LV1) accounted for more than 45.8% of the covariance between demographic/behavioral measurements and mean functional connectivity profiles (**Figure 4a**), with permutation tests confirming the significant correlation of corresponding composite scores along spa-LV1 (r = 0.66 $p_{perm} < 0.05$, **Figure 4b**). For the same latent variable, bootstrap-derived 95% CIs for loading coefficients

showed a reliable involvement of age (-0.63 [-0.78, -0.35]), group (0.68 [0.52, 0.79]), spa-E (0.64 [0.29, 0.81]), and spa-D (0.64 [0.38, 0.80]), but not sex (-0.23 [-0.51, 0.17]) (**Figure 4c**). They additionally pointed to robust positive contributions to spa-LV1 from bilateral medio-lateral inferior temporal gyri, bilateral superior frontal gyri, bilateral postcentral gyri, right posterior middle temporal gyrus, right marginal sulcus, right prefrontal cortex, and right parieto-occipital fissure, as well as large negative contributions from bilateral intraparietal sulci, bilateral posterior fusiform gyri, left inferior frontal sulcus, right precentral sulcus, and right insula (**Figure 4d**).

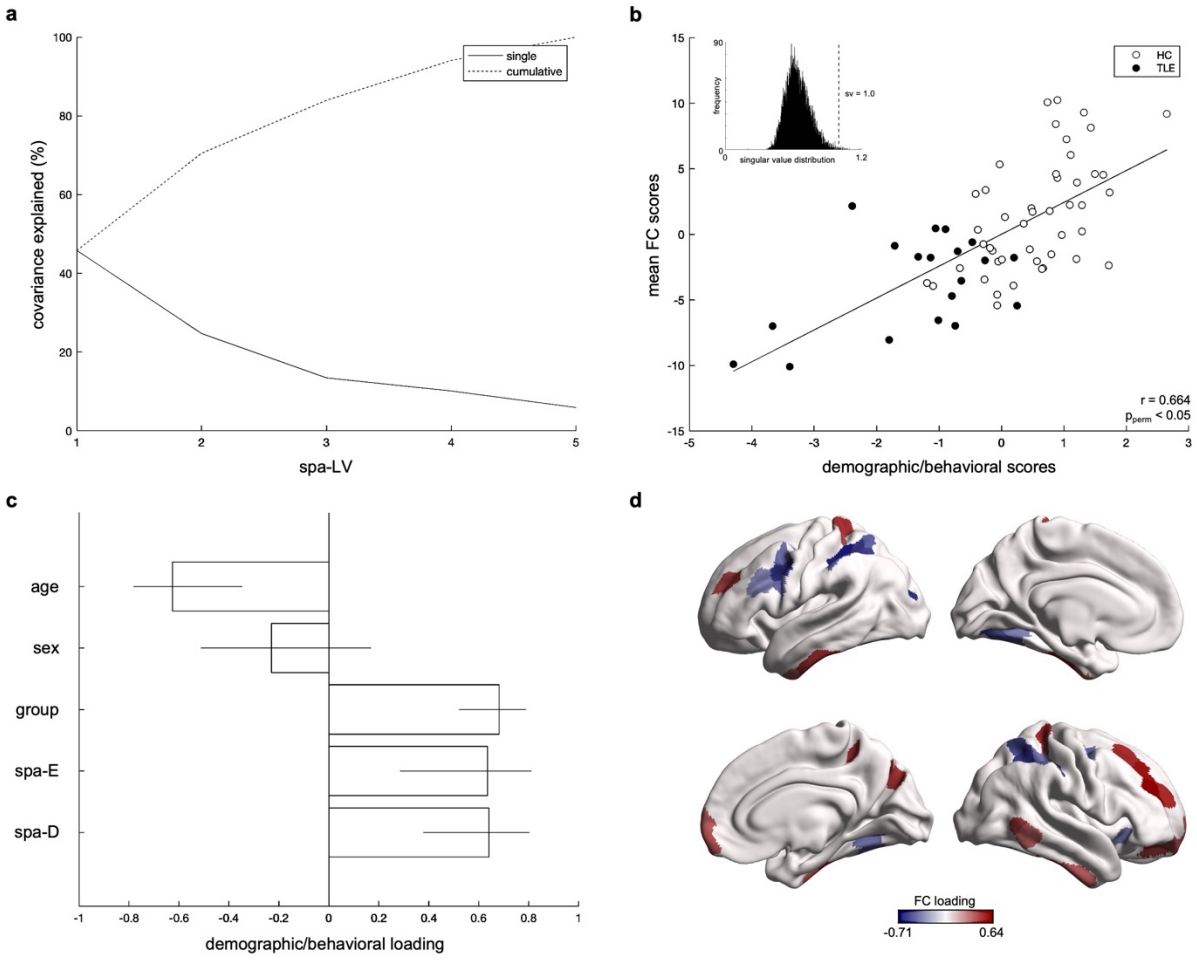

Figure 4. PLS results for Spatial. *(a)* spa-LV1 accounted for 45.8% of the total covariance between demographic/behavioral measurements and mean FC profiles. *(b)* the correlation between composite scores along sem-LV1 was significant ($r = 0.66$, $p_{perm} < 0.05$) as attested by 10,000 permutations (inset: dashed line "sv" represents the actual singular value). *(c)* age, group, spa-E, and spa-D (but not sex) showed robust contributions to epi-LV1. *(d)* whole-brain pattern of reliable mean FC loadings along epi-LV1. Note: the reliability of loading coefficients was determined via 95% CIs calculated over 10,000 bootstraps.

Comparison analyses

We ran supplementary analyses on the previously derived raw PLS mean functional connectome loadings (**Figure 5a**), stratifying them along canonical cortical networks to examine lower-dimensional patterns of overall task contribution (**Figure 5b, spider diagram**).

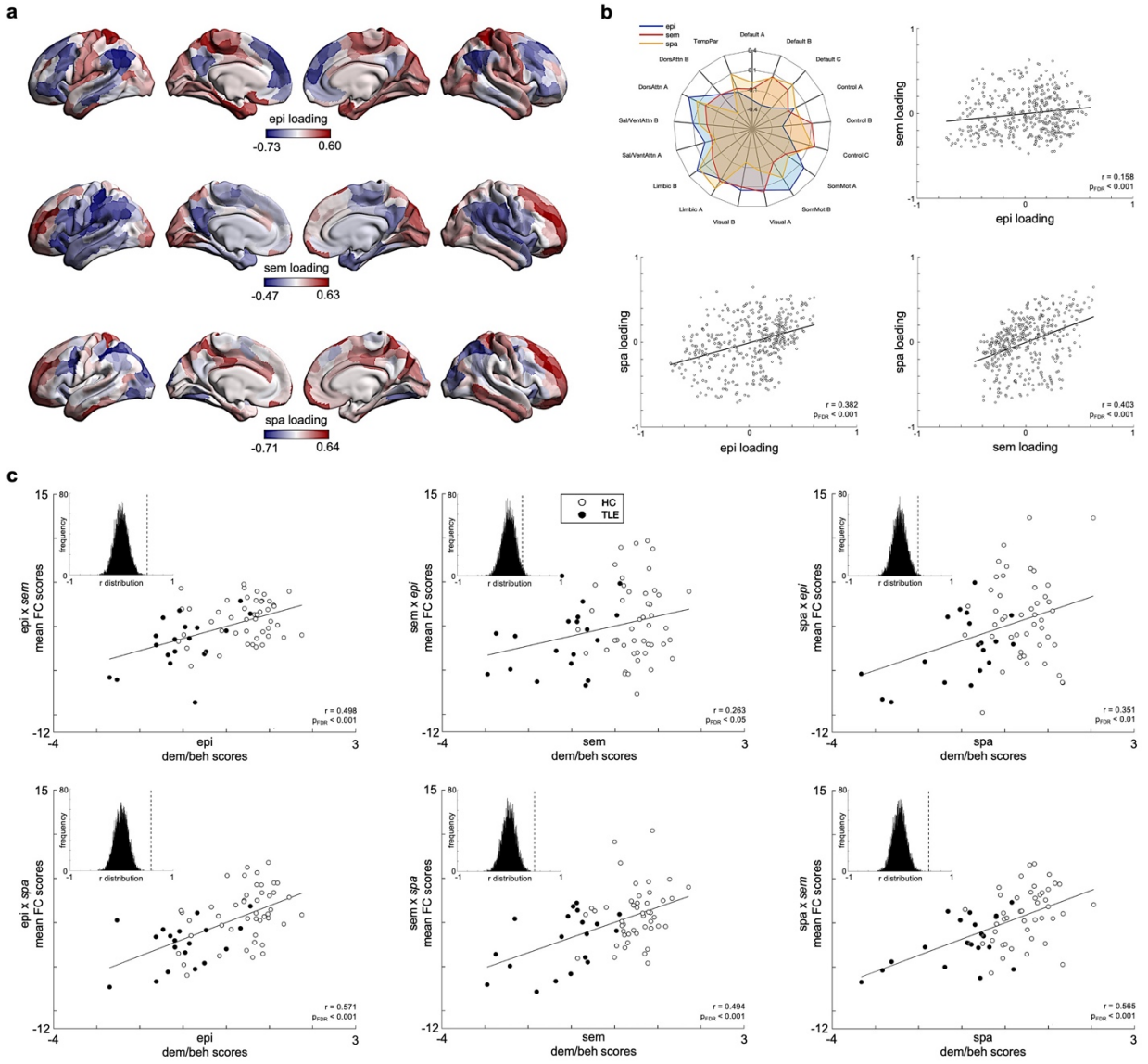

Figure 5. comparative results. *(a)* task-specific non-thresholded mean FC loadings. *(b)* spider diagram: task loadings stratified according to the 17 Yeo networks; scatterplots: correlations between non-thresholded loadings for each task pair. FDR-adjustment of p-values is performed in addition to permutations. *(c)* latent associations between cross-module mean FC and corresponding demographic/behavioral scores (inset: the actual correlation coefficient shown as a dashed line displayed against a null distribution derived from 10,000 permutations). FDR-adjustment of p-values is performed in addition to permutations. Note: associations are computed along previously defined significant latent variables (*i.e.*, epi-LV1, sem-LV1, and spa-LV1). Abbreviations: DorsAttn (Dorsal Attention), SomMot (Somato-motor), Sal/VentAttn (Salience/Ventral Attention), and TempPar (Temporo-parietal).

In descending order, mean positive loadings across tasks included Limbic A (0.195), DorsAttn A (0.171), Limbic B (0.170), Visual A (0.097), SomMot B (0.094), Control C (0.087), Sal/VentAttn B (0.049), Visual B (0.036), and SomMot A (0.016), whereas mean negative loadings consisted of DorsAttn B (-0.150), Default A (-0.147), Sal/VentAttn A (-0.084), Control A (-0.057), Default B (-0.052), Control B (-0.033), Default C (-0.030), and TempPar (-0.028). We uncovered significant associations between whole-brain patterns across all task pairs, as verified by permutation tests and corrections for multiple comparisons (epi x sem: $r = 0.16$, epi x spa: $r = 0.38$, sem x spa: $r = 0.40$, FDR-adjusted $ps < 0.001$, **Figure 5b, scatterplots**). What is more, all three functional connectivity manifolds derived in preceding steps yielded hybrid composite scores that showed strong correlations with corresponding demographic/behavioral scores along previously established LVs. Indeed, while these cross-module latent associations were inferior to their baseline values (epi-LV1: $r = 0.66$, sem-LV1: $r = 0.73$, spa-LV1: $r = 0.66$, permutation $ps < 0.05$, **Figures 2b, 3b, and 4b**), they nonetheless showed significance even after multiple comparisons corrections of permutation results (epi-LV1: $r_{epi\ x\ sem} = 0.50$, $p_{FDR} < 0.001$ & $r_{epi\ x\ spa} = 0.57$, $p_{FDR} < 0.001$; sem-LV1: $r_{sem\ x\ epi} = 0.26$, $p_{FDR} < 0.05$ & $r_{sem\ x\ spa} = 0.49$, $p_{FDR} < 0.001$; spa-LV1: $r_{spa\ x\ epi} = 0.35$, $p_{FDR} < 0.01$ & $r_{spa\ x\ sem} = 0.57$, $p_{FDR} < 0.001$, **Figure 5c**).

4.5 DISCUSSION

In this study, we aimed to uncover whole-brain patterns of task-based functional integration that underlie phenotypic variations in relational memory performance across cognitive domains and neurological diagnostic status. While there is ample research to support cross-cohort differences in behavior and function pertaining to domain-specific relational cognition, integrated assessments of its discrete elements (*i.e.*, episodic memory, semantic memory, and spatial memory), remain

scarce even to this day. An impediment to examining all three axes of relational memory within the same individuals across healthy and clinical groups has been the lack of a standardized evaluative protocol. With our recent development and validation of the iREP, which is optimized for the scanner environment, we can tap into episodic, semantic, and spatial aspects of relational memory in a controlled setting, making investigations of between-group variations in behavioral, structural, and functional phenotypes more expedient. Our first study involving iREP examined a group of healthy individuals in whom we demonstrated the presence of neural correlates underlying spatial processing that integrated cortical thickness and intrinsic connectivity across medial and lateral temporal cortices (Tavakol et al., 2021). In an ensuing project, we established that compared to controls, TLE patients presented with a hierarchy of deficits across relational cognitive domains, with most noticeable deficiencies observed in episodic memory, followed by spatial memory, and semantic memory last (Tavakol et al., 2022). Here, we leveraged data from the same participants to identify latent associations between behavior and function, addressing for the first time, systematic task-based functional patterns that can distinguish relational memory domains as well as diagnostic groups.

We conducted three separate PLS correlation schemes, one for each module of the iREP (*i.e.*, episodic, semantic, and spatial), to detect optimal associations between demographic/behavioral factors (*i.e.*, age, sex, group, and module-specific outcomes on easy and difficult conditions) and average functional connectivity profiles computed for corresponding iREP tasks. The advantage of using PLS correlation analysis lies within its mathematical approach to condensing complex multifactorial interactions into latent manifolds that optimize the shared information between two datasets. These saliences can be thought of as hidden feature spaces into which the original datasets

can be projected to generate novelty composite scores for each input matrix that are maximally correlated along PLS components called latent variables. Not only can saliences be used to determine the level of convergence between composite scores extracted within the same PLS protocol, but they can additionally be exploited to determine the association between baseline and hybrid scores derived across separate procedures. In this way, PLS correlation analysis represents a unique method for addressing unique and shared patterns of cortical connectivity across the different relational memory domains while simultaneously elucidating associations with other factors, such as demographic and behavioral variables of interest.

Broadly, we found younger age, HC group membership, and higher behavioral scores to strongly contribute to the first LVs across respective PLS schemes, a general finding that supports previous behavioral observations (Tavakol et al., 2022). What is specifically noteworthy in terms of behavioral performances across the six arms of the iREP (*i.e.*, Epi-E, Epi-D, Sem-E, Sem-D, Spa-E, and Spa-D) is that all of them, except for Sem-E, showed reliable loadings along corresponding first LVs, which lends further weight to the omnibus and PLS results our previous findings where, on the one hand, we did not observe a significant between-group difference, and on the other, Sem-E loadings were found to be unreliable contributors to LV1. Specific to the episodic regimen, we identified large positive loadings along epi-LV1 from the medial temporal lobes (MTL), including the left parahippocampal gyrus, with equally large negative contributions from the default mode network (DMN). These findings are in line with a plethora of evidence pointing to a role of the MTL in episodic memory (Ankudowich et al., 2016; Ankudowich et al., 2017; Li et al., 2021; Liu et al., 2022; Penfield & Milner, 1958; Scoville & Milner, 1957; Sormaz et al., 2017; Subramaniapillai et al., 2022; Subramaniapillai et al., 2019; Tavakol et al., 2022) and the

downregulating of the so-called “task-negative” DMN when attention is directed outwards (Fox et al., 2006; Fox et al., 2005; Raichle et al., 2001). With respect to the semantic PLS protocol, a comparatively small share of the neocortex displayed any form of contribution to sem-LV1, which is likely due to relatively high behavioral outcomes in both cohorts where the amount of variance that explains group differences remains exceptionally low. Therefore, it is reasonable to suggest that the neocortical connectivity patterns observed in this study, which demonstrate strong bilateral contributions from dorsolateral prefrontal cortices (DLPFC), potentially entail routine executive functions, such as working memory processing and motor planning, which, while important for certain facets of semantic memory, are not specific to it per se. Interestingly, the ATL, which is regarded as a transmodal hub within the semantic system (Alam et al., 2021; Hoffman & Morcom, 2018; Jackson, 2021; Patterson & Lambon Ralph, 2016; Rice et al., 2018; Rice et al., 2015; Rogers et al., 2004; Schapiro et al., 2013) showed a bias towards a positive TLE diagnosis based on uncorrected loadings. Given how significantly variations in socio-demographic variables and general executive/cognitive functions contribute to cross-cohort disparities in semantic accuracies (Tavakol et al., 2022), it is possible that the ATL may have been involved in overcompensating for TLE-related structural and functional alterations of the MTL (Bernhardt et al., 2016; Bernhardt et al., 2019; Bernhardt et al., 2015; Postma et al., 2020). Future studies should explore the relative contributions of the ATL, MTL, and prefrontal networks in sustaining semantic process, and to determine the degree of functional synergy between them. Regarding the spatial regimen, we found, as expected based on our findings in (Tavakol et al., 2021), involvement of the medial and lateral temporal lobes. Of note, in the episodic and spatial modules, where we had previously shown considerable TLE-related cognitive deficits, our TLE group exhibited a heightened

recruitment of brain regions, such as the DLPFC, pointing to potentially compensatory functional mechanisms.

Finally, while all three brain loading patterns presented with their unique idiosyncrasies, our comparative analyses did point to a strong degree of convergence across relational memory domains. In fact, the stratification of non-thresholded task-specific connectivity coefficients according to canonical Yeo networks allowed us to observe telling general trends, where the limbic system, which encompasses hippocampal and parahippocampal regions, showed highest average contributions across tasks, with noticeable negative connectivity loadings observed for DMN and attention networks. This finding points to an underlying relational memory motif shared across domains, which can discriminate between diagnostic groups. Moreover, the observation that these cortical loading patterns were significantly correlated across all task pairs demonstrates yet again a level of functional convergence between episodic, semantic, and spatial memory. Furthermore, we also saw that connectivity manifolds derived for any one iREP module can have predictive power over the latent associations of the remaining two tasks, as attested by cross-module analytical procedures, where hybrid connectome scores were significantly correlated with baseline demographic/behavioral scores along the same LVs. Even so, the original effect sizes derived in the separate PLS regimens were still superior to their matching cross-module counterparts, which speaks to the specificity of connectivity saliences, proving that while there is shared neocortical information across latent task-specific connectome features, these properties are nonetheless unique to each relational memory domain.

5 GENERAL DISCUSSION

The objective of my PhD was to streamline the study of relational memory in healthy and clinical populations. To this end, we developed the *integrated Relational Evaluation Paradigm*, or iREP, a multidomain cognitive task battery that is optimized for administration inside the MRI environment, which incorporates difficulty-adjusted modules that tax episodic, semantic, and spatial domains of mnemonic processing. The iREP is a python-based, user-friendly, and open-access platform currently in use at the MICA lab within the McConnell Brain Imaging Centre at the Montreal Neurological Institute and Hospital as part of ongoing multimodal neuroimaging initiatives (3T protocol: https://github.com/MICA-MNI/micaopen/tree/master/task-fMRI; 7T protocol: https://github.com/MICA-MNI/micaopen/tree/master/7T_task_fMRI). In this work, we presented three complementary projects in which we leveraged the iREP to examine specific and shared multivariate profiles of relational memory domains in healthy controls and patients diagnosed with TLE, who constitute a firmly established model of human memory dysfunction (Barrett Jones et al., 2022; Breier et al., 1996; Helmstaedter et al., 1995; Li et al., 2021; Mayeux et al., 1980; Penfield & Milner, 1958; Rugg et al., 1991; Scoville & Milner, 1957; Sideman et al., 2018; Voets et al., 2009; Yoo et al., 2006; Zanao et al., 2023). In *Project I* (Tavakol et al., 2021), we administered the iREP to a group of healthy participants while they were being scanned, thus deriving behavioral measures in addition to morphological and functional markers of the neocortex and hippocampus. We discovered consolidated structure-function substrates within medial and lateral temporal lobe regions that relate to behavioral differences in spatial cognition. In *Project II* (Tavakol et al., 2022), we compared a cohort of TLE patients with age- and sex-matched healthy individuals along the full gamut of iREP outcome measures. Using omnibus tests in conjunction with multivariate associative analytics, we established a graded pattern of cognitive impairments

in TLE patients relative to controls that presented itself as significant episodic memory deficits, milder yet recognizable spatial memory deficiencies, with mixed findings in semantic memory. Age, diagnostic group, and hippocampal volume were additively associated with behavioral scores. In *Project III*, we conducted additional group comparisons within the same two cohorts. Here, we specifically addressed the relation between task-based functional connectomes and socio-demographic variables in addition to iREP task accuracies. We ascertained the presence of overlapping, albeit distinctive functional neocortical topographies across relational memory domains that varied commensurately with changes in age, TLE diagnosis, and behavioral performance. With this work, we demonstrated the validity and practicality of the iREP as an integrated framework for studying episodic, semantic, and spatial dimensions of memory within single subjects across different populations. Collectively, our results revealed that interindividual and between-group differences in relational memory can be determined from a multivariate perspective, which unifies behavior, clinical presentation, socio-demographics, and brain anatomy and function.

Beyond homogenizing assessments of relational memory domains in a single neuroimaging framework, another novelty of the iREP is its spatial module, which we designated as the *conformational shift spatial task*, or CSST, in *Project I*. In fact, the episodic and semantic tasks are simple pictorial adaptations of pre-established lexicon-based paired associates paradigms (Payne et al., 2012; Sormaz et al., 2017; Wang et al., 2018). While it is true that stimulus modality modulates functional dynamics, especially for word processing, which is mainly left-lateralized, higher order and network-level neural topographies remain relatively stable across symbolic and word-based stimuli that represent the same construct (Krieger-Redwood et al., 2015; Patterson &

Lambon Ralph, 2016; Rice et al., 2015; Rogers et al., 2004; Schapiro et al., 2013). Furthermore, pictorial-based cognitive assessment protocols with comparable task parameters and design features to our own are commonly used and reported in the literature (Alam et al., 2021; Ankudowich et al., 2016; Ankudowich et al., 2017; Davey et al., 2015; Rice et al., 2018; Subramaniapillai et al., 2022; Subramaniapillai et al., 2019). These considerations speak to the construct-validity of the episodic and semantic modules of the iREP, leaving out the spatial task, which we specifically addressed in *Project I*.

We wanted first to validate this spatial component of the iREP along the behavioral dimension. To do this, we administered our relational memory battery to a group of healthy individuals as they underwent multimodal neuroimaging. We also examined our participants on complementary cognitive assessment tools, including the Four Mountains Task (FMT), which is a an established test of allocentric spatial processing (Bird et al., 2010; Chan et al., 2016; Hartley et al., 2007; Hartley & Harlow, 2012; Moodley et al., 2015; Ritchie et al., 2018), and the mnemonic similarity task (MST), which assesses the capacity to orthogonalize similar memory traces, otherwise known as pattern separation (Li et al., 2021; Stark et al., 2013). We then cross-correlated performance scores across paradigms and found that the spatial iREP and FMT showed the strongest pairwise association. The spatial module was additionally correlated with the semantic iREP, but neither with the episodic iREP nor the MST. We interpreted these behavioral results as evidence of the relative specificity of the spatial module to tap into spatial aspects of relational cognition with some overlap with semantic processes. This association between spatial and semantic scores may point to a convergence of anatomical and functional properties across these two dimensions of relational memory, including the role of place and grid cells in domain-invariant information

organization (Bellmund et al., 2018; Constantinescu et al., 2016; Epstein et al., 2017; Mok & Love, 2019; Sormaz et al., 2017; Whittington et al., 2020).

Having established the construct-validity of the spatial iREP along the behavioral dimension, we sought to relate performance scores with MRI-derived structural markers. Our analyses revealed neocortical clusters confined within medial and lateral temporal areas, including the right posterior parahippocampus, where gray matter thickness significantly correlated with spatial iREP accuracies. These findings corroborate what is already known about the involvement of the MTL in spatial cognition, including the role of the parahippocampal cortex in memory for scenes and configuration of objects (Abrahams et al., 1999; Aguirre et al., 1996; Bohbot et al., 2015; Bohbot et al., 2000; Bohbot et al., 1998; Epstein & Kanwisher, 1998), with increased gray matter of the entorhinal and parahippocampal cortices linked with better performance on videogame platforms that require rapid processing of geometric relationships and dynamic pathfinding behaviors (Kühn & Gallinat, 2014; Momi et al., 2018). While the involvement of lateral temporal regions in spatial cognition is unclear, our structural findings are in line with evidence from virtual reality paradigms that suggest a participation of these areas in sustaining navigation (Bush et al., 2017; Doeller et al., 2010), with one meta-analysis implicating bilateral lateral temporal cortices in the processing of familiar virtual environments (Boccia et al., 2014).

To functionally contextualize our anatomical findings, we conducted seed-based resting-state fMRI connectivity analyses centered on each temporal lobe cluster. We found that spatial accuracies were significantly modulated by the connectivity of the hippocampus to the lateral temporal cortex, and that of the posterior parahippocampal gyrus to a region stretching medially

from the middle frontal and precentral gyri to the paracentral lobule and superior anterior cingulate. Furthermore, meta-analytical results obtained for the NeuroSynth term "navigation" revealed a whole-brain topography presenting with robust hippocampus-parahippocampus involvement, with the average cortical thickness across co-activated areas showing a significant correlation with spatial iREP scores. While the function of the hippocampus in supporting spatial memory is well-established across animal (Aggleton et al., 1986; Burgess et al., 2007; O'Keefe & Nadel, 1978; Sargolini et al., 2006), clinical (Milner, 1965; Rains & Milner, 1994; Smith & Milner, 1981, 1989), and neuroimaging studies (Abrahams et al., 1999; Aguirre et al., 1996; Ghaem et al., 1997; Hassabis et al., 2009; Kim & Maguire, 2018; Maguire et al., 1998; Maguire et al., 2000; Robin et al., 2018), the parahippocampus has also been shown to be functionally involved in various forms of spatial processing, including object-location retrieval (Owen et al., 1996), local geometry encoding (Epstein & Kanwisher, 1998; Epstein, 2008), fine-grained spatial judgment (Hirshhorn et al., 2012), and 3D space representation (Kim & Maguire, 2018). Overall, our findings point to a fronto-limbic network underlying interindividual differences in spatial memory capacity, with an integrated structure-function substrate within medial and lateral temporal cortical areas.

In *Project II*, our goal was to analyze the extent to which various clinical and demographic factors may contribute to relational memory phenotypes. Thus, we expanded our behavioral analyses to include measurements from all iREP modules within control and TLE cohorts while additionally incorporating other salient variables, such as age, sex, diagnostic status, and hippocampal volume. Initially, we confirmed the difficulty manipulation within iREP modules for each group separately, effectively showing that both healthy individuals and TLE patients scored significantly higher on the "easy" condition of each task relative to its corresponding "difficult" one. We then ran omnibus

analyses to elucidate between-group differences in relational memory performance, and found that, out of six iREP measurements (*i.e.*, Epi-E, Epi-D, Sem-E, Sem-D, Spa-E, Spa-D), controls outperformed TLE patients on all outcomes, except for Sem-E, where both groups showed similar results. When additionally accounting for the effects of socio-demographics and general executive/cognitive functions, we observed that between-group differences persisted on Epi-D and Spa-D. Complementary partial least squares (PLS) analyses further identified a latent multivariate dimension along which iREP performance accuracies were positively associated with younger age, absence of TLE diagnosis, and greater hippocampal volume. Episodic contributions to this latent component were larger than spatial ones, which, in turn, were larger than semantic ones.

Our results lend additional support to an already firmly established scientific corpus showing episodic memory deficits in TLE (Hoppe et al., 2007; Spiers et al., 2001; Tavakol et al., 2019; Thom, 2014; Viskontas et al., 2000), and while spatial memory impairments are less well-defined, overall observations in the general population and individuals who present with hippocampal damage implicate the hippocampus both structurally (Abrahams et al., 1999; Hartley & Harlow, 2012; Maguire et al., 2000) and functionally (Bicanski & Burgess, 2018; Byrne et al., 2007; Dhindsa et al., 2014; Hartley et al., 2007; Tavakol et al., 2021) in sustaining allocentric spatial processing. In animal models of epilepsy, it has also been shown that disruptions of hippocampal sharp-wave ripples (100-200 Hz) contribute to downregulating the consolidation of spatial memory traces (Ego-Stengel & Wilson, 2009; Gelinas et al., 2016; Girardeau et al., 2009). Furthermore, navigational impairments in TLE patients have been reported on virtual reality paradigms (Cánovas et al., 2011; Glikmann-Johnston et al., 2008; Rosas et al., 2013), with underlying factors, such as age of epilepsy onset, level of intelligence, and epilepsy duration

further compacting spatial memory deficits (Amlerova et al., 2013). Even when controlling for salient covariates, such as age, sex, executive function and attention, and mild cognitive impairment (Lähde et al., 2021; Lutz & Helmstaedter, 2005; Nasreddine et al., 2005), cross-cohort differences in relational memory performance persisted along episodic and spatial dimensions, thus indicating that these results were not driven entirely by disparities in socio-demographic factors or other cognitive domains. Therefore, these mnemonic deficits could be pointing to underlying disease-related changes including subregional structural pathology (Bernhardt et al., 2015), disruptions in connectivity patterns (Bernhardt et al., 2016), and functional reorganization (Postma et al., 2020).

On the other hand, group effects on semantic scores vanished when accounting for socio-demographic and cognitive covariates. Unlike the episodic and spatial components of the iREP, which include an encoding and a retrieval phase, the semantic module is entirely retrieval-based, meaning that the conceptual associations required to successfully complete this task had previously been encoded into long-term memory, which is supported by both hippocampal and non-hippocampal neocortical processes (Klinzing et al., 2019). This consideration agrees with the complementary learning systems model, which proposes a gradual organization of semantic knowledge across the neocortex, which is based on rapid hippocampal encoding of non-overlapping episodic representations (McClelland et al., 1995; O'Reilly et al., 2014). Other models, like the multiple trace theory, posit that the hippocampus is merely transiently involved in semantic cognition, making the semantic system relatively resilient against lesions to this area (Nadel et al., 2000). Further evidence suggests that the neocortex can even form long-term arbitrary associations independent of the hippocampus via a temporal pole-mediated process known as “fast-mapping”

(Sharon et al., 2011), which is in line with the hub-and-spoke framework, where it is the ATL, and not the hippocampus, that integrates conceptual information across modalities (Patterson & Lambon Ralph, 2016; Rogers et al., 2004; Schapiro et al., 2013). Thus, the absence of a clear-cut group effect on semantic scores within our cohorts likely reflects this purportedly limited role of the hippocampus in semantic information processing. Moreover, the comparatively low semantic contributions to the shared PLS-derived component further speaks to this possibility. It should also be noted that TLE-related semantic deficiencies have either been reported using visual confrontation naming paradigms, which may not directly tap into semantic association processes (Bell et al., 2001; Giovagnoli et al., 2005), or have been found in patients who had undergone anterior temporal resection (Lambon Ralph et al., 2012). In fact, while the semantic iREP is a valid test of general conceptual knowledge (Sormaz et al., 2017; Tavakol et al., 2021; Wang et al., 2018), findings in other semantic protocols similar to the one we have used suggest that TLE patients show little signs of impairment on tests of general associations (Giovagnoli et al., 2005; Helmstaedter, 2002; Lambon Ralph et al., 2010), with task difficulty representing an important variable in teasing out behavioral deficits (Lambon Ralph et al., 2012). With *Project II*, we thus showcased the phenotypic granularity of TLE-associated relational memory dysfunction, demonstrating the presence of a graded pattern of behavioral impairments in which the episodic system seems to be most affected by the disease, followed by spatial cognition, while semantic processing appears to be relatively well preserved.

With *Project III*, our final study, we aimed to provide a network-level functional basis for our previous behavioral findings. Thus, we computed task-based functional connectomes for each iREP module in the same participants as in the previous study, and conducted separate domain-

specific PLS analyses in which we evaluated latent associations between joint demographic-behavioral factors and task-based connectivity profiles. To further assess the generalizability of functionally informative network topographies across relational memory domains, we additionally ran hybrid analyses in which the PLS-derived connectome saliences of one task were used to fit data from the other two modules.

In accordance with findings from *Project II*, we observed that within each domain-specific PLS scheme, a unique whole-brain functional connectivity profile was associated with an additive demographic-behavioral pattern defined by younger age, absence of TLE diagnosis, and higher performance scores. As in the previous study, contributions from Sem-E accuracies were negligible. Indeed, the share of the neocortex exhibiting an informative functional topography was relatively small in the semantic PLS regimen, which is likely due to the comparatively low amount of variance in semantic iREP accuracies across groups. What we did observe, however, was a strong bilateral contribution from dorsolateral prefrontal cortices (DLPFC), which implies that during the semantic task, the brain of healthy controls may have been actively involved in routine executive functions, such as working memory and motor planning. Surprisingly, functional involvement of the ATL, which is believed to be a core hub of the semantic processing system (Alam et al., 2021; Hoffman & Morcom, 2018; Jackson, 2021; Patterson & Lambon Ralph, 2016; Rice et al., 2018; Rice et al., 2015; Rogers et al., 2004; Schapiro et al., 2013) was associated with a positive TLE diagnosis based on raw connectivity loadings. Given that between-group differences in semantic scores were primarily driven by socio-demographic factors and neurobehavioral disparities along other cognitive domains (Tavakol et al., 2022), it is conceivable that the ATL may have been overcompensating for pathophysiological alterations seen in TLE

(Bernhardt et al., 2016; Bernhardt et al., 2019; Bernhardt et al., 2015; Postma et al., 2020). This possibility must be explored in prospective studies aimed at understanding the relative contributions of the ATL, MTL, and prefrontal areas to semantic cognition, and to establish whether these regions may be working synergistically as the evidence we have provided here suggests.

Findings from our spatial analyses revealed robust medial and lateral temporal cortical contributions to performance scores in healthy individuals, which supports past results relative to the consolidated structural-functional involvement of these regions in spatial memory (Tavakol et al., 2021). Medial temporal lobes also displayed large positive loading values in the episodic regimen, with substantial involvement of the parahippocampal gyrus in the control group, further supporting prior findings in the episodic memory literature (Ankudowich et al., 2016; Ankudowich et al., 2017; Li et al., 2021; Liu et al., 2022; Penfield & Milner, 1958; Scoville & Milner, 1957; Sormaz et al., 2017; Subramaniapillai et al., 2022; Subramaniapillai et al., 2019; Tavakol et al., 2022). We detected equally large contributions of the DMN in TLE patients, suggesting atypically heightened whole-brain integration of "task-negative" cortical regions (Fox et al., 2006; Fox et al., 2005; Raichle et al., 2001). Of note, in the episodic and spatial modules where TLE patients showed greatest behavioral deficits, our TLE group exhibited an overreliance on regions of the brain, such as the DLPF, that appeared to have been compensating for disease-related structural and functional anomalies (Bernhardt et al., 2016; Bernhardt et al., 2019; Bernhardt et al., 2015; Postma et al., 2020).

Finally, our comparative analyses pointed to a strong level of convergence of functionally informative whole-brain dynamics across relational memory domains. For instance, the limbic system, which encompasses hippocampal and parahippocampal regions, showed the highest average contributions across tasks in the control group, with noticeable reductions in whole-brain integration of DMN and attention networks. This observation suggests that there is a low-resolution relational memory motif within limbic regions that is shared across domains in the healthy brain, which makes it of potential use in differentiating diagnostic groups. Our analyses further showed that neocortical loading patterns were significantly correlated across all iREP modules, which further speaks to the functional convergence of the different dimensions of relational processing. Moreover, while connectivity topographies were mutually informative across domains, the original effect sizes calculated separately for each task were still larger in magnitude than corresponding hybrid values. These observations clearly denote the existence of a multivariate relational memory profile that presents itself as converging, albeit specific domain-dependent fronto-limbic and temporal connectivity motifs that vary in tandem with modulations in age, diagnostic group, and behavioral phenotype.

Taken together, the projects we have described establish the iREP as a construct-valid assessment platform that offers a wholistic approach to studying relational memory. They further demonstrate the existence of core features of episodic, semantic, and spatial cognition that are shared across domains while additionally identifying unique neural biomarkers that covary with interindividual differences in socio-demographics and mnemonic aptitudes. With this work, we have laid the foundations of an integrated memory framework that we hope will be actively implemented by the neuroscientific community to optimize the study of human cognition in different populations.

6 REFERENCES

Abrahams, S., Morris, R. G., Polkey, C. E., Jarosz, J. M., Cox, T. C., Graves, M., & Pickering, A. (1999). Hippocampal involvement in spatial and working memory: a structural MRI analysis of patients with unilateral mesial temporal lobe sclerosis. *Brain and cognition*, *41*(1), 39-65. https://doi.org/10.1006/brcg.1999.1095

Aggleton, P. R., Hunt Pr Fau - Rawlins, J. N., & Rawlins, J. N. (1986). The effects of hippocampal lesions upon spatial and non-spatial tests of working memory. *Behavioural brain research*(0166-4328 (Print)).

Aguirre, G. K., & D'Esposito, M. (1997). Environmental knowledge is subserved by separable dorsal/ventral neural areas. *The Journal of neuroscience : the official journal of the Society for Neuroscience*, *17*(7), 2512-2518. https://doi.org/10.1523/JNEUROSCI.17-07-02512.1997

Aguirre, G. K., Detre Ja Fau - Alsop, D. C., Alsop Dc Fau - D'Esposito, M., & D'Esposito, M. (1996). The parahippocampus subserves topographical learning in man. *Cerebral cortex*(1047-3211 (Print)).

Alam, T. R. J. G., Krieger-Redwood, K., Evans, M., Rice, G. E., Smallwood, J., & Jefferies, E. (2021). Intrinsic connectivity of anterior temporal lobe relates to individual differences in semantic retrieval for landmarks. *Cortex*, *134*, 76-91.

Alexander-Bloch, A. F., Shou, H., Liu, S., Satterthwaite, T. D., Glahn, D. C., Shinohara, R. T., Vandekar, S. N., & Raznahan, A. (2018). On testing for spatial correspondence between maps of human brain structure and function. *NeuroImage*(1095-9572 (Electronic)).

Allone, C., Buono, V. L., Corallo, F., Pisani, L. R., Pollicino, P., Bramanti, P., & Marino, S. (2017). Neuroimaging and cognitive functions in temporal lobe epilepsy: A review of the literature. *Journal of the neurological sciences*, *381*, 7-15.

Amlerova, J., Laczo, J., Vlcek, K., Javurkova, A., Andel, R., & Marusic, P. (2013). Risk factors for spatial memory impairment in patients with temporal lobe epilepsy. *Epilepsy & behavior : E&B*, *26*(1), 57-60. https://doi.org/10.1016/j.yebeh.2012.10.025

Ankudowich, E., Pasvanis, S., & Rajah, M. N. (2016). Changes in the modulation of brain activity during context encoding vs. context retrieval across the adult lifespan. *NeuroImage*, *139*, 103-113.

Ankudowich, E., Pasvanis, S., & Rajah, M. N. (2017). Changes in the correlation between spatial and temporal source memory performance and BOLD activity across the adult lifespan. *Cortex*, *91*, 234-249.

Aslaksen, P. M., Bystad, M. K., Ørbo, M. C., & Vangberg, T. R. (2018). The relation of hippocampal subfield volumes to verbal episodic memory measured by the California Verbal Learning Test II in healthy adults. *Behavioural brain research*, *351*, 131-137.

Astur, R. S., Taylor, L. B., Mamelak, A. N., Philpott, L., & Sutherland, R. J. (2002). Humans with hippocampus damage display severe spatial memory impairments in a virtual Morris water task. *Behavioural brain research*, *132*(1), 77-84.

Astur, R. S., Tropp, J., Sava, S., Constable, R. T., & Markus, E. J. (2004). Sex differences and correlations in a virtual Morris water task, a virtual radial arm maze, and mental rotation. *Behavioural brain research*, *151*(1-2), 103-115.

Attwell, D., & Laughlin, S. B. (2001). An energy budget for signaling in the grey matter of the brain. *Journal of Cerebral Blood Flow & Metabolism*, *21*(10), 1133-1145.

Barrett Jones, S., A. Miller, L., Kleitman, S., Nikpour, A., & Lah, S. (2022). Semantic and episodic memory in adults with temporal lobe epilepsy. *Applied Neuropsychology: Adult*, *29*(6), 1352-1361.

Baumann, O., & Mattingley, J. B. (2021). Extrahippocampal contributions to spatial navigation in humans: a review of the neuroimaging evidence. *Hippocampus*, *31*(7), 640-657.

Beattie, J. F., Martin, R. C., Kana, R. K., Deshpande, H., Lee, S., Curé, J., & Ver Hoef, L. (2017). Hippocampal dentation: Structural variation and its association with episodic memory in healthy adults. *Neuropsychologia*, *101*, 65-75.

Bell, B., Lin, J. J., Seidenberg, M., & Hermann, B. (2011). The neurobiology of cognitive disorders in temporal lobe epilepsy. *Nature Reviews Neurology*, *7*(3), 154-164.

Bell, B. D., Hermann, B. P., Woodard, A. R., Jones, J. E., Rutecki, P. A., Sheth, R., Dow, C. C., & Seidenberg, M. (2001). Object naming and semantic knowledge in temporal lobe epilepsy. *Neuropsychology*, *15*(4), 434-443. https://doi.org/10.1037//0894-4105.15.4.434

Bellmund, J. L. S., Gärdenfors, P., Moser, E. I., & Doeller, C. F. (2018). Navigating cognition: Spatial codes for human thinking. *Science (New York, N.Y.)*, *362*(6415). https://doi.org/10.1126/science.aat6766

Benjamini, Y., & Hochberg, Y. (1995). Controlling the False Discovery Rate: A Practical and Powerful Approach to Multiple Testing. *Journal of the Royal Statistical Society: Series B (Methodological)*, *57*(1), 289-300. https://doi.org/10.1111/j.2517-6161.1995.tb02031.x

Bernhardt, B. C., Bernasconi, A., Liu, M., Hong, S.-J., Caldairou, B., Goubran, M., Guiot, M. C., Hall, J., & Bernasconi, N. (2016). The spectrum of structural and functional imaging abnormalities in temporal lobe epilepsy. *Annals of neurology*, *80*(1), 142-153. https://doi.org/10.1002/ana.24691

Bernhardt, B. C., Fadaie, F., Liu, M., Caldairou, B., Gu, S., Jefferies, E., Smallwood, J., Bassett, D. S., Bernasconi, A., & Bernasconi, N. (2019). Temporal lobe epilepsy: Hippocampal pathology modulates connectome topology and controllability. *Neurology*, *92*(19), e2209-e2220.

Bernhardt, B. C., Hong, S.-J., Bernasconi, A., & Bernasconi, N. (2015). Magnetic resonance imaging pattern learning in temporal lobe epilepsy: classification and prognostics. *Annals of neurology*, *77*(3), 436-446. https://doi.org/10.1002/ana.24341

Bicanski, A., & Burgess, N. (2018). A neural-level model of spatial memory and imagery. *eLife*, *7*. https://doi.org/10.7554/eLife.33752

Binder, J. R., & Desai, R. H. (2011). The neurobiology of semantic memory. *Trends in cognitive sciences*, *15*(11), 527-536. https://doi.org/10.1016/j.tics.2011.10.001

Binder, J. R., Desai, R. H., Graves, W. W., & Conant, L. L. (2009). Where is the semantic system? A critical review and meta-analysis of 120 functional neuroimaging studies. *Cerebral cortex (New York, N.Y. : 1991)*, *19*(12), 2767-2796. https://doi.org/10.1093/cercor/bhp055

Bird, C. M., Chan, D., Hartley, T., Pijnenburg, Y. A., Rossor, M. N., & Burgess, N. (2010). Topographical short-term memory differentiates Alzheimer's disease from frontotemporal lobar degeneration. *Hippocampus*, *20*(10), 1154-1169.

Biswal, B. B., Kylen, J. V., & Hyde, J. S. (1997). Simultaneous assessment of flow and BOLD signals in resting-state functional connectivity maps. *NMR in Biomedicine*, *10*(4-5), 165-170.

Boccia, M., Nemmi, F., & Guariglia, C. (2014). Neuropsychology of environmental navigation in humans: review and meta-analysis of FMRI studies in healthy participants. *Neuropsychology review*, *24*, 236-251.

Bohbot, V. D., Allen, J. J. B., Dagher, A., Dumoulin, S. O., Evans, A. C., Petrides, M., Kalina, M., Stepankova, K., & Nadel, L. (2015). Role of the parahippocampal cortex in memory for the configuration but not the identity of objects: converging evidence from patients with selective thermal lesions and fMRI. *Frontiers in human neuroscience*, *9*, 431.

Bohbot, V. D., Allen, J. J. B., & Nadel, L. (2000). Memory deficits characterized by patterns of lesions to the hippocampus and parahippocampal cortex. *Annals of the New York Academy of Sciences*, *911*(1), 355-368.

Bohbot, V. D., Iaria, G., & Petrides, M. (2004). Hippocampal function and spatial memory: evidence from functional neuroimaging in healthy participants and performance of patients with medial temporal lobe resections. *Neuropsychology*, *18*(3), 418.

Bohbot, V. D., Jech, R., Ruzicka, E., Nadel, L., Kalina, M., Stepankova, K., & Bures, J. (2002). Rat spatial memory tasks adapted for humans: characterization in subjects with intact brain and subjects with medial temporal lobe lesions. *Physiol Res*, *51*(Suppl 1), S49-S56.

Bohbot, V. D., Kalina, M., Stepankova, K., Spackova, N., Petrides, M., & Nadel, L. (1998). Spatial memory deficits in patients with lesions to the right hippocampus and to the right parahippocampal cortex. *Neuropsychologia*, *36*(11), 1217-1238.

Bohbot, V. D., McKenzie, S., Konishi, K., Fouquet, C., Kurdi, V., Schachar, R., Boivin, M., & Robaey, P. (2012). Virtual navigation strategies from childhood to senescence: evidence for changes across the life span. *Frontiers in aging neuroscience*, 28.

Bozeat, S., Lambon Ralph, M. A., Patterson, K., Garrard, P., & Hodges, J. R. (2000). Non-verbal semantic impairment in semantic dementia. *Neuropsychologia*, *38*(9), 1207-1215. https://doi.org/10.1016/s0028-3932(00)00034-8

Breier, J. I., Plenger, P. M., Castillo, R., Fuchs, K., Wheless, J. W., Thomas, A. B., Brookshire, B. L., Willmore, L. J., & Papanicolaou, A. (1996). Effects of temporal lobe epilepsy on spatial and figural aspects of memory for a complex geometric figure. *Journal of the International Neuropsychological society*, *2*(6), 535-540.

Buchbinder, B. R. (2016). Handbook of Clinical Neurology 3rd Series. In J. C. Masdeu & R. G. González (Eds.), *Handbook of Clinical Neurology* (Vol. 135, pp. v-vi). Elsevier. https://doi.org/https://doi.org/10.1016/B978-0-444-53485-9.09996-7

Buckner, R. L., Krienen, F. M., & Yeo, B. T. T. (2013). Opportunities and limitations of intrinsic functional connectivity MRI. *Nature Neuroscience*, *16*(7), 832-837.

Burgess, N., Barry, C., & O'Keefe, J. (2007). An oscillatory interference model of grid cell firing. *Hippocampus*, *17*(9), 801-812.

Bush, D., Bisby, J. A., Bird, C. M., Gollwitzer, S., Rodionov, R., Diehl, B., McEvoy, A. W., Walker, M. C., & Burgess, N. (2017). Human hippocampal theta power indicates movement onset and distance travelled. *Proceedings of the National Academy of Sciences*, *114*(46), 12297-12302.

Byrne, P., Becker, S., & Burgess, N. (2007). Remembering the past and imagining the future: a neural model of spatial memory and imagery. *Psychological review*, *114*(2), 340-375. https://doi.org/10.1037/0033-295X.114.2.340

Cahalane, D. J., Charvet, C. J., & Finlay, B. L. (2012). Systematic, balancing gradients in neuron density and number across the primate isocortex. *Frontiers in neuroanatomy*, *6*.

Caldairou, B., Bernhardt, B. C., Kulaga-Yoskovitz, J., Kim, H., Bernasconi, N., & Bernasconi, A. (2016, 2016). *A surface patch-based segmentation method for hippocampal subfields*

Cánovas, R., León, I., Serrano, P., Roldán, M. D., & Cimadevilla, J. M. (2011). Spatial navigation impairment in patients with refractory temporal lobe epilepsy: evidence from a new virtual reality-based task. *Epilepsy & behavior : E&B*, *22*(2), 364-369. https://doi.org/10.1016/j.yebeh.2011.07.021

Cardinale, F., Chinnici, G., Bramerio, M., Mai, R., Sartori, I., Cossu, M., Lo Russo, G., Castana, L., Colombo, N., & Caborni, C. (2014). Validation of FreeSurfer-estimated brain cortical thickness: comparison with histologic measurements. *Neuroinformatics*, *12*, 535-542.

Chan, D., Gallaher, L. M., Moodley, K., Minati, L., Burgess, N., & Hartley, T. (2016). The 4 Mountains Test: A Short Test of Spatial Memory with High Sensitivity for the Diagnosis of Pre-dementia Alzheimer's Disease. *Journal of visualized experiments : JoVE*(116). https://doi.org/10.3791/54454

Chen, Y., Chen, K., Ding, J., Zhang, Y., Yang, Q., Lv, Y., Guo, Q., & Han, Z. (2019). Neural substrates of amodal and modality-specific semantic processing within the temporal lobe: a lesion-behavior mapping study of semantic dementia. *Cortex*, *120*, 78-91.

Cohen, N. J., & Eichenbaum, H. (1993). *Memory, amnesia, and the hippocampal system*. MIT press.

Cole, M. W., Ito, T., Cocuzza, C., & Sanchez-Romero, R. (2021). The functional relevance of task-state functional connectivity. *Journal of Neuroscience*, *41*(12), 2684-2702.

Collins, A. M., & Quillian, M. R. (1972). Experiments on semantic memory and language comprehension.

Collins, C. E., Airey, D. C., Young, N. A., Leitch, D. B., & Kaas, J. H. (2010). Neuron densities vary across and within cortical areas in primates. *Proceedings of the National Academy of Sciences*, *107*(36), 15927-15932.

Collins, D. L., Zijdenbos, A. P., Paus, T., & Evans, A. C. (2003). Use of registration for cohort studies. *Medical image registration*.

Constantinescu, A. O., O'Reilly, J. X., & Behrens, T. E. J. (2016). Organizing conceptual knowledge in humans with a gridlike code. *Science (New York, N.Y.)*, *352*(6292), 1464-1468. https://doi.org/10.1126/science.aaf0941

Cordes, D., Haughton, V. M., Arfanakis, K., Wendt, G. J., Turski, P. A., Moritz, C. H., Quigley, M. A., & Meyerand, M. E. (2000). Mapping functionally related regions of brain with functional connectivity MR imaging. *American journal of neuroradiology*, *21*(9), 1636-1644.

Cornwell, B. R., Johnson, L. L., Holroyd, T., Carver, F. W., & Grillon, C. (2008). Human hippocampal and parahippocampal theta during goal-directed spatial navigation predicts performance on a virtual Morris water maze. *Journal of Neuroscience*, *28*(23), 5983-5990.

Cox, R. W. (1996). AFNI: software for analysis and visualization of functional magnetic resonance neuroimages. *Computers and Biomedical research*, *29*(3), 162-173.

Cruces, R. R., Royer, J., Herholz, P., Larivière, S., De Wael, R. V., Paquola, C., Benkarim, O., Park, B.-y., Degré-Pelletier, J., & Nelson, M. C. (2022). Micapipe: a pipeline for multimodal neuroimaging and connectome analysis. *NeuroImage*, *263*, 119612.

Cutler, R. A., Duff, M. C., & Polyn, S. M. (2019). Searching for Semantic Knowledge: A Vector Space Semantic Analysis of the Feature Generation Task. *Frontiers in human neuroscience*, *13*, 341-341. https://doi.org/10.3389/fnhum.2019.00341

Dadar, M., Fonov, V. S., Collins, D. L., & Alzheimer's Disease Neuroimaging, I. (2018). A comparison of publicly available linear MRI stereotaxic registration techniques. *NeuroImage*, *174*, 191-200.

Dale, A. M., Fischl, B., & Sereno, M. I. (1999). Cortical surface-based analysis: I. Segmentation and surface reconstruction. *NeuroImage*, *9*(2), 179-194.

Davey, J., Cornelissen, P. L., Thompson, H. E., Sonkusare, S., Hallam, G., Smallwood, J., & Jefferies, E. (2015). Automatic and controlled semantic retrieval: TMS reveals distinct contributions of posterior middle temporal gyrus and angular gyrus. *Journal of Neuroscience*, *35*(46), 15230-15239.

DeKraker, J., Haast, R. A. M., Yousif, M. D., Karat, B., Lau, J. C., Köhler, S., & Khan, A. R. (2022). Automated hippocampal unfolding for morphometry and subfield segmentation with HippUnfold. *eLife*, *11*. https://doi.org/10.7554/eLife.77945

Dhindsa, K., Drobinin, V., King, J., Hall, G. B., Burgess, N., & Becker, S. (2014). Examining the role of the temporo-parietal network in memory, imagery, and viewpoint transformations. *Frontiers in human neuroscience*, *8*, 709-709. https://doi.org/10.3389/fnhum.2014.00709

Dodge, N. C., Thomas, K. G. F., Meintjes, E. M., Molteno, C. D., Jacobson, J. L., & Jacobson, S. W. (2020). Reduced hippocampal volumes partially mediate effects of prenatal alcohol exposure on spatial navigation on a virtual water maze task in children. *Alcoholism: Clinical and Experimental Research*, *44*(4), 844-855.

Doeller, C. F., Barry, C., & Burgess, N. (2010). Evidence for grid cells in a human memory network. *Nature*, *463*(7281), 657-661.

Ego-Stengel, V., & Wilson, M. A. (2009). Disruption of ripple-associated hippocampal activity during rest impairs spatial learning in the rat. *Hippocampus*, NA-NA. https://doi.org/10.1002/hipo.20707

Eichenbaum, H. (2017). Prefrontal–hippocampal interactions in episodic memory. *Nature Reviews Neuroscience*, *18*(9), 547-558.

Eichenbaum, H. (2018). What Versus Where: Non-spatial Aspects of Memory Representation by the Hippocampus. *Current topics in behavioral neurosciences*, *37*, 101-117. https://doi.org/10.1007/7854_2016_450

Eichenbaum, H., & Cohen, N. J. (2001). *From Conditioning to Conscious Recollection: Memory Systems of the Brain*. Oxford University Press.

Eichenbaum, H., Dudchenko, P., Wood, E., Shapiro, M., & Tanila, H. (1999). The hippocampus, memory, and place cells: is it spatial memory or a memory space? *Neuron*, *23*(2), 209-226. https://doi.org/10.1016/s0896-6273(00)80773-4

Ekstrom, A. D., Kahana, M. J., Caplan, J. B., Fields, T. A., Isham, E. A., Newman, E. L., & Fried, I. (2003). Cellular networks underlying human spatial navigation. *Nature*, *425*(6954), 184-188.

Engel Jr, J. (2001). A proposed diagnostic scheme for people with epileptic seizures and with epilepsy: report of the ILAE Task Force on Classification and Terminology. *Epilepsia*, *42*(6), 796-803.

Epstein, R., & Kanwisher, N. (1998). A cortical representation of the local visual environment. *Nature*, *392*(6676), 598-601.

Epstein, R. A. (2008). Parahippocampal and retrosplenial contributions to human spatial navigation. *Trends in cognitive sciences*, *12*(10), 388-396.

Epstein, R. A., Patai, E. Z., Julian, J. B., & Spiers, H. J. (2017). The cognitive map in humans: spatial navigation and beyond. *Nature Neuroscience*, *20*(11), 1504-1513.

Fischl, B. (2012). FreeSurfer. *NeuroImage*, *62*(2), 774-781.

Fischl, B., Sereno, M. I., Tootell, R. B. H., & Dale, A. M. (1999). High-resolution intersubject averaging and a coordinate system for the cortical surface. *Human brain mapping*, *8*(4), 272-284.

Foreman, N., Warry, R., & Murray, P. (1990). Development of reference and working spatial memory in preschool children. *Journal of General Psychology*, *117*(3), 267.

Foreman, N. P., Arber, M., & Savage, J. (1984). Spatial memory in preschool infants. *Developmental Psychobiology: The Journal of the International Society for Developmental Psychobiology*, *17*(2), 129-137.

Fox, M. D., Corbetta, M., Snyder, A. Z., Vincent, J. L., & Raichle, M. E. (2006). Spontaneous neuronal activity distinguishes human dorsal and ventral attention systems. *Proceedings of the National Academy of Sciences*, *103*(26), 10046-10051.

Fox, M. D., Snyder, A. Z., Vincent, J. L., Corbetta, M., Van Essen, D. C., & Raichle, M. E. (2005). The human brain is intrinsically organized into dynamic, anticorrelated functional networks. *Proceedings of the National Academy of Sciences*, *102*(27), 9673-9678.

Gelinas, J. N., Khodagholy, D., Thesen, T., Devinsky, O., & Buzsáki, G. (2016). Interictal epileptiform discharges induce hippocampal–cortical coupling in temporal lobe epilepsy. *Nature Medicine*, *22*(6), 641-648. https://doi.org/10.1038/nm.4084

Ghaem, O., Mellet, E., Crivello, F., Tzourio, N., Mazoyer, B., Berthoz, A., & Denis, M. (1997). Mental navigation along memorized routes activates the hippocampus, precuneus, and insula. *Neuroreport*, *8*(3), 739-744.

Giovagnoli, A. R., Erbetta, A., Villani, F., & Avanzini, G. (2005). Semantic memory in partial epilepsy: verbal and non-verbal deficits and neuroanatomical relationships. *Neuropsychologia*, *43*(10), 1482-1492. https://doi.org/10.1016/j.neuropsychologia.2004.12.010

Girardeau, G., Benchenane, K., Wiener, S. I., Buzsáki, G., & Zugaro, M. B. (2009). Selective suppression of hippocampal ripples impairs spatial memory. *Nature Neuroscience*, *12*(10), 1222-1223. https://doi.org/10.1038/nn.2384

Glasser, M. F., Sotiropoulos, S. N., Wilson, J. A., Coalson, T. S., Fischl, B., Andersson, J. L., Xu, J., Jbabdi, S., Webster, M., & Polimeni, J. R. (2013). The minimal preprocessing pipelines for the Human Connectome Project. *NeuroImage*, *80*, 105-124.

Glikmann-Johnston, Y., Saling, M. M., Chen, J., Cooper, K. A., Beare, R. J., & Reutens, D. C. (2008). Structural and functional correlates of unilateral mesial temporal lobe spatial memory impairment. *Brain : a journal of neurology*, *131*(Pt 11), 3006-3018. https://doi.org/10.1093/brain/awn213

Goodrich-Hunsaker, N. J., & Hopkins, R. O. (2010). Spatial memory deficits in a virtual radial arm maze in amnesic participants with hippocampal damage. *Behavioral neuroscience*, *124*(3), 405.

Goubran, M., Ntiri, E. E., Akhavein, H., Holmes, M., Nestor, S., Ramirez, J., Adamo, S., Ozzoude, M., Scott, C., & Gao, F. (2020). *Hippocampal segmentation for brains with extensive atrophy using three-dimensional convolutional neural networks* (1065-9471).

Greve, D. N., & Fischl, B. (2009). Accurate and robust brain image alignment using boundary-based registration. *NeuroImage*, *48*(1), 63-72.

Guderian, S., Dzieciol, A. M., Gadian, D. G., Jentschke, S., Doeller, C. F., Burgess, N., Mishkin, M., & Vargha-Khadem, F. (2015). Hippocampal volume reduction in humans predicts impaired allocentric spatial memory in virtual-reality navigation. *Journal of Neuroscience*, *35*(42), 14123-14131.

Hafting, T., Fyhn, M., Molden, S., Moser, M.-B., & Moser, E. I. (2005). Microstructure of a spatial map in the entorhinal cortex. *Nature*, *436*(7052), 801-806.

Han, L., Kashyap, A. L., Finin, T., Mayfield, J., & Weese, J. (2013). UMBC_EBIQUITY-CORE: Semantic Textual Similarity Systems. Second Joint Conference on Lexical and

Computational Semantics (*SEM), Volume 1: Proceedings of the Main Conference and the Shared Task, Atlanta.

Hannula, D. E., Tranel, D., & Cohen, N. J. (2006). The long and the short of it: relational memory impairments in amnesia, even at short lags. *Journal of Neuroscience*, *26*(32), 8352-8359.

Hartley, T., Bird, C. M., Chan, D., Cipolotti, L., Husain, M., Vargha-Khadem, F., & Burgess, N. (2007). The hippocampus is required for short-term topographical memory in humans. *Hippocampus*, *17*(1), 34-48. https://doi.org/10.1002/hipo.20240

Hartley, T., & Harlow, R. (2012). An association between human hippocampal volume and topographical memory in healthy young adults. *Frontiers in human neuroscience*, *6*, 338-338. https://doi.org/10.3389/fnhum.2012.00338

Hassabis, D., Chu, C., Rees, G., Weiskopf, N., Molyneux, P. D., & Maguire, E. A. (2009). Decoding neuronal ensembles in the human hippocampus. *Current biology : CB*, *19*(7), 546-554. https://doi.org/10.1016/j.cub.2009.02.033

He, T., Kong, R., Holmes, A. J., Nguyen, M., Sabuncu, M. R., Eickhoff, S. B., Bzdok, D., Feng, J., & Yeo, B. T. T. (2020). Deep neural networks and kernel regression achieve comparable accuracies for functional connectivity prediction of behavior and demographics. *NeuroImage*, *206*, 116276.

Helmstaedter, C. (2002). Effects of chronic epilepsy on declarative memory systems. *Progress in brain research*, *135*, 439-453. https://doi.org/10.1016/S0079-6123(02)35041-6

Helmstaedter, C., Gleissner, U., Di Perna, M., & Elger, C. E. (1997). Relational verbal memory processing in patients with temporal lobe epilepsy. *Cortex; a journal devoted to the study of the nervous system and behavior*, *33*(4), 667-678. https://doi.org/10.1016/s0010-9452(08)70724-x

Helmstaedter, C., Pohl, C., & Elger, C. E. (1995). Relations Between verbal and nonverbal memory performance: evidence of confounding effects Particulary in patients with right temporal lobe epilepsy. *Cortex*, *31*(2), 345-355.

Hirshhorn, M., Grady, C., Rosenbaum, R. S., Winocur, G., & Moscovitch, M. (2012). Brain regions involved in the retrieval of spatial and episodic details associated with a familiar environment: an fMRI study. *Neuropsychologia*, *50*(13), 3094-3106.

Hoffman, P., & Morcom, A. M. (2018). Age-related changes in the neural networks supporting semantic cognition: A meta-analysis of 47 functional neuroimaging studies. *Neuroscience & Biobehavioral Reviews*, *84*, 134-150.

Höller, Y., Höhn, C., Schwimmbeck, F., Plancher, G., & Trinka, E. (2020). Effects of Antiepileptic Drug Tapering on Episodic Memory as Measured by Virtual Reality Tests. *Frontiers in neurology*, *11*, 93-93. https://doi.org/10.3389/fneur.2020.00093

Hoppe, C., Elger, C. E., & Helmstaedter, C. (2007). Long-term memory impairment in patients with focal epilepsy. *Epilepsia*, *48 Suppl 9*, 26-29. https://doi.org/10.1111/j.1528-1167.2007.01397.x

Iaria, G., Petrides, M., Dagher, A., Pike, B., & Bohbot, V. D. (2003). Cognitive strategies dependent on the hippocampus and caudate nucleus in human navigation: variability and change with practice. *Journal of Neuroscience*, *23*(13), 5945-5952.

Jackson, R. L. (2021). The neural correlates of semantic control revisited. *NeuroImage*, *224*, 117444.

Jacobs, J., Weidemann, C. T., Miller, J. F., Solway, A., Burke, J. F., Wei, X.-X., Suthana, N., Sperling, M. R., Sharan, A. D., & Fried, I. (2013). Direct recordings of grid-like neuronal activity in human spatial navigation. *Nature Neuroscience*, *16*(9), 1188-1190.

Jefferies, E. (2013). The neural basis of semantic cognition: converging evidence from neuropsychology, neuroimaging and TMS. *Cortex; a journal devoted to the study of the nervous system and behavior*, *49*(3), 611-625. https://doi.org/10.1016/j.cortex.2012.10.008

Jenkinson, M., Beckmann, C. F., Behrens, T. E. J., Woolrich, M. W., & Smith, S. M. (2012). Fsl. *NeuroImage*, *62*(2), 782-790.

Jokeit, H., Okujava, M., & Woermann, F. G. (2001). Memory fMRI lateralizes temporal lobe epilepsy. *Neurology*, *57*(10), 1786-1793. https://doi.org/10.1212/wnl.57.10.1786

Kebets, V., Holmes, A. J., Orban, C., Tang, S., Li, J., Sun, N., Kong, R., Poldrack, R. A., & Yeo, B. T. T. (2019). Somatosensory-Motor Dysconnectivity Spans Multiple Transdiagnostic Dimensions of Psychopathology. *Biological psychiatry*, *86*(10), 779-791. https://doi.org/10.1016/j.biopsych.2019.06.013

Kim, H., Bernhardt, B. C., Kulaga-Yoskovitz, J., Caldairou, B., Bernasconi, A., & Bernasconi, N. (2014, 2014). *Multivariate hippocampal subfield analysis of local MRI intensity and volume: application to temporal lobe epilepsy*

Kim, H., Park, J. Y., & Kim, K. K. (2018). Spatial learning and memory using a radial arm maze with a head-mounted display. *Psychiatry investigation*, *15*(10), 935.

Kim, J. S., Singh, V., Lee, J. K., Lerch, J., Ad-Dab'bagh, Y., MacDonald, D., Lee, J. M., Kim, S. I., & Evans, A. C. (2005). Automated 3-D extraction and evaluation of the inner and outer cortical surfaces using a Laplacian map and partial volume effect classification. *NeuroImage*, *27*(1), 210-221.

Kim, M., & Maguire, E. A. (2018). Hippocampus, retrosplenial and parahippocampal cortices encode multicompartment 3D space in a hierarchical manner. *Cerebral cortex*, *28*(5), 1898-1909.

Kim, M., & Maguire, E. A. (2019). Can we study 3D grid codes non-invasively in the human brain? Methodological considerations and fMRI findings. *NeuroImage*, *186*, 667-678.

Klinzing, J. G., Niethard, N., & Born, J. (2019). Mechanisms of systems memory consolidation during sleep. *Nature Neuroscience*, *22*(10), 1598-1610. https://doi.org/10.1038/s41593-019-0467-3

Kolarik, B. S., Shahlaie, K., Hassan, A., Borders, A. A., Kaufman, K. C., Gurkoff, G., Yonelinas, A. P., & Ekstrom, A. D. (2016). Impairments in precision, rather than spatial strategy, characterize performance on the virtual Morris Water Maze: A case study. *Neuropsychologia*, *80*, 90-101.

Konkel, A., Warren, D. E., Duff, M. C., Tranel, D., & Cohen, N. J. (2008). Hippocampal amnesia impairs all manner of relational memory. *Frontiers in human neuroscience*, *2*, 286.

Krieger-Redwood, K., Teige, C., Davey, J., Hymers, M., & Jefferies, E. (2015). Conceptual control across modalities: graded specialisation for pictures and words in inferior frontal and posterior temporal cortex. *Neuropsychologia*, *76*, 92-107. https://doi.org/https://doi.org/10.1016/j.neuropsychologia.2015.02.030

Kühn, S., & Gallinat, J. (2014). Amount of lifetime video gaming is positively associated with entorhinal, hippocampal and occipital volume. *Molecular psychiatry*, *19*(7), 842-847.

Kulaga-Yoskovitz, J., Bernhardt, B. C., Hong, S.-J., Mansi, T., Liang, K. E., Van Der Kouwe, A. J. W., Smallwood, J., Bernasconi, A., & Bernasconi, N. (2015). Multi-contrast submillimetric 3 Tesla hippocampal subfield segmentation protocol and dataset. *Scientific data*, *2*(1), 1-9.

Kuperberg, G. R., Broome, M. R., McGuire, P. K., David, A. S., Eddy, M., Ozawa, F., Goff, D., West, W. C., Williams, S. C. R., & van der Kouwe, A. J. W. (2003). Regionally localized

thinning of the cerebral cortex in schizophrenia. *Archives of general psychiatry*, *60*(9), 878-888.

Kwong, K. K., Belliveau, J. W., Chesler, D. A., Goldberg, I. E., Weisskoff, R. M., Poncelet, B. P., Kennedy, D. N., Hoppel, B. E., Cohen, M. S., & Turner, R. (1992). Dynamic magnetic resonance imaging of human brain activity during primary sensory stimulation. *Proceedings of the National Academy of Sciences*, *89*(12), 5675-5679.

la Fougère, C., Grant, S., Kostikov, A., Schirrmacher, R., Gravel, P., Schipper, H. M., Reader, A., Evans, A., & Thiel, A. (2011). Where in-vivo imaging meets cytoarchitectonics: the relationship between cortical thickness and neuronal density measured with high-resolution [18F] flumazenil-PET. *NeuroImage*, *56*(3), 951-960.

Lähde, N., Basnyat, P., Lehtinen, H., Rainesalo, S., Rosti-Otajärvi, E., & Peltola, J. (2021). EpiTrack is a feasible tool for assessing attention and executive functions in patients with refractory epilepsy. *Epilepsy & behavior : E&B*, *115*, 107691-107691. https://doi.org/10.1016/j.yebeh.2020.107691

Lambon Ralph, M. A., Cipolotti, L., Manes, F., & Patterson, K. (2010). Taking both sides: do unilateral anterior temporal lobe lesions disrupt semantic memory? *Brain : a journal of neurology*, *133*(11), 3243-3255. https://doi.org/10.1093/brain/awq264

Lambon Ralph, M. A., Ehsan, S., Baker, G. A., & Rogers, T. T. (2012). Semantic memory is impaired in patients with unilateral anterior temporal lobe resection for temporal lobe epilepsy. *Brain : a journal of neurology*, *135*(Pt 1), 242-258. https://doi.org/10.1093/brain/awr325

Levy, L. J., Astur, R. S., & Frick, K. M. (2005). Men and women differ in object memory but not performance of a virtual radial maze. *Behavioral neuroscience*, *119*(4), 853.

Lewejohann, L., Pickel, T., Sachser, N., & Kaiser, S. (2010). Wild genius-domestic fool? Spatial learning abilities of wild and domestic guinea pigs. *Frontiers in Zoology*, *7*(1), 1-8.

Li, Q., Tavakol, S., Royer, J., Larivière, S., Vos De Wael, R., Park, B.-y., Paquola, C., Zeng, D., Caldairou, B., & Bassett, D. S. (2021). Atypical neural topographies underpin dysfunctional pattern separation in temporal lobe epilepsy. *Brain*, *144*(8), 2486-2498.

Liu, W., Shi, Y., Cousins, J. N., Kohn, N., & Fernández, G. (2022). Hippocampal-medial prefrontal event segmentation and integration contribute to episodic memory formation. *Cerebral cortex*, *32*(5), 949-969.

Lowe, M. J., Dzemidzic, M., Lurito, J. T., Mathews, V. P., & Phillips, M. D. (2000). Correlations in low-frequency BOLD fluctuations reflect cortico-cortical connections. *NeuroImage*, *12*(5), 582-587.

Lutz, M. T., & Helmstaedter, C. (2005). EpiTrack: tracking cognitive side effects of medication on attention and executive functions in patients with epilepsy. *Epilepsy & behavior : E&B*, *7*(4), 708-714. https://doi.org/10.1016/j.yebeh.2005.08.015

Magiorkinis, E., Sidiropoulou, K., & Diamantis, A. (2010). Hallmarks in the history of epilepsy: epilepsy in antiquity. *Epilepsy & Behavior*, *17*(1), 103-108.

Maguire, E. A., Burgess, N., Donnett, J. G., Frackowiak, R. S. J., Frith, C. D., & O'Keefe, J. (1998). Knowing where and getting there: a human navigation network. *Science*, *280*(5365), 921-924.

Maguire, E. A., Gadian, D. G., Johnsrude, I. S., Good, C. D., Ashburner, J., Frackowiak, R. S., & Frith, C. D. (2000). Navigation-related structural change in the hippocampi of taxi drivers. *Proceedings of the National Academy of Sciences of the United States of America*, *97*(8), 4398-4403. https://doi.org/10.1073/pnas.070039597

Mandolesi, L., Petrosini, L., Menghini, D., Addona, F., & Vicari, S. (2009). Children's radial arm maze performance as a function of age and sex. *International Journal of Developmental Neuroscience*, *27*(8), 789-797.

Mayeux, R., Brandt, J., Rosen, J., & Benson, D. F. (1980). Interictal memory and language impairment in temporal lobe epilepsy. *Neurology*, *30*(2), 120-120.

McClelland, J. L., McNaughton, B. L., & O'Reilly, R. C. (1995). Why there are complementary learning systems in the hippocampus and neocortex: insights from the successes and failures of connectionist models of learning and memory. *Psychological review*, *102*(3), 419-457. https://doi.org/10.1037/0033-295X.102.3.419

McCormick, C., Protzner, A. B., Barnett, A. J., Cohn, M., Valiante, T. A., & McAndrews, M. P. (2014). Linking DMN connectivity to episodic memory capacity: What can we learn from patients with medial temporal lobe damage? *NeuroImage: Clinical*, *5*, 188-196. https://doi.org/https://doi.org/10.1016/j.nicl.2014.05.008

McIntosh, A. R., & Lobaugh, N. J. (2004). Partial least squares analysis of neuroimaging data: applications and advances. *NeuroImage*, *23 Suppl 1*, S250-263. https://doi.org/10.1016/j.neuroimage.2004.07.020

McNaughton, B. L., Battaglia, F. P., Jensen, O., Moser, E. I., & Moser, M.-B. (2006). Path integration and the neural basis of the'cognitive map'. *Nature Reviews Neuroscience*, *7*(8), 663-678.

Medea, B., Karapanagiotidis, T., Konishi, M., Ottaviani, C., Margulies, D., Bernasconi, A., Bernasconi, N., Bernhardt, B. C., Jefferies, E., & Smallwood, J. (2018). How do we decide what to do? Resting-state connectivity patterns and components of self-generated thought linked to the development of more concrete personal goals. *Experimental brain research*, *236*, 2469-2481.

Milner, B. (1965). Visually-guided maze learning in man: Effects of bilateral hippocampal, bilateral frontal, and unilateral cerebral lesions. *Neuropsychologia*, *3*(4), 317-338.

Mok, R. M., & Love, B. C. (2019). A non-spatial account of place and grid cells based on clustering models of concept learning. *Nature communications*, *10*(1), 5685-5685. https://doi.org/10.1038/s41467-019-13760-8

Momi, D., Smeralda, C., Sprugnoli, G., Ferrone, S., Rossi, S., Rossi, A., Di Lorenzo, G., & Santarnecchi, E. (2018). Acute and long-lasting cortical thickness changes following intensive first-person action videogame practice. *Behavioural brain research*, *353*, 62-73.

Moodley, K., Minati, L., Contarino, V., Prioni, S., Wood, R., Cooper, R., D'Incerti, L., Tagliavini, F., & Chan, D. (2015). Diagnostic differentiation of mild cognitive impairment due to Alzheimer's disease using a hippocampus-dependent test of spatial memory. *Hippocampus*, *25*(8), 939-951.

Moraleda Barreno, E., Broglio Schenon, C., Rodríguez Fernández, F., & Gómez García, A. M. (2013). Development of different spatial frames of reference for orientation in small-scale environments. *Psicothema*.

Morris, R. G. M. (1981). Spatial localization does not require the presence of local cues. *Learning and motivation*, *12*(2), 239-260.

Morris, R. G. M., Garrud, P., Rawlins, J. N. P. a., & O'Keefe, J. (1982). Place navigation impaired in rats with hippocampal lesions. *Nature*, *297*(5868), 681-683.

Moscovitch, M., Cabeza, R., Winocur, G., & Nadel, L. (2016). Episodic Memory and Beyond: The Hippocampus and Neocortex in Transformation. *Annual review of psychology*, *67*, 105-134. https://doi.org/10.1146/annurev-psych-113011-143733

Moscovitch, M., Rosenbaum, R. S., Gilboa, A., Addis, D. R., Westmacott, R., Grady, C., McAndrews, M. P., Levine, B., Black, S., & Winocur, G. (2005). Functional neuroanatomy of remote episodic, semantic and spatial memory: a unified account based on multiple trace theory. *Journal of anatomy*, *207*(1), 35-66.

Nadel, L., & Moscovitch, M. (1997). Memory consolidation, retrograde amnesia and the hippocampal complex. *Current opinion in neurobiology*, *7*(2), 217-227.

Nadel, L., Samsonovich, A., Ryan, L., & Moscovitch, M. (2000). Multiple trace theory of human memory: computational, neuroimaging, and neuropsychological results. *Hippocampus*, *10*(4), 352-368. https://doi.org/10.1002/1098-1063(2000)10:4<352::AID-HIPO2>3.0.CO;2-D

Nasreddine, Z. S., Phillips, N. A., Bédirian, V., Charbonneau, S., Whitehead, V., Collin, I., Cummings, J. L., & Chertkow, H. (2005). The Montreal Cognitive Assessment, MoCA: a brief screening tool for mild cognitive impairment. *Journal of the American Geriatrics Society*, *53*(4), 695-699. https://doi.org/10.1111/j.1532-5415.2005.53221.x

Nelson, D. L., McEvoy, C. L., & Schreiber, T. A. (2004). The University of South Florida free association, rhyme, and word fragment norms. *Behavior Research Methods, Instruments, & Computers*, *36*(3), 402-407.

Neylan, T. C. (2000). Memory and the medial temporal lobe: Patient HM. *The Journal of Neuropsychiatry and Clinical Neurosciences*, *12*(1), 103-103.

O'Keefe, J., & Dostrovsky, J. (1971). The hippocampus as a spatial map: preliminary evidence from unit activity in the freely-moving rat. *Brain research*.

O'Keefe, J., & Nadel, L. (1978). *The Hippocampus as a Cognitive Map*. Oxford University Press.

O'Reilly, R. C., Bhattacharyya, R., Howard, M. D., & Ketz, N. (2014). Complementary learning systems. *Cognitive science*, *38*(6), 1229-1248. https://doi.org/10.1111/j.1551-6709.2011.01214.x

Ogawa, S., Tank, D. W., Menon, R., Ellermann, J. M., Kim, S. G., Merkle, H., & Ugurbil, K. (1992). Intrinsic signal changes accompanying sensory stimulation: functional brain mapping with magnetic resonance imaging. *Proceedings of the National Academy of Sciences*, *89*(13), 5951-5955.

Olsen, R. K., Moses, S. N., Riggs, L., & Ryan, J. D. (2012). The hippocampus supports multiple cognitive processes through relational binding and comparison. *Frontiers in human neuroscience*, *6*, 146-146. https://doi.org/10.3389/fnhum.2012.00146

Olton, D. S., & Samuelson, R. J. (1976). Remembrance of places passed: spatial memory in rats. *Journal of experimental psychology: Animal behavior processes*, *2*(2), 97.

Olton, D. S., Walker, J. A., & Gage, F. H. (1978). Hippocampal connections and spatial discrimination. *Brain research*, *139*(2), 295-308.

Othman, M. Z., Hassan, Z., & Has, A. T. C. (2022). Morris water maze: a versatile and pertinent tool for assessing spatial learning and memory. *Experimental Animals*, *71*(3), 264-280.

Owen, A. M., Milner, B., Petrides, M., & Evans, A. C. (1996). A specific role for the right parahippocampal gyrus in the retrieval of object-location: A positron emission tomography study. *Journal of cognitive neuroscience*, *8*(6), 588-602.

Paquola, C., Benkarim, O., DeKraker, J., Lariviere, S., Frässle, S., Royer, J., Tavakol, S., Valk, S., Bernasconi, A., & Bernasconi, N. (2020). Convergence of cortical types and functional motifs in the human mesiotemporal lobe. *eLife*, *9*, e60673.

Patel, S. A., Frick, K. M., Newhouse, P. A., & Astur, R. S. (2022). Estradiol effects on spatial memory in women. *Behavioural brain research*, *417*, 113592.

Patterson, K., & Lambon Ralph, M. A. (2016). Chapter 61 - The Hub-and-Spoke Hypothesis of Semantic Memory. In G. Hickok & S. L. Small (Eds.), *Neurobiology of Language* (pp. 765-775). Academic Press. https://doi.org/https://doi.org/10.1016/B978-0-12-407794-2.00061-4

Paulin, T., Roquet, D., Kenett, Y. N., Savage, G., & Irish, M. (2020). The effect of semantic memory degeneration on creative thinking: A voxel-based morphometry analysis. *NeuroImage*, *220*, 117073.

Payne, J. D., Tucker, M. A., Ellenbogen, J. M., Wamsley, E. J., Walker, M. P., Schacter, D. L., & Stickgold, R. (2012). Memory for semantically related and unrelated declarative information: the benefit of sleep, the cost of wake. *PloS one*, *7*(3), e33079-e33079. https://doi.org/10.1371/journal.pone.0033079

Penfield, W., & Milner, B. (1958). Memory deficit produced by bilateral lesions in the hippocampal zone. *AMA archives of Neurology & Psychiatry*, *79*(5), 475-497.

Perlmutter, M., Metzger, R., Nezworski, T., & Miller, K. (1981). Spatial and temporal memory in 20 and 60 year olds. *Journal of Gerontology*, *36*(1), 59-65.

Pezdek, K. (1983). Memory for items and their spatial locations by young and elderly adults. *Developmental Psychology*, *19*(6), 895.

Phuong, T. H., Houot, M., Méré, M., Denos, M., Samson, S., & Dupont, S. (2021). Cognitive impairment in temporal lobe epilepsy: contributions of lesion, localization and lateralization. *Journal of neurology*, *268*, 1443-1452.

Plachti, A., Eickhoff, S. B., Hoffstaedter, F., Patil, K. R., Laird, A. R., Fox, P. T., Amunts, K., & Genon, S. (2019). Multimodal parcellations and extensive behavioral profiling tackling the hippocampus gradient. *Cerebral cortex*, *29*(11), 4595-4612.

Postma, T. S., Cury, C., Baxendale, S., Thompson, P. J., Cano-López, I., de Tisi, J., Burdett, J. L., Sidhu, M. K., Caciagli, L., Winston, G. P., Vos, S. B., Thom, M., Duncan, J. S., Koepp, M. J., & Galovic, M. (2020). Hippocampal Shape Is Associated with Memory Deficits in Temporal Lobe Epilepsy. *Annals of neurology*, *88*(1), 170-182. https://doi.org/10.1002/ana.25762

Przeździk, I., Faber, M., Fernández, G., Beckmann, C. F., & Haak, K. V. (2019). The functional organisation of the hippocampus along its long axis is gradual and predicts recollection. *Cortex*, *119*, 324-335.

Qiu, Y., Wu, Y., Liu, R., Wang, J., Huang, H., & Huang, R. (2019). Representation of human spatial navigation responding to input spatial information and output navigational strategies: An ALE meta-analysis. *Neuroscience & Biobehavioral Reviews*, *103*, 60-72.

Quillian, M. R. (1966). *Semantic memory*. Air Force Cambridge Research Laboratories, Office of Aerospace Research ….

Raichle, M. E., MacLeod, A. M., Snyder, A. Z., Powers, W. J., Gusnard, D. A., & Shulman, G. L. (2001). A default mode of brain function. *Proceedings of the National Academy of Sciences*, *98*(2), 676-682.

Rains, G. D., & Milner, B. (1994). Right-hippocampal contralateral-hand effect in the recall of spatial location in the tactual modality. *Neuropsychologia*, *32*(10), 1233-1242.

Rice, G. E., Hoffman, P., Binney, R. J., & Lambon Ralph, M. A. (2018). Concrete versus abstract forms of social concept: an fMRI comparison of knowledge about people versus social

terms. *Philosophical Transactions of the Royal Society B: Biological Sciences*, *373*(1752), 20170136.

Rice, G. E., Lambon Ralph, M. A., & Hoffman, P. (2015). The roles of left versus right anterior temporal lobes in conceptual knowledge: an ALE meta-analysis of 97 functional neuroimaging studies. *Cerebral cortex*, *25*(11), 4374-4391.

Ritchie, K., Carrière, I., Howett, D., Su, L., Hornberger, M., O'Brien, J. T., Ritchie, C. W., & Chan, D. (2018). Allocentric and egocentric spatial processing in middle-aged adults at high risk of late-onset Alzheimer's disease: the PREVENT dementia study. *Journal of Alzheimer's Disease*, *65*(3), 885-896.

Robin, J., Buchsbaum, B. R., & Moscovitch, M. (2018). The primacy of spatial context in the neural representation of events. *Journal of Neuroscience*, *38*(11), 2755-2765.

Rogers, T. T., Lambon Ralph, M. A., Garrard, P., Bozeat, S., McClelland, J. L., Hodges, J. R., & Patterson, K. (2004). Structure and deterioration of semantic memory: a neuropsychological and computational investigation. *Psychological review*, *111*(1), 205.

Romero, J. E., Coupe, P., & Manjón, J. V. (2017). HIPS: A new hippocampus subfield segmentation method. *NeuroImage*, *163*, 286-295.

Rosas, H. D., Liu, A. K., Hersch, S., Glessner, M., Ferrante, R. J., Salat, D. H., van Der Kouwe, A., Jenkins, B. G., Dale, A. M., & Fischl, B. (2002). Regional and progressive thinning of the cortical ribbon in Huntington's disease. *Neurology*, *58*(5), 695-701.

Rosas, K., Parrón, I., Serrano, P., & Cimadevilla, J. M. (2013). Spatial recognition memory in a virtual reality task is altered in refractory temporal lobe epilepsy. *Epilepsy & behavior : E&B*, *28*(2), 227-231. https://doi.org/10.1016/j.yebeh.2013.05.010

Rugg, M. D., Roberts, R. C., Rotter, D. D., Pickles, C. D., & Nagy, M. E. (1991). Event-related potentials related to recognition memory: Effects of unilateral temporal lobectomy and temporal lobe epilepsy. *Brain*, *114*(5), 2313-2332.

Rugg, M. D., & Vilberg, K. L. (2013). Brain networks underlying episodic memory retrieval. *Current opinion in neurobiology*, *23*(2), 255-260. https://doi.org/10.1016/j.conb.2012.11.005

Ryan, J. D., & Cohen, N. J. (2003). Evaluating the neuropsychological dissociation evidence for multiple memory systems. *Cognitive, Affective, & Behavioral Neuroscience*, *3*, 168-185.

Sargolini, F., Fyhn, M., Hafting, T., McNaughton, B. L., Witter, M. P., Moser, M.-B., & Moser, E. I. (2006). Conjunctive representation of position, direction, and velocity in entorhinal cortex. *Science*, *312*(5774), 758-762.

Savelli, F., Yoganarasimha, D., & Knierim, J. J. (2008). Influence of boundary removal on the spatial representations of the medial entorhinal cortex. *Hippocampus*, *18*(12), 1270-1282.

Schapiro, A. C., McClelland, J. L., Welbourne, S. R., Rogers, T. T., & Lambon Ralph, M. A. (2013). Why bilateral damage is worse than unilateral damage to the brain. *Journal of cognitive neuroscience*, *25*(12), 2107-2123.

Schindler, A., & Bartels, A. (2013). Parietal cortex codes for egocentric space beyond the field of view. *Current biology : CB*, *23*(2), 177-182. https://doi.org/10.1016/j.cub.2012.11.060

Schmidbauer, V., Nenning, K.-H., Schwarz, M., Foesleitner, O., Mayr-Geisl, G., Yildirim, M. S., Pirker, S., Moser, D., Denk, D., & Prayer, D. (2022). Imaging visuospatial memory in temporal lobe epilepsy—Results of an fMRI study. *PloS one*, *17*(2), e0264349.

Schoenfeld, R., Schiffelholz, T., Beyer, C., Leplow, B., & Foreman, N. (2017). Variants of the Morris water maze task to comparatively assess human and rodent place navigation. *Neurobiology of Learning and Memory*, *139*, 117-127.

Scoville, W. B., & Milner, B. (1957). Loss of recent memory after bilateral hippocampal lesions. *Journal of neurology, neurosurgery, and psychiatry*, *20*(1), 11.

Seidenberg, M., Guidotti, L., Nielson, K. A., Woodard, J. L., Durgerian, S., Antuono, P., Zhang, Q., & Rao, S. M. (2009). Semantic memory activation in individuals at risk for developing Alzheimer disease. *Neurology*, *73*(8), 612-620.

Sepeta, L. N., Berl, M. M., & Gaillard, W. D. (2018). Imaging episodic memory during development and childhood epilepsy. *Journal of neurodevelopmental disorders*, *10*(1), 1-10.

Serra, L., Raimondi, S., Di Domenico, C., Maffei, S., Lardone, A., Liparoti, M., Sorrentino, P., Caltagirone, C., Petrosini, L., & Mandolesi, L. (2021). The beneficial effects of physical exercise on visuospatial working memory in preadolescent children. *AIMS neuroscience*, *8*(4), 496.

Sharon, T., Moscovitch, M., & Gilboa, A. (2011). Rapid neocortical acquisition of long-term arbitrary associations independent of the hippocampus. *Proceedings of the National Academy of Sciences of the United States of America*, *108*(3), 1146-1151. https://doi.org/10.1073/pnas.1005238108

Sideman, N., Chaitanya, G., He, X., Doucet, G., Kim, N. Y., Sperling, M. R., Sharan, A. D., & Tracy, J. I. (2018). Task activation and functional connectivity show concordant memory laterality in temporal lobe epilepsy. *Epilepsy & Behavior*, *81*, 70-78.

Sidhu, M. K., Stretton, J., Winston, G. P., Bonelli, S., Centeno, M., Vollmar, C., Symms, M., Thompson, P. J., Koepp, M. J., & Duncan, J. S. (2013). A functional magnetic resonance

imaging study mapping the episodic memory encoding network in temporal lobe epilepsy. *Brain*, *136*(6), 1868-1888. https://doi.org/10.1093/brain/awt099

Sierk, A., Manthey, A., King, J., Brewin, C. R., Bisby, J. A., Walter, H., Burgess, N., & Daniels, J. K. (2019). Allocentric spatial memory performance predicts intrusive memory severity in posttraumatic stress disorder. *Neurobiology of Learning and Memory*, *166*, 107093.

Smith, M. L., & Milner, B. (1981). The role of the right hippocampus in the recall of spatial location. *Neuropsychologia*, *19*(6), 781-793.

Smith, M. L., & Milner, B. (1989). Right hippocampal impairment in the recall of spatial location: encoding deficit or rapid forgetting? *Neuropsychologia*, *27*(1), 71-81.

Smith, S. M., Fox, P. T., Miller, K. L., Glahn, D. C., Fox, P. M., Mackay, C. E., Filippini, N., Watkins, K. E., Toro, R., & Laird, A. R. (2009). Correspondence of the brain's functional architecture during activation and rest. *Proceedings of the National Academy of Sciences*, *106*(31), 13040-13045.

Smith, S. M., Nichols, T. E., Vidaurre, D., Winkler, A. M., Behrens, T. E. J., Glasser, M. F., Ugurbil, K., Barch, D. M., Van Essen, D. C., & Miller, K. L. (2015). A positive-negative mode of population covariation links brain connectivity, demographics and behavior. *Nature Neuroscience*, *18*(11), 1565-1567.

Snowden, J. S., Harris, J. M., Saxon, J. A., Thompson, J. C., Richardson, A. M., Jones, M., & Kobylecki, C. (2019). Naming and conceptual understanding in frontotemporal dementia. *Cortex*, *120*, 22-35.

Snowden, J. S., Harris, J. M., Thompson, J. C., Kobylecki, C., Jones, M., Richardson, A. M., & Neary, D. (2018). Semantic dementia and the left and right temporal lobes. *Cortex*, *107*, 188-203.

Solomon, S. H., & Schapiro, A. C. (2020). Semantic Search as Pattern Completion across a Concept. *Trends in cognitive sciences*, *24*(2), 95-98. https://doi.org/10.1016/j.tics.2019.12.003

Solstad, T., Boccara, C. N., Kropff, E., Moser, M.-B., & Moser, E. I. (2008). Representation of geometric borders in the entorhinal cortex. *Science*, *322*(5909), 1865-1868.

Sormaz, M., Jefferies, E., Bernhardt, B. C., Karapanagiotidis, T., Mollo, G., Bernasconi, N., Bernasconi, A., Hartley, T., & Smallwood, J. (2017). Knowing what from where: Hippocampal connectivity with temporoparietal cortex at rest is linked to individual differences in semantic and topographic memory. *NeuroImage*, *152*, 400-410. https://doi.org/10.1016/j.neuroimage.2017.02.071

Spiers, H. J., Maguire, E. A., & Burgess, N. (2001). Hippocampal amnesia. *Neurocase*, *7*(5), 357-382. https://doi.org/10.1076/neur.7.5.357.16245

Squire, L. R. (2009). The legacy of patient HM for neuroscience. *Neuron*, *61*(1), 6-9.

Stark, S. M., Yassa, M. A., Lacy, J. W., & Stark, C. E. L. (2013). A task to assess behavioral pattern separation (BPS) in humans: Data from healthy aging and mild cognitive impairment. *Neuropsychologia*, *51*(12), 2442-2449.

Styner, M., Oguz, I., Xu, S., Brechbühler, C., Pantazis, D., Levitt, J. J., Shenton, M. E., & Gerig, G. (2006). Framework for the statistical shape analysis of brain structures using SPHARM-PDM. *The insight journal*(1071), 242.

Subramaniapillai, S., Rajagopal, S., Ankudowich, E., Pasvanis, S., Misic, B., & Rajah, M. N. (2022). Age-and episodic memory-related differences in task-based functional connectivity in women and men. *Journal of cognitive neuroscience*, *34*(8), 1500-1520.

Subramaniapillai, S., Rajagopal, S., Elshiekh, A., Pasvanis, S., Ankudowich, E., & Rajah, M. N. (2019). Sex differences in the neural correlates of spatial context memory decline in healthy aging. *Journal of cognitive neuroscience*, *31*(12), 1895-1916.

Suhrawardī, Y. y. i. H. a. (1998). *Suhrawardi: the shape of light: hayakal al-nur*. Fons Vitae.

Tallarita, G. M., Parente, A., & Giovagnoli, A. R. (2019). The visuospatial pattern of temporal lobe epilepsy. *Epilepsy & Behavior*, *101*, 106582. https://doi.org/https://doi.org/10.1016/j.yebeh.2019.106582

Tavakol, S., Kebets, V., Royer, J., Li, Q., Auer, H., DeKraker, J., Jefferies, E., Bernasconi, N., Bernasconi, A., Helmstaedter, C., Caciagli, L., Frauscher, B., Smallwood, J., & Bernhardt, B. (2022). Differential Memory Impairment Across Relational Domains in Temporal Lobe Epilepsy. *bioRxiv*, 2022.2011.2001.514752. https://doi.org/10.1101/2022.11.01.514752

Tavakol, S., Li, Q., Royer, J., Vos de Wael, R., Larivière, S., Lowe, A., Paquola, C., Jefferies, E., Hartley, T., Bernasconi, A., Bernasconi, N., Smallwood, J., Bohbot, V., Caciagli, L., & Bernhardt, B. (2021). A Structure-Function Substrate of Memory for Spatial Configurations in Medial and Lateral Temporal Cortices. *Cerebral cortex (New York, N.Y. : 1991)*, *31*(7), 3213-3225. https://doi.org/10.1093/cercor/bhab001

Tavakol, S., Royer, J., Lowe, A. J., Bonilha, L., Tracy, J. I., Jackson, G. D., Duncan, J. S., Bernasconi, A., Bernasconi, N., & Bernhardt, B. C. (2019). Neuroimaging and connectomics of drug-resistant epilepsy at multiple scales: From focal lesions to macroscale networks. *Epilepsia*, *60*(4), 593-604. https://doi.org/10.1111/epi.14688

Thom, M. (2014). Review: Hippocampal sclerosis in epilepsy: a neuropathology review. *Neuropathology and applied neurobiology*, *40*(5), 520-543. https://doi.org/10.1111/nan.12150

Thornberry, C., Cimadevilla, J. M., & Commins, S. (2021). Virtual Morris water maze: Opportunities and challenges. *Reviews in the Neurosciences*, *32*(8), 887-903.

Tolman, E. C. (1948). Cognitive maps in rats and men. *Psychological review*, *55*(4), 189.

Travis, S. G., Huang, Y., Fujiwara, E., Radomski, A., Olsen, F., Carter, R., Seres, P., & Malykhin, N. V. (2014). High field structural MRI reveals specific episodic memory correlates in the subfields of the hippocampus. *Neuropsychologia*, *53*, 233-245.

Trimmel, K., van Graan, A. L., Caciagli, L., Haag, A., Koepp, M. J., Thompson, P. J., & Duncan, J. S. (2018). Left temporal lobe language network connectivity in temporal lobe epilepsy. *Brain : a journal of neurology*, *141*(8), 2406-2418. https://doi.org/10.1093/brain/awy164

Tulving, E. (1972). Episodic and semantic memory. *Organization of memory*, *1*(381-403), 1.

Tulving, E. (1983). *Elements of Episodic Memory*. Oxford University Press.

Tulving, E. (2002). Episodic memory: from mind to brain. *Annual review of psychology*, *53*, 1-25. https://doi.org/10.1146/annurev.psych.53.100901.135114

Valk, S. L., Bernhardt, B. C., Böckler, A., Trautwein, F.-M., Kanske, P., & Singer, T. (2016). Socio-cognitive phenotypes differentially modulate large-scale structural covariance networks. *Cerebral cortex*, bhv319.

Vidal-Piñeiro, D., Sneve, M. H., Amlien, I. K., Grydeland, H., Mowinckel, A. M., Roe, J. M., Sørensen, Ø., Nyberg, L. H., Walhovd, K. B., & Fjell, A. M. (2021). The functional foundations of episodic memory remain stable throughout the lifespan. *Cerebral cortex*, *31*(4), 2098-2110.

Viskontas, I. V., McAndrews, M. P., & Moscovitch, M. (2000). Remote episodic memory deficits in patients with unilateral temporal lobe epilepsy and excisions. *The Journal of*

neuroscience : the official journal of the Society for Neuroscience, *20*(15), 5853-5857. https://doi.org/10.1523/JNEUROSCI.20-15-05853.2000

Voets, N. L., Adcock, J. E., Stacey, R., Hart, Y., Carpenter, K., Matthews, P. M., & Beckmann, C. F. (2009). *Functional and structural changes in the memory network associated with left temporal lobe epilepsy* (1065-9471).

Vorhees, C. V., & Williams, M. T. (2006). Morris water maze: procedures for assessing spatial and related forms of learning and memory. *Nature protocols*, *1*(2), 848-858.

Vos de Wael, R., Larivière, S., Caldairou, B., Hong, S.-J., Margulies, D. S., Jefferies, E., Bernasconi, A., Smallwood, J., Bernasconi, N., & Bernhardt, B. C. (2018). Anatomical and microstructural determinants of hippocampal subfield functional connectome embedding. *Proceedings of the National Academy of Sciences*, *115*(40), 10154-10159.

Wagstyl, K., Ronan, L., Goodyer, I. M., & Fletcher, P. C. (2015). Cortical thickness gradients in structural hierarchies. *NeuroImage*, *111*, 241-250.

Wang, H., Suh, J. W., Das, S. R., Pluta, J. B., Craige, C., & Yushkevich, P. A. (2012). Multi-atlas segmentation with joint label fusion. *IEEE transactions on pattern analysis and machine intelligence*, *35*(3), 611-623.

Wang, X., Bernhardt, B. C., Karapanagiotidis, T., De Caso, I., Gonzalez Alam, T. R. D. J., Cotter, Z., Smallwood, J., & Jefferies, E. (2018). The structural basis of semantic control: Evidence from individual differences in cortical thickness. *NeuroImage*, *181*, 480-489. https://doi.org/10.1016/j.neuroimage.2018.07.044

Watson, J. B. (1924). *Behaviorism*. W. W. Norton & Company, Inc.

West, G. L., Konishi, K., Diarra, M., Benady-Chorney, J., Drisdelle, B. L., Dahmani, L., Sodums, D. J., Lepore, F., Jolicoeur, P., & Bohbot, V. D. (2018). Impact of video games on plasticity of the hippocampus. *Molecular psychiatry*, *23*(7), 1566-1574.

West, G. L., Patai, Z. E., Coutrot, A., Hornberger, M., Bohbot, V. D., & Spiers, H. J. (2023). Landmark-dependent navigation strategy declines across the human life-span: evidence from over 37,000 participants. *Journal of cognitive neuroscience*, *35*(3), 452-467.

Whalley, M. G., Rugg, M. D., Smith, A. P. R., Dolan, R. J., & Brewin, C. R. (2009). Incidental retrieval of emotional contexts in post-traumatic stress disorder and depression: an fMRI study. *Brain and cognition*, *69*(1), 98-107.

Whitlock, J. R., Sutherland, R. J., Witter, M. P., Moser, M.-B., & Moser, E. I. (2008). Navigating from hippocampus to parietal cortex. *Proceedings of the National Academy of Sciences*, *105*(39), 14755-14762.

Whittington, J. C. R., Muller, T. H., Mark, S., Chen, G., Barry, C., Burgess, N., & Behrens, T. E. J. (2020). The Tolman-Eichenbaum machine: unifying space and relational memory through generalization in the hippocampal formation. *Cell*, *183*(5), 1249-1263.

Winocur, G. (1982). Radial-arm maze behavior by rats with dorsal hippocampal lesions: Effects of cuing. *Journal of comparative and physiological psychology*, *96*(2), 155.

Woodard, J. L., Seidenberg, M., Nielson, K. A., Antuono, P., Guidotti, L., Durgerian, S., Zhang, Q., Lancaster, M., Hantke, N., & Butts, A. (2009). Semantic memory activation in amnestic mild cognitive impairment. *Brain*, *132*(8), 2068-2078.

Worsley, K. J., Taylor, J., Carbonell, F., Chung, M., Duerden, E., Bernhardt, B., Lyttelton, O., Boucher, M., & Evans, A. (2009, 2009). *A Matlab toolbox for the statistical analysis of univariate and multivariate surface and volumetric data using linear mixed effects models and random field theory*

Xiao, F., Caciagli, L., Wandschneider, B., Joshi, B., Vos, S. B., Hill, A., Galovic, M., Long, L., Sone, D., Trimmel, K., Sander, J. W., Zhou, D., Thompson, P. J., Baxendale, S., Duncan, J. S., & Koepp, M. J. (2021). Effect of Anti-seizure Medications on Functional Anatomy of Language: A Perspective From Language Functional Magnetic Resonance Imaging. *Frontiers in neuroscience*, *15*, 787272-787272. https://doi.org/10.3389/fnins.2021.787272

Yeo, B. T. T., Krienen, F. M., Sepulcre, J., Sabuncu, M. R., Lashkari, D., Hollinshead, M., Roffman, J. L., Smoller, J. W., Zöllei, L., & Polimeni, J. R. (2011). The organization of the human cerebral cortex estimated by intrinsic functional connectivity. *Journal of neurophysiology*.

Yoo, H. J., Lee, S. A., Kim, S. Y., Kang, J. G., & Lee, J. G. (2006). Compromised memory function in schizophrenia and temporal lobe epilepsy. *The Journal of Neuropsychiatry and Clinical Neurosciences*, *18*(2), 199-207.

Zammit, A. R., Ezzati, A., Zimmerman, M. E., Lipton, R. B., Lipton, M. L., & Katz, M. J. (2017). Roles of hippocampal subfields in verbal and visual episodic memory. *Behavioural brain research*, *317*, 157-162.

Zanao, T. A., Seitz-Holland, J., O'Donnell, L. J., Zhang, F., Rathi, Y., Lopes, T. M., Pimentel-Silva, L. R., Yassuda, C. L., Makris, N., & Shenton, M. E. (2023). Exploring the impact of hippocampal sclerosis on white matter tracts memory in individuals with mesial temporal lobe epilepsy. *Epilepsia Open*.

Zhuang, X., Yang, Z., Sreenivasan, K. R., Mishra, V. R., Curran, T., Nandy, R., & Cordes, D. (2019). Multivariate group-level analysis for task fMRI data with canonical correlation analysis. *NeuroImage*, *194*, 25-41.